

**Control of Hydrological Regime
on the Cropping Pattern
in the Context of Climate Change
in Mahanadi Delta**

Thesis submitted by

Amit Ghosh

[Index No. 224/16/Oce.Stud./25]

Doctor of Philosophy (Science)

School of Oceanographic Studies

Jadavpur University

Kolkata, West Bengal

India


2022



Date 07.12.2022

CERTIFICATE FROM THE SUPERVISOR

This is to certify that the thesis entitled "*Control of hydrological regimes on the cropping pattern in the context of climate change*" submitted by **Sri Amit Ghosh**, who got his name registered on 25-11-2016, (Index No 224/16/Oce.Stud./25) for the award of PhD (Science) degree of Jadavpur University is absolutely based upon his own work under the supervision of **Prof. Tuhin Ghosh** and that neither his thesis nor any part of the thesis has been submitted for any degree/diploma or any other academic award anywhere before.


(Prof. Tuhin Ghosh)

Prof. Tuhin Ghosh
School of Oceanographic Studies
Jadavpur University
Kolkata-700032
India

Acknowledgements

As I prepare to submit my doctoral dissertation, I reflect on how many individuals and organisations have assisted and supported me.

Before anything else, I would like to express my profound gratitude to Professor Tuhin Ghosh of the School of Oceanographic Studies at Jadavpur University, who served as my supervisor during the course of this research. His insightful counsel, fruitful conversations, innovative ideas, and unwavering support through thick and thin have been and continue to be extremely inspirational. Without his support, I never would have finished this thesis. Moreover, I'd like to thank Prof. Rabindra N. Bhattacharya, Honorary Adjunct Professor (Economics), School of Oceanographic Studies, Jadavpur University, Kolkata, for his insightful comments and support.

Dr. Rabindranath Samal, Senior Scientist at the Chilika Development Authority in the Department of Forest and Environment in the Government of Odisha, was instrumental in providing laboratory facility for the soil analysis that was essential to this research. He has my gratitude. I would like to express my sincere thanks to Dr. Pradipta R. Muduli, Scientific Officer at the Wetland Research and Training Center (WRTC), Chilika Development Authority, Department of Forest and Environment, Government of Odisha, Barkul, Balugaon, as well as the rest of the WRTC's staff and the project's personnel for their assistance in soil analysis.

I would like to thank the Vice-Chancellor, Registrar, Secretary, and Doctoral Committee of the Faculty of Science of Jadavpur University for giving all the necessary resources and support. Without the assistance and support of University administrators and employees, it would have been difficult to complete the research.

I am thankful to Prof. Sugata Hazra, professor at the School of Oceanographic Studies, and Dr. Avbhra Chanda, Assistant Professor at the School of Oceanographic Studies, as well as the rest of the faculty, researchers and staff at the School of Oceanographic Studies, Mr. Subhas Acharya, ex-joint director of the Sundarban

Development Board, Government of West Bengal, Dr. P V Raju, Senior Scientist, National remote Sensing Centre, ISRO, Govt. India, Mr. Sunil S. Kulkarni, Scientist, National Remote Sensing Service Centre, ISRO, Government of India, Dr. Gianlucal Franseschini, Senior Environmental officer, Food and Agriculture Organization of the United Nations, Rome, for their helpful ideas and conversations and support during the course of my study.

I will remember my friends and research scholars Somnath da, Souvik, Sumana, Shruti di Sourav da and Anirban da with fondness because they made it easy for me to do my Ph.D. research and because they were friendly, worked hard, and cared about each other.

I am insufficient if I do not express my sincere appreciation to my family members for their support and encouragement.

A handwritten signature in black ink that reads "Amit Ghosh". The signature is written in a cursive, flowing style with a large initial 'A'.

Contents

Acknowledgements	i
Contents	iii
List of Figures	vi
List of Tables	xii
Executive Summary	xiv
Abbreviations and acronyms	xviii
1 Introduction	1
1.1 Climate change and agriculture	1
1.2 Changes in the climate and agriculture in the deltas	2
1.3 Objectives	3
1.4 Problem Statement	4
1.5 Research hypothesis	4
1.6 Organizational scheme for the thesis	4
2 Literature review	6
2.1 Introduction	6
2.2 Climate projections	7
2.2.1 Climate models	8
2.2.2 Projection scenarios	11
2.3 Changes in hydrological regime and climate and their impacts on agriculture	13

<i>Contents</i>	iv
2.3.1 Impacts of elevated CO ₂	14
2.3.2 Impacts of extreme events	14
2.3.3 Impacts of hydrological regime	14
2.4 Crop model	15
2.5 The effects of climate change on the agricultural sector in the Ma- hanadi Delta	19
3 Study area	21
3.1 Biophysical environment	21
3.2 Socio-economic profile	22
4 Methodology and data used	29
4.1 Impacts of extreme events	29
4.1.1 Flood	29
4.1.2 Cyclone	32
4.1.3 Land cover mapping	33
4.2 Soil suitability assessment	34
4.2.1 Soil data collection	34
Allocation of sampling locations	34
Collection of soil samples	34
4.2.2 Soil data analysis	35
Soil texture	35
Soil pH and electric conductivity	38
Cation Exchange Capacity (CEC)	39
4.2.3 Spatial interpolation of soil properties	40
4.2.4 Suitability assessment	41
4.3 Assessment of crop water requirements	41
4.3.1 Climate data preparation	41
4.3.2 Agro-climatic zone and hydrological regime	44
4.3.3 Assessment of crop water needs and the effects of climate change on agriculture	44
5 Results and Discussion	45
5.1 Impacts of extreme events	45

<i>Contents</i>	v
5.2 Soil analysis	52
5.2.1 Soil data and ratings	52
5.2.2 Soil suitability	61
5.3 Water requirement and yield response to climate change	61
5.3.1 Paddy	62
5.3.2 Wheat	62
5.3.3 Black and green grams	63
5.3.4 Groundnut	63
5.4 Decadal occurrences of dry spells	68
6 Conclusion and recommendations	88
References	91
A Land cover legend–class diagram	109
B The path taken while collecting soil samples	113

List of Figures

2.1	A comparison of the temperature rise predicted by models and that which has actually been seen since the beginning of the twentieth century [source: (Change et al., 2006)]	7
2.2	The cascading pyramid of uncertainties in the assessment emission problem [source: Schneider (1983)]	8
2.3	connections between climate system's elements, general circulation model [source: Karl and Trenberth (2003)]	9
2.4	Emission scenarios (source: IPCC (2001))	12
2.5	The increase in average global temperature under different RCP scenarios [source: IPCC (2013)]	13
2.6	Impact of elevated CO ₂ on photosynthesis [source: Lemon (2019)] . .	15
2.7	Crop soil suitability modelling based on different knowledge systems and scale of analysis [Source: Bouma (1999)]	17
2.8	The main components of the soil-plant-atmosphere continuum in Aquacrop [source: Steduto et al. (2009)]	18
3.1	Study area	23
3.2	Geological map of the delta [after Mahalik (1984)]	24
3.3	rainfall temperature graph	25
3.4	Decadal population growth in the delta	26
3.5	Crop calendar of major crops in the delta	26
3.6	Geomorphology of the study area	27
3.7	Land cover of the delta	27
4.1	Graphical representation of the liner decay function used to estimate the surge height and inundation extent	32

4.2	Phases of the random forest classification model: samples, variables, probabilities, classes, data, tree counts, and input data are indicated by the letters i, j, p, c, s, t, and d, respectively. [Source: Belgiu and Drăguț (2016)]	33
4.3	Distribution of soil sampling locations	35
4.4	Route map used to visit the sampling locations	36
4.5	Experimental and fitted variogram for the pH samples	40
4.6	Comparisons of different climate models [source: Janes and Macadam (2017)]	42
5.1	Extent of inundated areas at various return periods	47
5.2	Flood risk map of the delta	48
5.3	Inundation due to storm surge	49
5.4	Gust wind of storms at various return periods	50
5.5	Wind profile of storm at various return period at Paradeep and Puri .	50
5.6	Wind risk map of the delta	51
5.7	Effects of extreme climatic events on Kharif rice production in Odisha	51
5.8	Spatial distribution of soil pH in the study area	53
5.9	Spatial distribution of soil electric conductivity (salinity $\mu\text{S}/\text{cm}$) in the study area	54
5.10	Spatial distribution of soil potassium in the study area	55
5.11	Spatial distribution of soil drainage class in the study area	56
5.12	Spatial distribution of soil calcium in the study area	57
5.13	Spatial distribution of soil magnesium in the study area	58
5.14	Spatial distribution of soil sodium in the study area	59
5.15	Spatial distribution of proportion of silt (%) in the study area	60
5.16	Spatial distribution of proportion of clay (%) in the study area	60
5.17	Spatial distribution of multi-crop suitability in the study area	61
5.18	Average annual rainfall distribution in the study area, a) historical, b)2020s, c) 2050s, d) 2080s	63
5.19	Average mean temperature distribution in the study area, a) historical, b)2020s, c) 2050s, d) 2080s	64
5.20	Average reference evapotranspiration distribution in the study area, a) historical, b)2020s, c) 2050s, d) 2080s	64

5.21	Yield response and irrigation requirement for the paddy in the baseline and future scenarios	65
5.22	Yield response and irrigation requirement for the wheat in the baseline and future scenarios	66
5.23	Yield response and irrigation requirement for black and green grams in the baseline and future scenarios	67
5.24	Yield response and irrigation requirement for potato in the baseline and future scenarios	68
5.25	Variations in flood timing trends across the Mahanadi basin [Source: Ganguli et al. (2022)]	69
5.26	Predicted longest dry spell days from 2021 to 2030 for the RCP 4.5 emission scenario using CNRM's CM5 model	70
5.27	Predicted average dry spell days from 2021 to 2030 for RCP 4.5 emission scenario using CNRM's CM5 model	71
5.28	Predicted longest dry spell days from 2021 to 2030 for RCP 8.5 emission scenario using CNRM's CM5 model	72
5.29	Predicted average dry spell days from 2021 to 2030 for RCP 8.5 emission scenario using CNRM's CM5 model	73
5.30	Predicted longest dry spell days from 2031 to 2040 for RCP 4.5 emission scenario using CNRM's CM5 model	74
5.31	Predicted average dry spell days from 2031 to 2040 for RCP 4.5 emission scenario using CNRM's CM5 model	74
5.32	Predicted longest dry spell days from 2031 to 2040 for RCP 8.5 emission scenario using CNRM's CM5 model	75
5.33	Predicted average dry spell days from 2031 to 2040 for RCP 8.5 emission scenario using CNRM's CM5 model	75
5.34	Predicted longest dry spell days from 2041 to 2050 for RCP 4.5 emission scenario using CNRM's CM5 model	76
5.35	Predicted average dry spell days from 2041 to 2050 for RCP 4.5 emission scenario using CNRM's CM5 model	76
5.36	Predicted longest dry spell days from 2041 to 2050 for RCP 8.5 emission scenario using CNRM's CM5 model	77

5.37	predicted average dry spell days from 2041 to 2050 for RCP 8.5 emission scenario using CNRM's CM5 model	77
5.38	Predicted longest dry spell days from 2051 to 2060 for RCP 4.5 emission scenario using CNRM's CM5 model	78
5.39	Predicted average dry spell days from 2051 to 2060 for RCP 4.5 emission scenario using CNRM's CM5 model	78
5.40	Predicted longest dry spell days from 2051 to 2060 for RCP 8.5 emission scenario using CNRM's CM5 model	79
5.41	Predicted average dry spell days from 2051 to 2060 for RCP 8.5 emission scenario using CNRM's CM5 model	79
5.42	Predicted longest dry spell days from 2061 to 2070 for RCP 4.5 emission scenario using CNRM's CM5 model	80
5.43	Predicted average dry spell days from 2061 to 2070 for RCP 4.5 emission scenario using CNRM's CM5 model	80
5.44	Predicted longest dry spell days from 2061 to 2070 for RCP 8.5 emission scenario using CNRM's CM5 model	81
5.45	Predicted average dry spell days from 2061 to 2070 for RCP 8.5 emission scenario using CNRM's CM5 model	81
5.46	Predicted longest dry spell days from 2071 to 2080 for RCP 4.5 emission scenario using CNRM's CM5 model	82
5.47	Predicted average dry spell days from 2071 to 2080 for RCP 4.5 emission scenario using CNRM's CM5 model	82
5.48	Predicted longest dry spell days from 2071 to 2080 for RCP 8.5 emission scenario using CNRM's CM5 model	83
5.49	Predicted average dry spell days from 2071 to 2080 for RCP 8.5 emission scenario using CNRM's CM5 model	83
5.50	Predicted longest dry spell days from 2081 to 2090 for RCP 4.5 emission scenario using CNRM's CM5 model	84
5.51	Predicted average dry spell days from 2081 to 2090 for RCP 4.5 emission scenario using CNRM's CM5 model	84
5.52	Predicted longest dry spell days from 2081 to 2090 for RCP 8.5 emission scenario using CNRM's CM5 model	85

5.53	Predicted average dry spell days from 2081 to 2090 for RCP 8.5 emission scenario using CNRM's CM5 model	85
5.54	Predicted longest dry spell days from 2091 to 2100 for RCP 4.5 emission scenario using CNRM's CM5 model	86
5.55	Predicted average dry spell days from 2091 to 2100 for RCP 4.5 emission scenario using CNRM's CM5 model	86
5.56	Predicted longest dry spell days from 2091 to 2100 for RCP 8.5 emission scenario using CNRM's CM5 model	87
5.57	Predicted average dry spell days from 2091 to 2100 for RCP 8.5 emission scenario using CNRM's CM5 model	87
6.1	Crop choice model based on the value of economic activity by Auffhammer (2018). The best crops are those with thick curves based on the value of economic activity.	90
A.1	Aquaculture	109
A.2	Bareland	109
A.3	Mono cropland	110
A.4	Double cropland	110
A.5	Tripple cropland	110
A.6	Forest plantation	110
A.7	River and stream class diagram	110
A.8	Forest	110
A.9	Rural settlement	111
A.10	Urban settlement	111
A.11	Scrub land	111
A.12	Sandy area	111
A.13	Mangrove	112
A.14	Wetland	112
A.15	Water body	112
B.1	Trip details for soil sample collection on 03/04/2018: travelled 203 kilometres and visited Bhubaneswar–Chandaka–Ranpur–Khordha . .	113
B.2	Trip details for soil sample collection on 04/04/2018: travelled 313 kilometres and visited Bhubaneswar–Rambha–Banpur–Khordha . .	114

B.3	Trip details for soil sample collection on 05/04/2018: travelled 268 kilometres and visited Bhubaneswar–Salipur–Paradeep–Tritol	115
B.4	Trip details for soil sample collection on 06/04/2018: travelled 206 kilometres and visited Bhubaneswar–Salipur–Tritol–Jagatsinghpur .	115
B.5	Trip details for soil sample collection on 07/04/2018: travelled 260 kilometres and visited Bhubaneswar–Paradeep–Nuagaon–Niali	116
B.6	Trip details for soil sample collection on 08/04/2018: travelled 180 kilometres and visited Bhubaneswar–Niali–Kakatpur–Nimapada . . .	116
B.7	Trip details for soil sample collection on 09/04/2018: travelled 194 kilometres and visited Bhubaneswar–Gop–Konark–Sakhigopal–Delang	117
B.8	Trip details for soil sample collection on 11/04/2018: travelled 241 kilometres and visited Bhubaneswar–Puri–Satapada–Sakhigopal . . .	117
B.9	Trip details for soil sample collection on 12/04/2018: travelled 264 kilometres and visited Bhubaneswar–Cuttack–Naraj–Banki–Kalapathar–Baghmari– Khordha	118

List of Tables

2.1	A list of general circulation models [source: Suppiah et al. (2007)] . . .	10
2.2	Increase in global mean temperature by RCPs [source: IPCC (2013)] .	13
3.1	Cultivated area of different crops in the delta in 2011 [source: Govt. of Odisha (2011a,e,d,c,b)]	25
3.2	Demographic profile of the study area [source: Govt. of India (2011)]	28
4.1	A list of flood events that were mapped using SAR data	30
4.2	Comparisons of average total annual precipitation (mm) from different models	43
4.3	Comparisons of average mean annual temperature (°C) from different models	43
4.4	Comparisons of total days per year with rainfall>1mm from different models	43
4.5	Comparisons of Average annual reference potential evapotranspiration (mm/m) from different models	43
4.6	Lookup table to convert De Martonne Aridity index values to climate type	44
5.1	Block wise flood affected population at various return period	46
5.2	Suitability rating for nutrient retention capacity based on the cation exchange capacity (cmol/kg) [after Fischer et al. (2021)]	52
5.3	Suitability rating based on the exchangeable sodium percentage - ESP (%) [after Fischer et al. (2021)]	53
5.4	Suitability rating based on electric conductivity (dS/m), presence of salinity [after Fischer et al. (2021)]	54

5.5	Suitability rating based on soil depth (cm) [after Fischer et al. (2021)]	55
5.6	Suitability rating based total exchangeable bases (cmol/kg) [after Fischer et al. (2021)]	56
5.7	Suitability rating based soil pH [after Fischer et al. (2021)]	57
5.8	Suitability rating based on soil texture class [after Fischer et al. (2021)]	58
5.9	Suitability rating based on soil drainage [after Fischer et al. (2021)] . .	59
5.10	Areal distribution of suitability categories in the study area	62

Executive Summary

Chapter 1: The founding of the IPCC in 1990 made it evident that climate change is a genuine problem that must be tackled in order to the planet sustainable. The manifestations of climate change and global warming are becoming prominent and disastrous. The hydrological and climatological systems are being modified by the growing global mean temperature. These factors influence the availability of water and the hydrological regime. These are the most influential elements on cropping patterns and techniques. Extreme climate events, such as tropical cyclones, floods, and storm surges, pose challenges for the agriculture sector and are difficult to manage.

Agriculture and livelihood in the Delta region are threatened by climate change. In the future decades, sea level rise will be one of the several issues that deltas will face. The objective of this study was to assess the effects of climate change on agricultural practises in the Mahanadi Delta.

Chapter 2: The presence of greenhouse gases is essential for preserving the equilibrium of the global temperature. Since the industrial revolution, however, the concentration of greenhouse gases has risen to an alarming level. Understanding the state of greenhouse gases in the atmosphere is essential for the research of climate change consequences. Climate projections are methods for projecting future situations and the related radiative forcing. There are a range of climate models available to meet various global and local objectives. In its fifth reassessment report, the IPCC introduced four typical concentration paths as four distinct climatic scenarios. RCP 2.6 represents the least amount of warming, whereas RCP 8.5 represents the most amount of warming.

Changes in the hydrological regime or climate as a whole affect the agricultural system in a variety of ways, apart from climatological dangers. For instance,

greater CO₂ enhances biomass output, higher temperatures accelerate crop maturation, and heat stress occurs during the flow and maturation phases, etc.

A crop model includes functions for simulating the development and yield of crops. There are a variety of growth simulation models available to handle various problems. Aquacrop is a model that simulates crop growth and calculates optimal yield and water needs.

There are several research on the implications of climate change on the behaviour of the Mahanadi Delta, but relatively few on the effects on agricultural production.

Chapter 3: Three rivers combine to form the Mahanadi delta: the Mahanadi, Bramhini, and Baitarini. The study area is comprised of the five administrative districts with an elevation zone lower than 5 metres. In the past, the Delta has experienced numerous climate change-related problems. These days, floods and cyclones are common occurrences. In the heavily populated delta, with an estimated population of 8 million, there is a constant risk of flooding. Agriculture is the primary source of income in the rural areas of the delta. The primary crop in the delta is rice. Other essential crops include oil seeds, cereals, peanuts, etc.

Chapter 4: To study of the effects of flooding in the delta, SAR data was utilised to create flood maps, while IMD rainfall data was used to study the return period. Using flood maps for a variety of return periods, the risk of flooding was calculated. The TCRM model was used to simulate the wind behaviour, which resulted in cyclone-related risk in the Delta. The LISS IV images were used to create a land cover map for the agricultural land damage assessment. In addition, storm surge effects on crops were modelled. A total of 72 soil samples were gathered from the delta region in order to determine the appropriateness of the region's soil for agriculture. To create the spatial distribution of soil attributes, the soil data were interpolated. The CNRM-CM5 model was chosen to obtain climate projection data. The Aquacrop crop model was used to evaluate crop water requirements using downscaled data for two RCPs (4.5 and 8.5).

Chapter 5: In the Mahanadi delta, flooding is one of the most common extreme phenomena. As the delta is heavily populated with a large number of agrarians, the livelihood is threaten in the flood affected the administrative blocks of the Kendapara and Bhadrak districts. Due to the low, flat topography in the northern

half of the delta, storm surge flooding is a typical occurrence in the delta during cyclones. The most frequent destructive force in the Mahanadi Delta is cyclone wind. During the 100-year return period, the wind gusts reach approximately 50 metres per second, which is catastrophic in nature. Several destructive cyclones have struck Mahanadi throughout the last century, primarily in September and November. The northern portion of the delta is susceptible to nearly all extreme occurrences, including floods, storm surge, high cyclonic wind speeds, and significant precipitation.

The delta is suited for growing a variety of crops. The bulk of marginal and unsuitable sites are situated around the coastline because to the excessive salt in these regions. A small parcel of moderately suitable land is located in the vicinity of the Khoorda region. Poor drainage conditions exist in this area. In the entire delta, rice is the most frequent crop, especially during the Kharif season. Some double and triple-cropping cropland are utilised for paddy cultivation. In the RCP 8.5 the yield rate fluctuation is greater in the 2080s. After 2040, the variability of irrigation requirement increases, and the variability of yield rate increases under RCP8.5. In this region's leftover moisture, black and green grams are cultivated. During the Rabi season, the delta produces a substantial amount of black and green gram. RCP4.5 predicts a higher yield rate in the distant future, notably after 2040. Length of dry periods is one of the most important criteria for the kharif harvest. In all studied decades, a maximum dry period of 13 days has occurred on average.

Chapter 6: Climate change is becoming increasingly dangerous, and its manifestations and consequences are becoming more catastrophic. Even the general population is becoming increasingly aware of the effects of climate change on the various precipitation and temperature patterns and expressions. Due to rising sea levels and a rise in the frequency of cyclones, climate change poses a huge threat to the world's low-lying coastal regions, such as the main deltas. The Mahanadi Delta is a large delta on India's eastern coast that confronts similar challenges. The majority of the delta is suitable for all major crops. Variations in temperature and precipitation can, however, reduce the yield and production of existing crop kinds. Adopting alternate crops is a commonly suggested adaptation method for dealing with climate change and variability. Suitable crop rotation and cropping

patterns can be implemented in response to anticipated climate change. However, food preferences and nutritional patterns are crucial considerations when proposing a substitute crop.

Abbreviations and acronyms

AgMIP	Agricultural Model Inter-comparison and Improvement Project
APSIM	Agricultural Production Systems Simulator
CEC	Cation Exchange Capacity
CNRM	National Centre for Meteorological Research
CTI	Compound topographic index
DEM	Digital elevation model
DSSAT	Decision Support System for Agro-Technology Transfer Model
FAO	Food and Agriculture Organization
GCM	General Circulation Model
GEV	Generalised extreme value
IBTrACS	International Best Track Archive for Climate Stewardship
IMD	India Meteorological Department
IPCC	Intergovernmental Panel on Climate Change
ISRO	Indian Space Research Organisation
IRS	India Remote Sensing Satellite
LISS IV	Linear Imaging Self-Scanning Sensor - 4
LST	Land surface temperature
NARDL	Non-linear autoregressive distributed lag
NDVI	Normalized difference vegetation index
NRSC	National Remote Sensing Centre
RCP	Representative Concentration Pathway
RCM	Regional Climate Model
SAR	Synthetic Aperture Radar
TCRM	Tropical Cyclone Risk Model

Introduction

“একখানি ছোট ক্ষেত আমি একেলা,
চারিদিকে বাঁকা জল করিছে খেলা।
পরপারে দেখি আঁকা
তরুছায়ামসীমাখা
গ্রামখানি মেঘে ঢাকা
প্রভাত বেলা -- ”

সোনার তরী - রবীন্দ্রনাথ ঠাকুর

The metaphor in the epigraph portrays the agony of a marginal farmer surrounded by swirling water around his small cropland. As the natural course to keep a rhythmic climate is ‘*styled*’, the experience is shared by the agricultural system as a whole. The climate system that surrounds our very lives is changing. Seemingly, the change is capricious. So, the issue of climate change has sought much attention in recent decades on its causes and consequences to find possible solutions, including adaptive and mitigation measures.

1.1 Climate change and agriculture

Upon the inception of the IPCC in 1990, it was clear that the concentrations of CO₂ are rising and so are the temperatures (IPCC, 2007). Climate change and global warming are unequivocal, and a mountain of studies confirm that the impacts are very real (IPCC, 2013). It will continue to rise if no proper actions are taken to curb the greenhouse gas emissions (IPCC, 2021). The rising global mean temperature leads to subsequent hydrological and climatological changes. These changes affect the availability of water and surface run-off and thus may affect

the hydrological regimes (Middelkoop et al., 2001). Plans for managing water resources are increasingly required to consider the consequences of climate change into account in order to accurately estimate future water availability (Wurbs et al., 2005). On the other hand, frequency of extreme climatic events like flood, cyclone, drought, heat wave are increasing in the warming globe (Rahmstorf and Coumou, 2011). These events pose different challenges on the agricultural sectors and are very complex to address (Cogato et al., 2019; Motha, 2011).

The climatic variabilities, especially the extreme events, have been a dilemma for farmers since the inception of agriculture in the fertile earth some millions years ago. Agricultural system is sensitive to climate change as well as a driver for climate change (Prasada et al., 2010). Climate change brings changes in the agro-ecological conditions (Allen et al., 1987) Therefore, variability in temperature, precipitation and soil moisture may act synergistic or antagonistically in determining the optimal temperature and water requirements for biomass production and growth (Karl et al., 2009). Cropping pattern and techniques rely on the availability of water resources, which is the single most critical factor in determining the survival and sustainability of agricultural systems. (Zingaro et al., 2017). The changes and variability of precipitation may affected the sustainability of such cropping practices (Amini Fasakhodi et al., 2010).

1.2 Changes in the climate and agriculture in the deltas

Deltas are formed by alluvial deposits at the edge of a standing body of water and carried downstream by a river near its mouth (Coleman, 1981). River deltas have been attractive for living since the inception of civilization due to the availability of fertile land, access to fishing, and the possibility to construct ports and harbours for trade and business. Hence, river deltas are more populated than the rest of the landscape. An estimated average population density in the deltas is around 500 persons per square kilometre compared to the world population density of 44.7 persons per square kilometre (Kuenzer and Renaud, 2012; UN, 2007).

Deltas are sensitive to climate change and the hydrological cycle. The changes in climate and subsequent hydrological changes could threaten the agriculture

and livelihoods of the communities (Tuan and Chinvanno, 2011). Because of its low elevation and open coastline, the delta region is particularly vulnerable to the effects of rising sea level.

The most likely climate-related changes to be seen throughout the 21st century include a rising sea levels, an overall increase in sea surface temperature, and climate change-induced extreme weather conditions like heavy precipitation cyclones and storm surges. The worldwide average sea level has climbed by about 20 centimetres since 1870. Between 1963 and 2003, the average annual amount of sea level rise was reported to be 1.8 millimetres (mm), while the rate reported for the period between 1993 and 2003 was 3.1 mm/year, a significant increase (IPCC, 2007). This could result in a 50% increase in delta surface areas that are vulnerable to coastal flooding. At deltas these changes are expected to have a range of physical, economic and social impacts (IPCC, 2013, 2007; Solomon et al., 2007). Natural resource and people of the deltas are now facing consequences of the increased human interference on climate system (Nicholls et al., 1999). The agricultural sector is one of the most significant of these (IPCC, 2007).

1.3 Objectives

Assessing the impact of climate change on cropping patterns in the Mahanadi Delta was the purpose of the study, which aimed to accomplish the following objectives in the process:

- To evaluate the effects that extreme events have had on the agricultural sector in the delta,
- To analyse the suitability of land for the major crops in the delta,
- To integrate water resource management and soil suitability for the feasibility of optimal cropping pattern under different climate scenarios in the delta.

1.4 Problem Statement

The dawn of the third millennium is attributed by human induced large scale changes in the earth's environments. It includes alteration of climate, land use and its productivity, atmospheric chemistry, water resources, and ecosystems, which may affect the sustainability of the earth (Eissa and Zaki, 2011). Among these, changing climate ranks high. Crop distribution, like natural vegetation, is well established to be heavily influenced by climate and soil (Cramer and Lee-mans, 1993). Deltas are suitable for crop production because of the availability of alluvial sediment. On the other hand, deltas are more vulnerable due to their proximity to the sea. Because of climate change and its severe manifestations, the Mahanadi Delta, one of the most major deltas in eastern India, is experiencing a number of negative impacts, including recurring crop losses. The development of adaptation mechanisms to mitigate and control the effects of climate change in the deltas relies on a thorough understanding of those effects. However, regional or local analyses are necessary to comprehend the implications in a regional context and make recommendations based on the findings.

1.5 Research hypothesis

The main hypothesis are:

1. The Mahanadi Delta, which is mostly an agricultural delta, is being negatively impacted by climate change in a number of ways that are having an effect on farming.
2. Changing climates and extreme events are putting great stress on crop production in the Delta.
3. Changing hydrological regimes as a result of climate change have negatively affected crop productivity in the delta.

1.6 Organizational scheme for the thesis

These are the chapters that make up the organisation of the thesis:

The 1st chapter provides an overview of the study as well as an explanation of the problem statement.

A summary of the previous researches and literatures that were reviewed for this study can be found in Chapter 2.

The climate, topography, socio-economic, and agricultural profiles of the study area are detailed in Chapter 3, along with other general descriptions of the study area.

In the 4th chapter, there is a discussion of the research methods that were applied in this study.

The results of the study as well as a pertinent discussion on the effects that climate change and extreme events have had on cropping systems are presented in Chapter 5.

The conclusion as well as any recommendations are presented in Chapter 6.

Literature review

2.1 Introduction

The presence of the greenhouse effect is what enables life to exist on earth (Selsis, F. et al., 2007). However, a continuous increase in the amount of greenhouse gases makes the climate out of tune, which is commonly referred to as “climate change” (Mitchell, 1989; Mikhaylov et al., 2020). In addition to land cover transitions and shifts in land use, one of the primary contributors to such change is the alteration of atmospheric composition that have been caused by anthropogenic activities (Karl and Trenberth, 2003). Clearly, the worldwide mean surface temperature has increased since the beginning of the Industrial Revolution (Change et al., 2006). As indicated in Fig. 2.1, the temperature has risen considerably from the beginning of the twentieth century.

The change in climatic behaviour is becoming a routine occurrence with far-reaching repercussions, ranging from the modification of agro-climatic zones to the disturbance of socio-economic balances., in spite of the significant uncertainty involved in the rate of change (IPCC, 2007). The implication is not homogeneous in all the regions. For instance, locations in the tropics are more susceptible to the effects of climate change than high-latitude regions in the northern hemisphere, which are less susceptible to the effects of climate change than regions in the tropical zones (Ramankutty et al., 2002). Because of the effects of climate change, agriculture is one of the most susceptible sector. A number of studies have been carried out in an effort to assess or quantify the effects that climate change will have on the agricultural sector. The following sections summarise some of the aspects of climate change related to agricultural sectors.

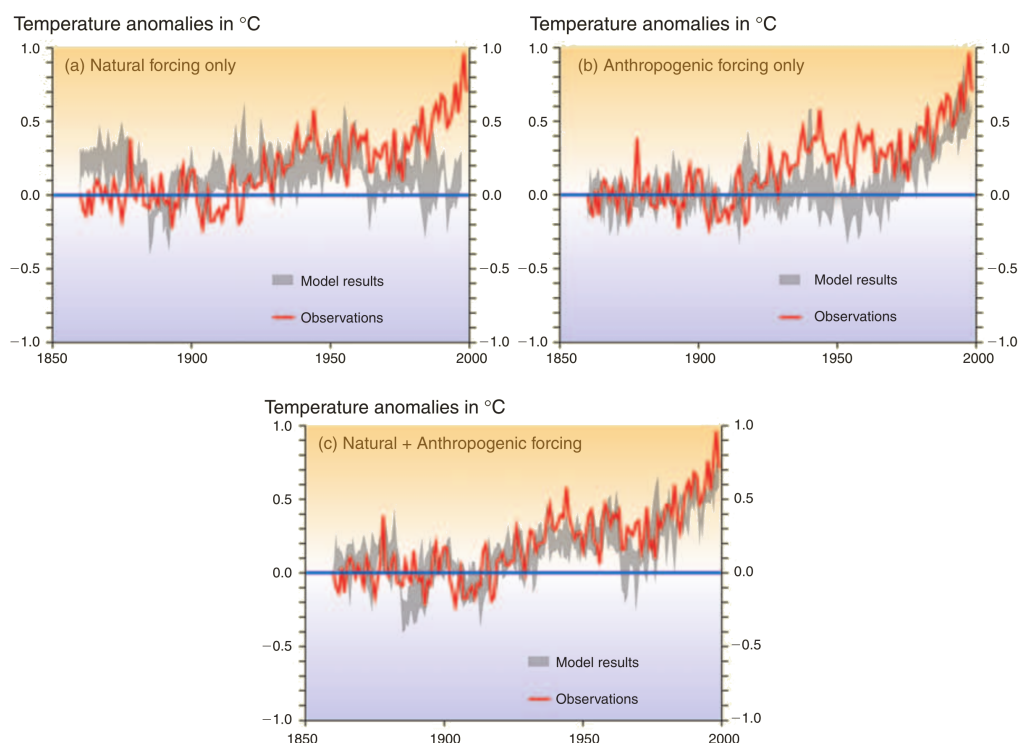


Figure 2.1: A comparison of the temperature rise predicted by models and that which has actually been seen since the beginning of the twentieth century [source: (Change et al., 2006)]

2.2 Climate projections

Data on what the future is expected to hold are required in order to conduct an assessment of the potential implications of climate change. There is a great deal of unpredictability around the emissions, the responses of the carbon cycle, and the developments in socio-economic conditions due to the probability and their manifestations (Fig. 2.2).

Climate projection is one of the most important tools for predicting the effects of future climates when all uncertainties are considered. It provides a reasonable description of the future climate scenarios for probable future conditions (IPCC, 2007).

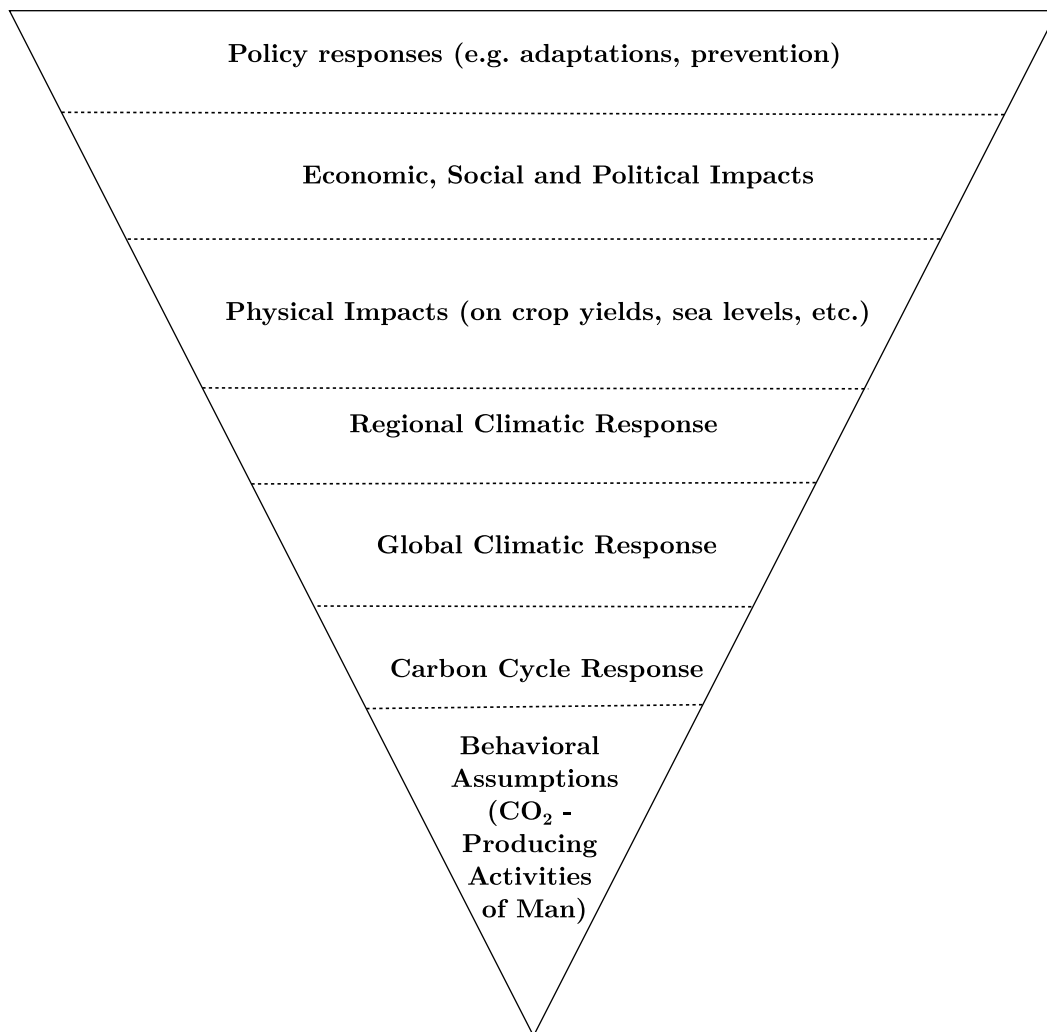


Figure 2.2: The cascading pyramid of uncertainties in the assessment emission problem [source: [Schneider \(1983\)](#)]

2.2.1 Climate models

A climate model is a mathematical representation in three dimensions of many climatological variables and how they interact, as well as many assumptions and flows through the earth's atmosphere, land, ocean, and sea ice (Fig. 2.3). There are two types of climate models: (i) the global climate model (abbreviated as GCM), which is the coarser resolution model for representing the entire globe, and (ii) the regional climate model (abbreviated as RCM), which reflects regional or local

behaviour at a finer, more detailed resolution ([Teutschbein and Seibert, 2010](#)).

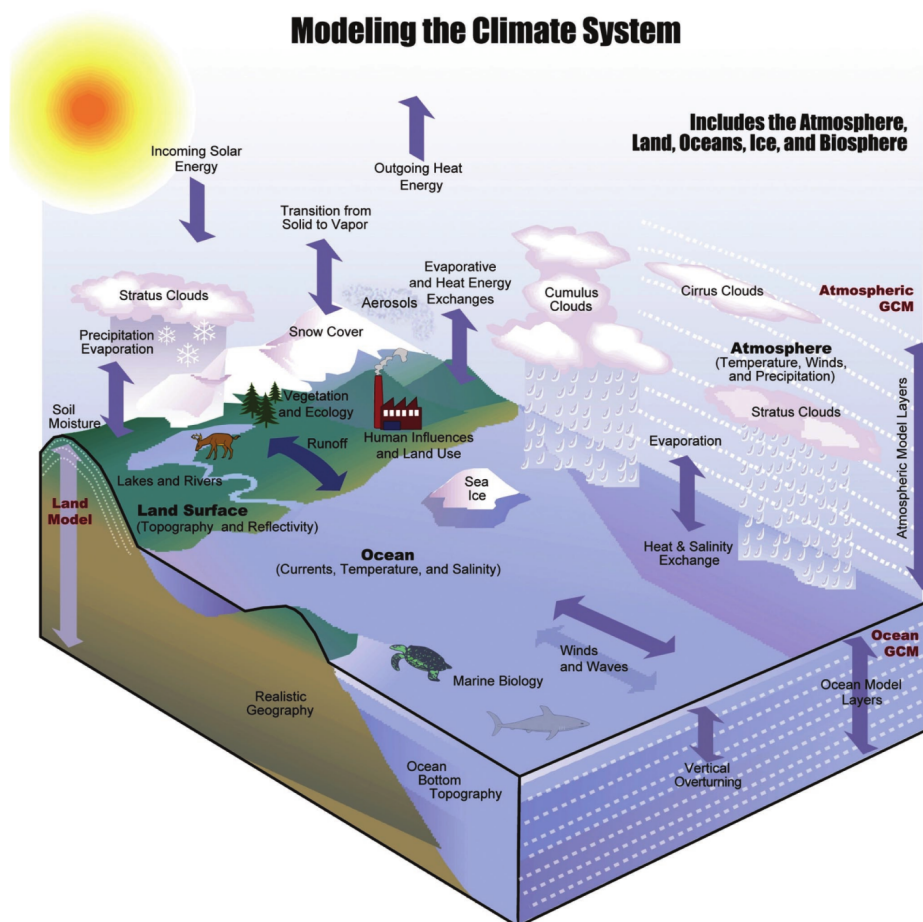


Figure 2.3: connections between climate system's elements, general circulation model [source: [Karl and Trenberth \(2003\)](#)]

Climate models are great instruments for predicting hydrological regimes and agricultural growth for various climate scenarios in order to gain a deeper understanding of the effects of abrupt changes in climate ([IPCC, 2007](#)). There are several different GCMs and RCMs that can be utilised ([Cotton and Pielke Sr, 2007](#)). A list of popular GCM models is given in Table 2.1

Table 2.1: A list of general circulation models [source: [Suppiah et al. \(2007\)](#)]

Model	Institutions	Resolution [°]	time span
BCC-CM1	Beijing Climate Center	1.9 × 1.9	1871–2100
BCCR-BCM2.0	Bjerknes Center for Climate Research	1.9 × 1.9	1850–2099
CCSM3	National Center for Atmospheric Research	1.4 × 1.4	1870–2099
CCCM3.1(T 47)	Canadian Center for Climate Modelling & Analysis	2.8×2.8	1850–2100
CCCM3.1(T 63)	Canadian Center for Climate Modelling & Analysis	1.9 × 1.9	1850–2100
CNRM-CM3	Météo-France/Centre National de Recherches Météorologiques	1.9 × 1.9	1860–2090
CSIRO-Mk3.0	CSIRO Atmospheric Research	1.9 × 1.9	1871–2100
ECHAM5/MPI-OM	Max Planck Institute for Meteorology	1.9 × 1.9	1860–2100
ECHO-G	Meteorological Institute of the University of Bonn, Meteorological Research Institute of KMA, and Model	3.9 × 3.9	1860–2100
FGOALS-g1.0	LASG/Institute of Atmospheric Physics	2.8 × 2.8	1850–2099
GFDL-CM2.0	US Dept. of Commerce/NOAA/-Geophysical Fluid Dynamics Laboratory	2.0 × 2.5	1861–2100
GFDL-CM2.1	US Dept. of Commerce/NOAA/-Geophysical Fluid Dynamics Laboratory	2.0 × 2.5	1861–2100
GISS-AOM	NASA/Goddard Institute for Space Studies	3.0 × 4.0	1850–2100
GISS-EH	NASA/Goddard Institute for Space Studies	4.0 × 5.0	1880–2099
GISS-ER	NASA/Goddard Institute for Space Studies	4.0 × 5.0	1880–2100
INM-CM3.0	Institute for Numerical Mathematics	4.0 × 5.0	1871–2100
IPSL-CM4	Institut Pierre Simon Laplace	2.5 × 3.75	1860–2100
MIROC3.2 (hires)	Center for Climate System Research	1.12 × 1.12	1900–2100
MIROC3.2 (medres)	Center for Climate System Research	2.8 × 2.8	1850–2100
MRI-CGCM2.3.2	Meteorological Research Institute	2.8 × 2.8	1851–2100
PCM	National Center for Atmospheric Research	2.8 × 2.8	1890–2099
UKMO-HadCM3	Hadley Center for Climate Prediction and Research/Met Office	2.5 × 3.75	1860–2099
UKMO-HadGEM1	Hadley Center for Climate Prediction and Research/Met Office	1.25 × 1.9	1860–2098

2.2.2 Projection scenarios

The use of climate scenarios allows researchers to study the potential consequences of anthropogenic climate change for a variety of alternative futures. The IPCC issued a report titled “Special Report on Emission Scenarios” (SRES) in 2000 to categorise all plausible scenarios into seven groupings. (Nakicenovic, 2000). Fig.2.4 concisely portrays all the possible future scenarios.

The IPCC Fifth Assessment Report (AR5) introduced a new mechanism for categorising different scenarios: the Representative Concentration Pathway (abbreviated as RCP) (IPCC, 2013). Four RCPs were explored based on greenhouse gas concentrations. Each RCP forecasts a distinct future climate based on the amount of greenhouse gases (GHG) generated in the coming years (Fig. 2.5). The scenarios are named after the maximum amount of radiative forcing (W/m^2) they represent: RCP-2.6, RCP-4.5, RCP-6 and RCP-8.5 (IPCC, 2013). The average global temperature is expected to rise in the 21st century (Table 2.2). The A1FI scenario in SRES is equivalent to a RCP8.5, and the B1 scenario in SRES is equivalent to a RCP4.5 (Rogelj et al., 2012).

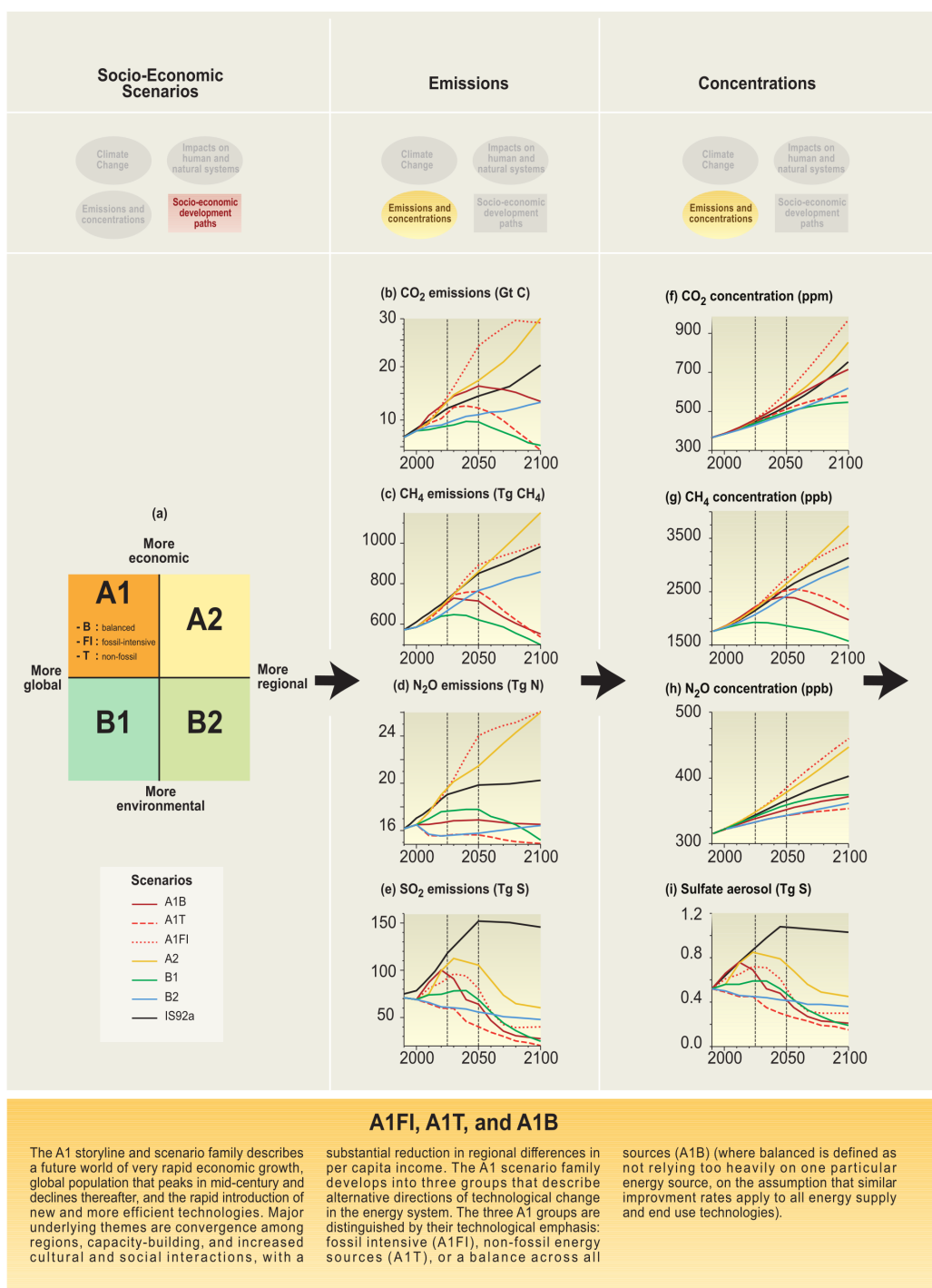


Figure 2.4: Emission scenarios (source: IPCC (2001))

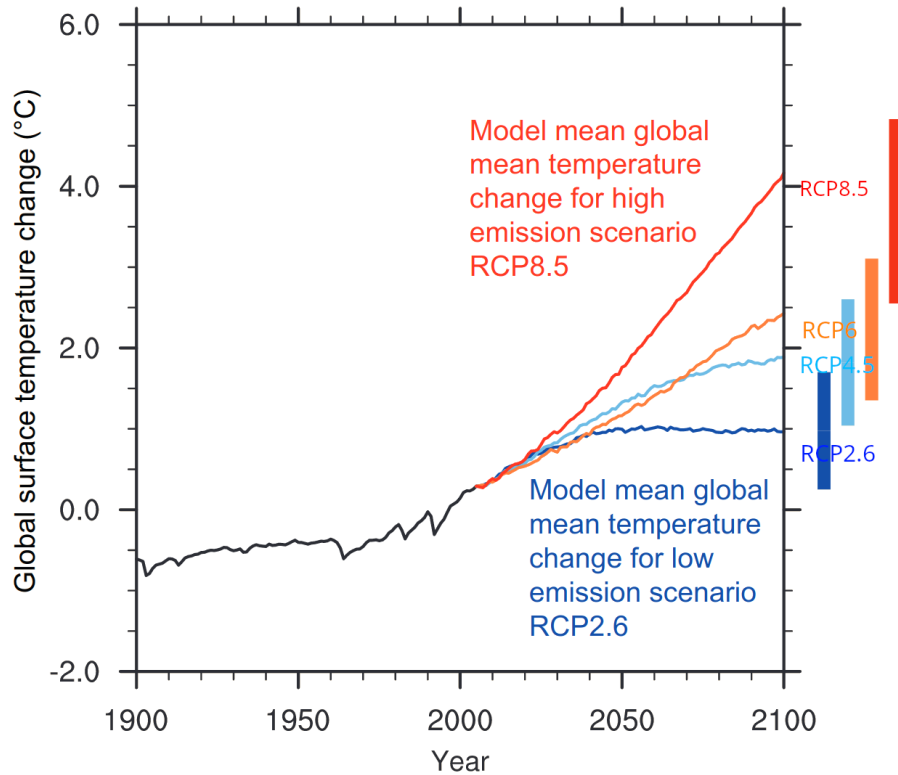


Figure 2.5: The increase in average global temperature under different RCP scenarios [source: IPCC (2013)]

Table 2.2: Increase in global mean temperature by RCPs [source: IPCC (2013)]

RCPs	2046–2065	2081–2100
	Mean [5–95% range]	Mean [5–95% range]
2.6	1.0 [0.4, 1.6]	1.0 [0.3, 1.7]
4.5	1.4 [0.9, 2.0]	1.8 [1.1, 2.6]
6	1.3 [0.8, 1.8]	2.2 [1.4, 3.1]
8.5	2.0 [1.4, 2.6]	3.7 [2.6, 4.8]

2.3 Changes in hydrological regime and climate and their impacts on agriculture

Climate change along with climate variability is influencing crop production year to year. IPCC (2007) listed the impacts of temperature on crop production. The

effects can be summed up briefly as follows:

- Elevated CO₂ level increases the biomass production.
- Higher temperatures accelerate the maturation of crops.
- Heat stress during flowering and reproduction.
- Increased climate variability, drought, and flooding may increase crop loss.

2.3.1 Impacts of elevated CO₂

Increase in CO₂ would be beneficial if no other climate related changes were not occurring (Parry, 1990). The photosynthetic rate can be increased by 30 to 100% with a doubling CO₂ concentration (IPCC, 2007). A typical response curve is given in Fig. 2.6 that shows the impact of increasing CO₂ on photosynthesis. Ortiz et al. (2008) predicted an increase in wheat production in the Indo-Gangetic plain for the 2050s. Therefore, it is beneficial for wheat production. Eitzinger et al. (2003) also predicted similar results. On contrary, Anwar et al. (2007) predicted a decrease in wheat production in Australia by 25% due to the elevated CO₂. Therefore, there are other factors that significantly influence yield.

2.3.2 Impacts of extreme events

Flood, cyclone and drought are the very common extreme weather events. Increasing and uncertainty of extreme weather events are common characteristics of climate scenarios (Frei et al., 2006). The impact of extremes event are complex in nature (Cogato et al., 2019). Drought and flood are most common disaster that damages the crops (Guo et al., 2019). These events sometimes create food security issues (Devereux, 2007).

2.3.3 Impacts of hydrological regime

Availability of water for crop production will be one of the limiting constraints in the agricultural sector (Fujihara et al., 2008). The changes in hydrological regimes will alter the agro-climatic zones, which may affect crop production and cropping

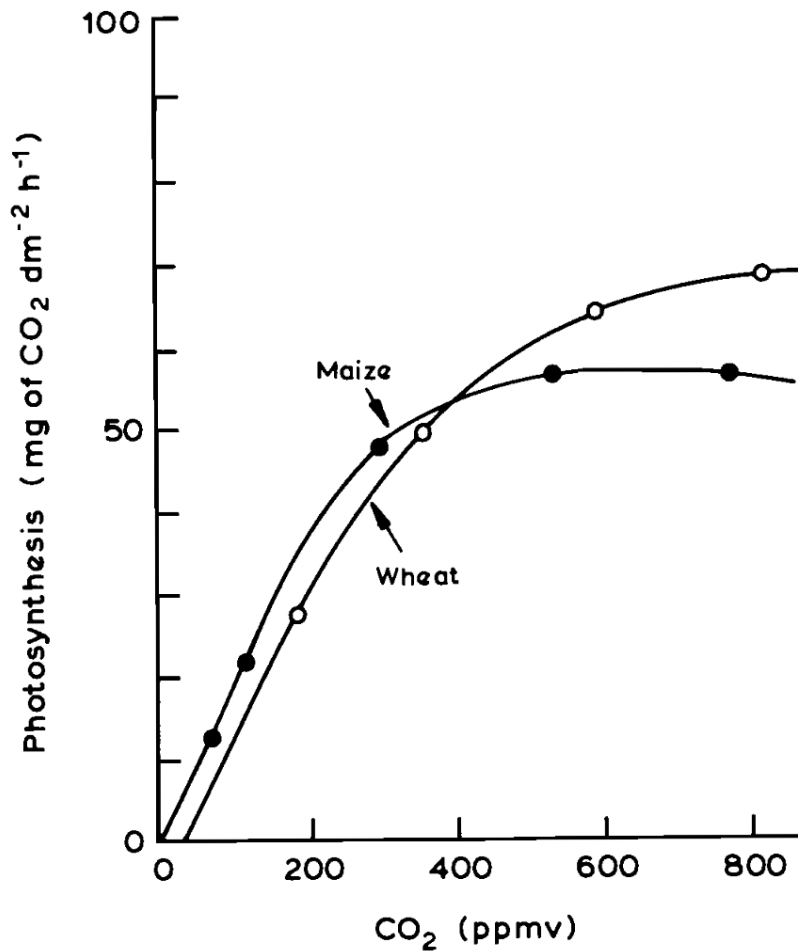


Figure 2.6: Impact of elevated CO₂ on photosynthesis [source: [Lemon \(2019\)](#)]

patterns ([Middelkoop et al., 2001](#)). The change in hydrological regimes may introduce new dry and wet spell characteristics that may affect the cropping pattern ([Mathew et al., 2021](#)).

2.4 Crop model

Crop models are used to estimate yield and quantify the effects of different variables. A crop model can provide helpful insights for lessening the adverse consequences of climate change and variability, which can be used to meet the challenges posed by these changes. ([Rosenzweig et al., 2014](#)). Over the years various crop model were introduced based different knowledge system and scales

(Fig. 2.7). The knowledge are divided into two axes, one ranging empirical to mechanical and other ranging from quantitative to qualitative. Bouma (1999) described the different knowledge system are as follows:

- K₁ = user knowledge;
- K₂ = expert knowledge;
- K₃ = knowledge that needs to be acquired through the use of semi-quantitative models;
- K₄ = knowledge obtained through the use of quantitative models with soil process are described in general terms; and
- k₅ = same as K₄ but process are described in details.

These knowledge can be integrated in soil model depending on the data availability and objectives. The land evaluation framework by FAO allows integration of these knowledge to prepare soil suitability for different crops (Verheye et al., 2009).

A crop model that deals with crop water requirements is based on the estimation of evapotranspiration of a crop. FAO defines “crop water requirement” as the demand for water that is required to compensate for the loss that occurs as a result of evapotranspiration, for it to be cultivated without any restrictions on the soil quality, including the amount of water and fertility in the soil, and for it to reach its full production potential within the context of a specific growing condition (Allen et al., 1998). Equation 2.1 is used solve the crop water requirements yield response of a crop.

$$ET_c = ET_o \times K_c, \quad (2.1)$$

where, K_c is the crop coefficient, and ET_c is the amount of evapotranspiration (in millimetres per day) that a crop produces and ET_o is the amount of reference crop evapotranspiration (in millimetres per day).

All the computer model for crop water requirements solve this equation in different ways. A short summery of the commons models used in crop are given below:

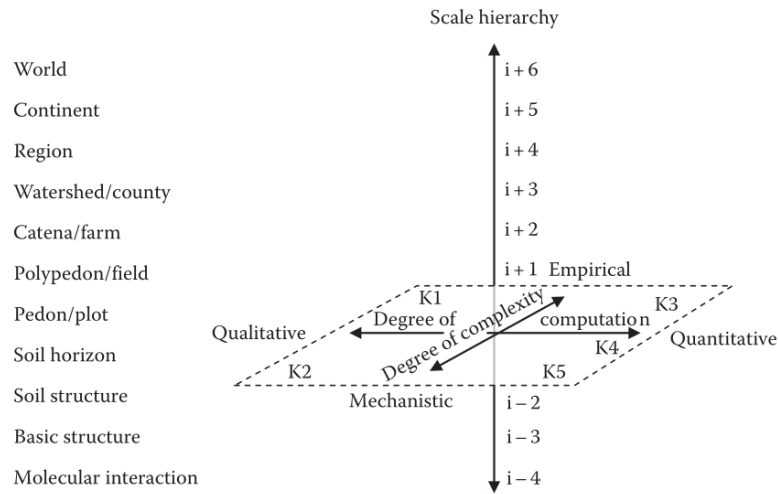


Figure 2.7: Crop soil suitability modelling based on different knowledge systems and scale of analysis [Source: Bouma (1999)]

AquaCrop was developed by Food and Agriculture Organization (Steduto et al., 2009). It is a crop water productivity model to improve water productivity in rain-fed and irrigated fields.

Doorenbos and Kassam (1979) provides the fundamental equation 2.2 to represent the relation of the yield response to water.

$$\left(\frac{Y_x - Y_a}{Y_x}\right) = K_y \left(\frac{ET_x - ET}{ET_x}\right), \quad (2.2)$$

where, Y_x is the maximum yield and Y_a is the actual yield, ET_x represent the maximum evapotranspiration and ET actual, the proportionality factor between a loss in relative yield and a decrease in relative evapotranspiration is denoted by the K_y . Within the framework of the Aquacrop model, the following procedures are carried out (Fig. 2.8):

- The ET is divided between soil evaporation and crop transpiration.
- Product of water productivity and cumulated crop transpiration is calculated
- Product of B and Harvest Index to estimate the actual yield is calculated,

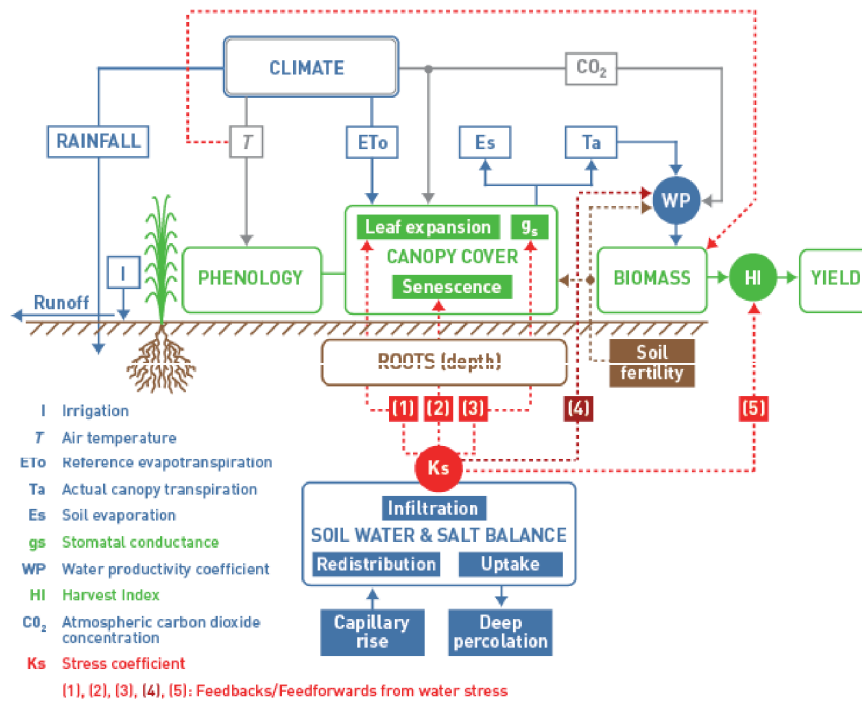


Figure 2.8: The main components of the soil-plant-atmosphere continuum in Aquacrop [source: [Steduto et al. \(2009\)](#)]

- Normalization of crop transpiration with reference evapotranspiration is carried out,
- Crop water use, growth, and yield are calculated in daily time increments.

Some of the other popular models are as follows: DSSAT is a crop simulation model that simulates about 42 crops. A database management system for managing crop, weather, and soil-related data is one of the components. The soil, plant, and atmosphere dynamics are modeled in the crop simulation models to simulate growth, development, and yield ([Jones et al., 2003](#)).

APSIM is a crop model for estimation of crop production, soil water, and nutrient flow simulation. In addition, it has components to deal with pasture production and crop residue decomposition. ([McCown et al., 1996](#)).

CropSyst is a user-friendly crop simulation model to estimate crop production and yield ([Stöckle et al., 2003](#)).

The CERES model is a set of improvised models to simulate the site specific crops (Timsina and Humphreys, 2006).

AgMIP is an effort to bring together the climate, crop, and economic modelling communities with state-of-the-art computational technology to produce an improved crop model (Rosenzweig et al., 2013). It lists several grid-based crop models for comparing crop yields around the world using different scenarios.

LPJmL simulates biophysical and biogeochemical processes for the most important crops in the world to estimate their production and yield. It draws on the LPJ-Dynamic Global Vegetation Model and its usage of crop functional types (CFTs) (Lapola et al., 2009; Rohwer et al., 2007). It mimics the short-term adjustments to the carbon and water cycles brought on by changes in land use, the unique phenology and periodic CO₂ fluxes of cultivated areas (Lapola et al., 2009).

2.5 The effects of climate change on the agricultural sector in the Mahanadi Delta

Various studies on the climate change have been conducted for this region particularly for the Mahanadi basin and Odisha state (Swain, 2014; Jin et al., 2018; Mishra and Jena, 2015b,a; Panda and Singh, 2016; Jena et al., 2014; Das et al., 2020; Mishra and Sethi; Nayak et al.; Mishra, 2017; Sahu et al., 2020; Bastia and Equeenuddin, 2016; Nibal and Damodar, 2020; Jena, 2018; Behera et al., 2016; Patnaik and Narayanan, 2009; Priyadarshi et al., 2019; Nageswararao et al., 2019). However, very few have concentrated on crop water requirement and soil suitability modelling. Pasupalak (2009) conducted a study on the threat of climate change on agriculture in the state of Odisha and came to the realisation that the results of the models do not indicate any negative change in the *kahrif* rice yield. In addition, the author came to the conclusion that the impact assessments carried out in the state of Odisha were not comprehensive enough to warrant drawing any conclusions. Gumma et al. (2015) used earth observation data to estimate production changes in rice yield in the context of changing climate and climate variability and concluded that rainfed rice would continue to dominate the share of cropland area in the state of Odisha. Senapati (2022) employed a nonlinear autoregressive distributed lag (NARDL) model to estimate statistical significance between

the role of climate variables and crop yield and concluded that the magnitude of positive rainfall deviations is greater than the corresponding negative rainfall deviation elasticities and that there is a significant asymmetry between the effect of rain on the yield of Odisha's most important crops. On the basis of panel data from thirteen different districts in Odisha, [Senapati and Goyari \(2020\)](#) investigated the factors that are most important for determining crop yields. The researchers concluded that climate change has a negative impact on crop yield in the districts studied. [Nayak et al. \(2019\)](#) studied the farmer's perceptions on risk source and management strategies to recommend adaptation strategies. [Duncan et al. \(2017\)](#) studied the factors that affect farmers' resilience in the Delta and argued that consideration of the system in which rice is cultivated is crucial in addition to a production boost and shock resistance to make farmers resilient to climate change. [Das and Mishra \(2017\)](#) investigated the susceptibility of agriculture to climate change and proposed some adaptation strategies. [Sahu and Mishra \(2013\)](#) carried out an empirical examination into farmers' perspectives on adaptations to climate change. The researchers identified the major factors that influence the farmers' behaviour.

Study area

The Mahanadi delta is traversed by three rivers: the Mahanadi, the Brahmani, and the Baitarini, all of which pour into the Bay of Bengal. The delta stretches along the coast for about 200 kilometers, from Chilika in the south to the Dhamra River in the north (Singh and Das, 2018). Five coastal districts Bhadrak, Kendrapara, Jagatsinghapur, Puri, and Khordha were selected that are located within 5 m of sea level and cover an area of about 13,000 km². These are further divided into 45 community development blocks (Fig. 3.1).

3.1 Biophysical environment

The River Mahanadi originates as a small stream in the south-east of Madhya Pradesh and flows over the eastern part of the Chhattisgarh Plain before entering the state of Odisha near Baloda Bazaar (Chakrapani and Subramanian, 1990). The river reaches the delta apex near Naraj after crossing the eastern ghat range. Young and older alluvium are the main geological strata (Fig. 3.2, Fig. 3.6). Flooding cyclones are most common extreme weather events in the delta region. For the period 1875–1987, the total number of floods were 125 in R. Mahanadi, 100 in R. Brahmani and 92 in R. Baitarini (Sinha, 1999). Recently, in the years 2003, 2008, 2011 and in 2014 the delta experienced major flood events which caused extensive damages to the crops and infrastructure in the delta. These rivers become flooded if there is excessive precipitation during the monsoon season (Mohanti and Swain, 2005). In delta regions, devastating flooding is caused by multiple factors, including the flat coastal topography, inadequate drainage, siltation on river bed, the failure of embankments, and the pouring of floodwaters over flood barriers. The circular shape of the Mahanadi basin has a lot to do with floods that

occurs there (Beura, 2015). The Hirakud Dam was constructed over the Mahanadi River approximately 15 kilometres away from Sambalpur. Its primary purpose was to control flooding in the delta while also providing additional services, such as irrigation (Panda et al., 2013). Only to a certain extent does it make a difference in the amount of flooding that occurs (Kar et al., 2010). Nevertheless, throughout the monsoon season there is a consistent risk of flooding in the densely populated delta. Out of a total annual rainfall of 1451 millimetres, the basin receives, on average, 1,088 millimetres of precipitation during the southwest monsoon, which lasts from the middle of June to the middle of October. (Fig. 3.3). Because of this, the delta is susceptible to annual floods, the severity of which increases along with the volume and intensity of the precipitation (Gosain et al., 2006). The situation is mentioned in several other studies, in the context of trend and characteristics of climatic variable like precipitation, temperature and stream-flow (Rao, 1993; Ghosh et al., 2010; Kar et al., 2010; Gosain et al., 2006). The Delta is prone to tropical cyclones and storm surges and has experienced severe damage and loss of life. A large number of tropical depressions or cyclones have been observed in the Bay of Bengal. The frequency has increased in recent years. For instance, the experienced 12 storms in 2006, which included both the depression and cyclonic storms that generated severe rainfall, whereas in 2007, it was 14. The intensity of cyclone also has increased as observed in last decade (1999, 2007, 2013). Unnikrishnan et al. (2011) predicted an increasing trend for the occurrence of cyclones during the late monsoon season in 2071–2100 compared to the baseline scenario in the Bay of Bengal.

3.2 Socio-economic profile

The Mahanadi Delta is home to eight million people and has a population density of 613 people per square kilometre, according to the Census completed in 2011 (Govt. of India, 2011). The population density is significantly more than that of Odisha (270 people per square kilometre) and India (382 people per square kilometre). Khordha is the most populous district with a population of 2.25 million, with 1.17 million men (52%) and 1.08 million females (48%) (Table 3.2). The line graph in Fig. 3.4 shows the positive decadal growth in population since 1901 in

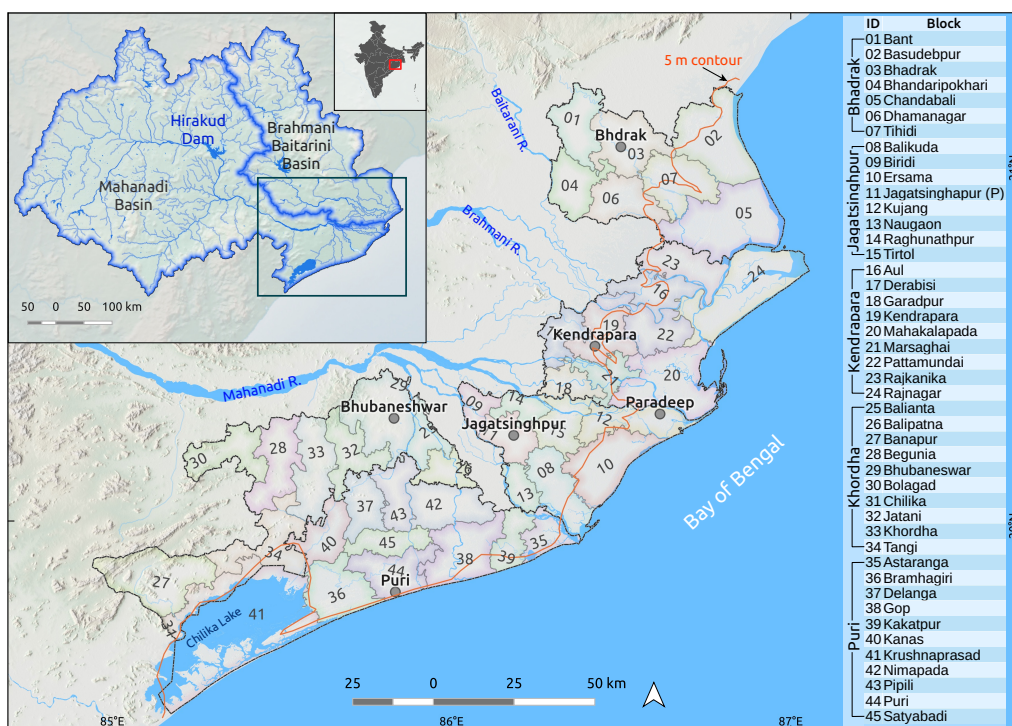


Figure 3.1: Study area

all the districts of the Mahanadi Delta. A drastic positive change can be noted after 1951. During the period of 2001 and 2011, the annual growth rate is 1.4 percent, which is placing growing demands on coastal resources. The people of this delta are mainly dependent on agriculture. According to Census 2001 and 2011, a shift has been observed in the composition of workers from agricultural to non-agricultural sector. Interestingly, while men make up a larger share of rural areas' growers, women considerably outnumber men in the agricultural labour force. In both rural and urban settings, the vast majority of working women are employed in the domestic sector. The dependency rate in the delta is 53 out of every 100 working-age residents, which is higher than the state and national averages and contributes to the area's pre-existing social vulnerabilities. Bhadrak, Kendrapara, and Jagatsinghpur districts are the socio-economically most vulnerable districts in the area with respect to climate change. Because of chronic crop failures and low returns from pre-existing livelihoods, migration is actually

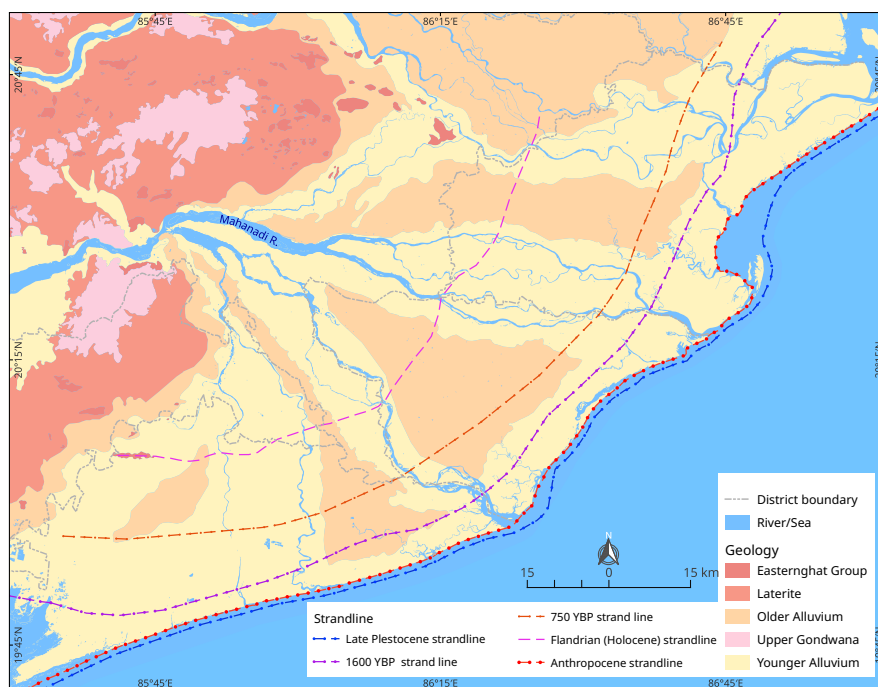


Figure 3.2: Geological map of the delta [after Mahalik (1984)]

starting in these coastal communities. This can be attributed to “distress-induced migration.” Khordha, Odisha’s most urbanised district with 42.93 percent urban population, and Puri, famous for religious tourism, serve as migration hubs for neighbouring rural communities (Samling et al., 2015).

Paddy is the main crop cultivated in the delta area. Other important crops include oilseed, grains, groundnut, black grams, green grams and so on (Table 3.1). There are three cropping seasons in the delta: i) Kharif, ii) Rabi, and iii) Zaid. A crop calendar of the major crops is shown in Fig. 3.5. Based on the cropping intensities, there are three types of cropland in the delta: i) mono cropland; ii) double cropland; and iii) triple cropland (Fig. 3.7)

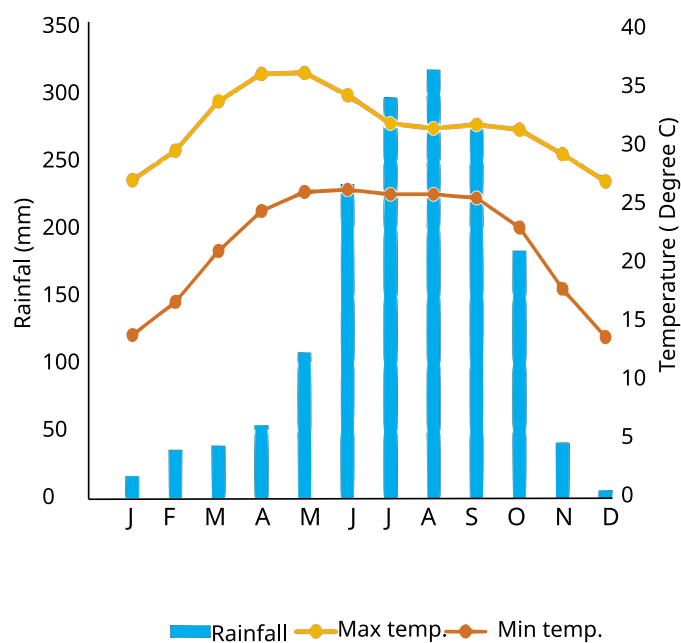


Figure 3.3: rainfall temperature graph

Table 3.1: Cultivated area of different crops in the delta in 2011 [source: Govt. of Odisha (2011a,e,d,c,b)]

District	Paddy	Other Cereals	Pulses	Oil Seeds
Bhadrak	26750	600	18340	26680
Jagatsinghpur	550	130	55680	10140
Kendrapara	2860	260	77790	12830
Puri	33050	230	71000	21920
Khordha	920	1090	4613	4820

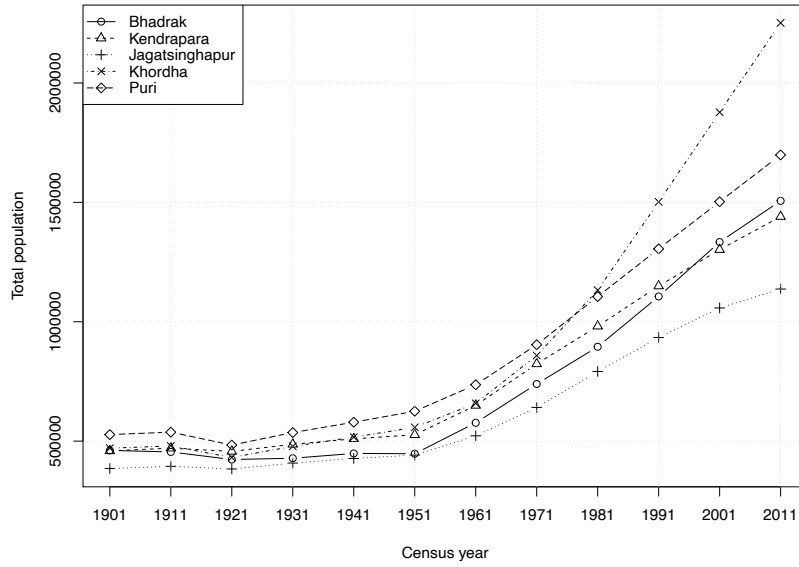


Figure 3.4: Decadal population growth in the delta

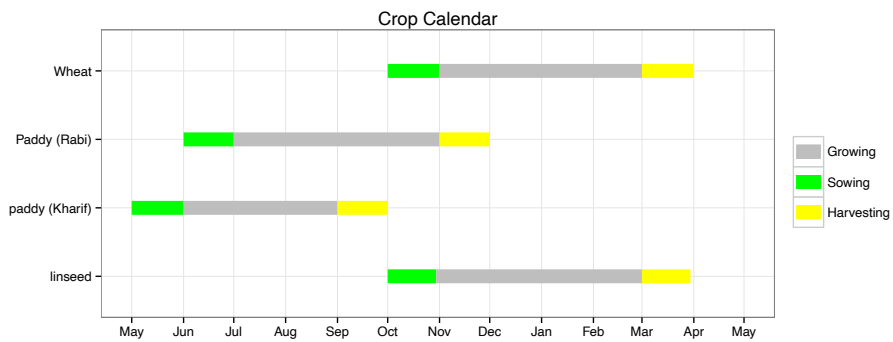


Figure 3.5: Crop calendar of major crops in the delta

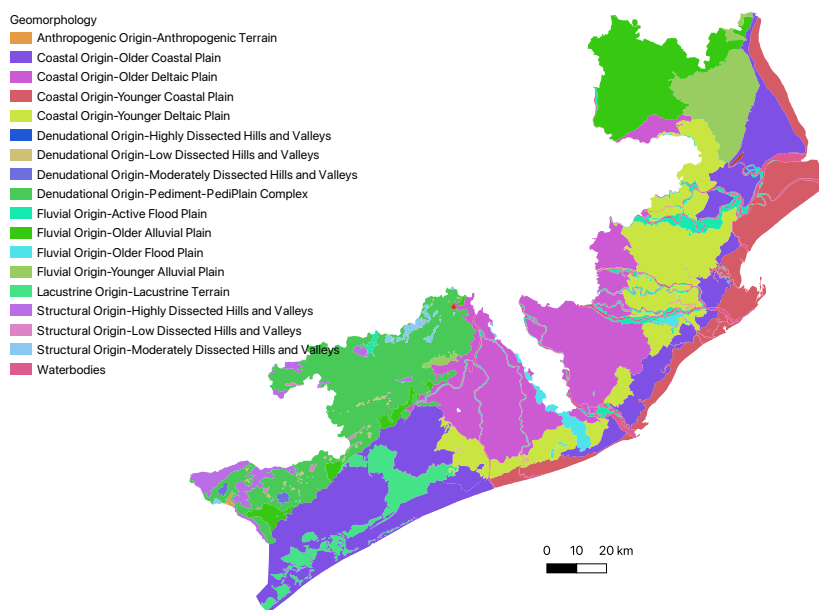


Figure 3.6: Geomorphology of the study area

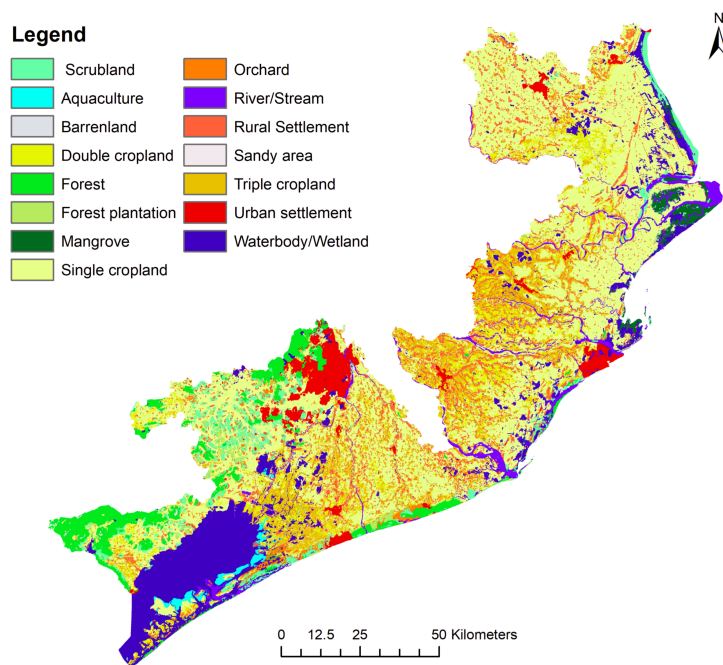


Figure 3.7: Land cover of the delta

Table 3.2: Demographic profile of the study area [source: Govt. of India (2011)]

District	Puri	Bhadrak	Kendrapara	Jagatsinghapur	Khordha	Total
Area in km²	3501	2451	2480	1669	2755	16799
Pop. density in person/km²	485.2	614.6	580.8	681.2	817.3	478.3
Population	1698730	1506337	1440361	1136971	2251673	8034072
% shared by districts	21.14	18.75	17.93	14.15	28.03	100
Male population	865380	760260	717814	577865	1167137	4088456
Proportion of male in %	21.17	18.6	17.56	14.13	28.55	100
Female population	833350	746077	722547	559106	1084536	3945616
Pop. aged below 6 years	172888	184560	161159	110249	237394	866250
% of Pop. aged below 6 years	19.96	21.31	18.6	12.73	27.4	100
SC population	325133	334896	309780	248152	297472	1515433
% of SC population	21.45	22.1	20.44	16.37	19.63	100
ST population	6129	30428	9484	7862	115051	168954
% of ST population	3.63	18.01	5.61	4.65	68.1	100

Methodology and data used

The methodological approaches employed in this study are as follows:

4.1 Impacts of extreme events

4.1.1 Flood

One of the major challenges in predicting flood extent and magnitude is a lack of adequate historical flood extent data. Recent advancements in the Synthetic Aperture Radar (SAR) remote sensing system make it possible to map the flood extent effectively. In this study, Radarsat 1/2 and Risat 1/2 SAR data were used to map the flood-inundated areas from 2000 to 2014 (Table 4.1). The satellite era is relatively new in comparison to the available rainfall records. So, SAR data from recent floods that happened at the same time as rain events with a certain return period were chosen. Rainfall data was procured from the India Meteorological Department (IMD). The technique of thresholding SAR backscattering values to map the inundated pixel was adopted in this study. An adequate threshold was estimated by inspecting the histogram of each data point (Hirose et al., 2001; Yamada, 2001). The Joint Research Centre's water body data was used to mask out the paramagnet water bodies. A slope value greater than 5 degrees was used to mask the terrain shadows. The estimation of the return period of annual maximum precipitation was carried out using the Gumbel extreme probability distribution model (Gumbel, 1941; Kidson and Richards, 2005).

Equation 4.1 illustrates the formula to fit the observed series of rainfall on the probability graph at different return periods, T .

$$X_T = \bar{X} + K\sigma_{n-1}, \quad (4.1)$$

where X_T represents the magnitude of the T -year precipitation events, K represents the frequency factor, and \bar{X} and σ_{n-1} represent the mean and standard deviation of the maximum amount of precipitation, respectively.

Table 4.1: A list of flood events that were mapped using SAR data

Sl. No.	Event date
1	06-06-05
2	07-08-05
3	24-09-05
4	27-10-05
5	09-07-06
6	04-08-06
7	19-08-06
8	26-08-06
9	02-09-06
10	04-09-06
11	26-09-06
12	04-07-07
13	06-07-07
14	13-07-07
15	21-08-07
16	23-08-07
17	23-09-07
18	24-09-07
19	17-06-08
20	19-07-08
21	20-09-08
22	21-09-08
23	14-07-09
24	22-07-09

25	24-07-09
26	27-07-09
27	29-07-09
28	08-09-09
29	12-09-09
30	18-06-11
31	22-06-11
32	05-09-11
33	08-09-11
34	12-09-11
35	14-09-11
36	01-10-11
37	12-10-13
38	14-10-13
39	15-10-13
40	17-10-13
41	25-10-13

Storm surge is another form of flooding that may damage crops by uprooting and salt-water inundation. It is an important extreme event due to the high frequency of tropical cyclones in this area. The projected water level on the onshore topography was used as the extent of storm surge flooding in the delta. A linear projection of water level would be the simplest approach to delineate the boundaries of inundation. However, it is assumed that it may overestimate the extent of inundation. (Dube et al., 2009). A linear decay function was used to estimate the rate of reduction in surge height (Eq. 4.2)

$$SDC = \frac{H_s - Z_s}{D_f - D_{cs}}, \quad (4.2)$$

where, SDC is the surge reduction factor, H_s is surge height, Z_s is the elevation at surge, D_f denotes the extent of inland inundation and D_{cs} is the extent of constant surge (Fig. 4.1). The reference information used to derive this factor was taken from the 1999 super cyclone. The maximum inundation extent reported

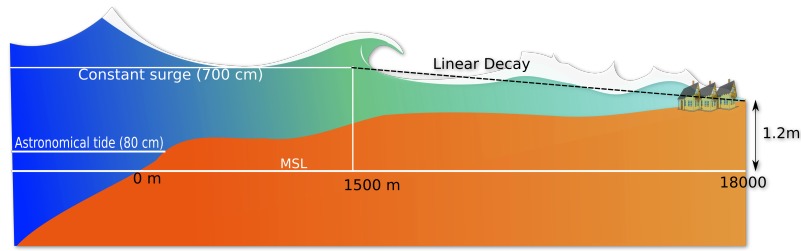


Figure 4.1: Graphical representation of the linear decay function used to estimate the surge height and inundation extent

was 18 km (Dube et al., 2009). The elevation information was derived from the SRTM digital elevation model, which has a spatial resolution of one arc second, equivalent to 30 m.

$$\begin{aligned}
 SDC_m &= \frac{700\text{cm} - 120\text{cm}}{18000 - 1500} \\
 &= 0.35\text{cm}/\text{m}
 \end{aligned}$$

4.1.2 Cyclone

The Tropical Cyclone Risk Model (TCRM) model was used to calculate wind hazards maps at nine return periods. The return periods include 5, 10, 25, 50, 100, 500, 1000, and 2000 years. Geoscience Australia has created this stochastic model of tropical cyclones to help estimate the potential wind damage that these storms can cause (Arthur et al., 2008). Using the IBTrACS data (Knapp et al., 2010) from 1981 to 2014, a set of 5,000 synthetic cyclone tracks was created. A parametric wind field and boundary layer model was applied to the tracks individually to capture the maximum wind speed over the lifespan of each event (Kepert, 2001; Powell et al., 2005; Fang et al., 2020). Each grid cell's highest wind speed within the model domain was fitted using the generalised extreme value (GEV) probability distribution (Hosking, 1990). Over the specified return times, the model predicts the highest possible gust wind speed for a duration of three seconds.

4.1.3 Land cover mapping

A land cover legend with 15 classes was prepared by taken into considerations the landscape of the delta (Di Gregorio, 2005). Indian Remote Sensing (IRS) satellite LISS IV images from the three cropping season were acquired from National Remote Sensing Centre (NRSC). The image were atmospherically corrected before performing the segmentation for object based image analysis. On field and high resolution image based training samples were collected to classify the image objects from the segmentation. Random forest algorithm wast used to classify the land cover map (Breiman, 2001). Random forest algorithm is an advance for of classification regression tree classification where over fitting is avoided by integrating the results of some random trees (Fig. 4.2). Some object were manually verified to improve the accuracy of the result. A separate accuracy assessment was conducted to asses the quality of land cover map.

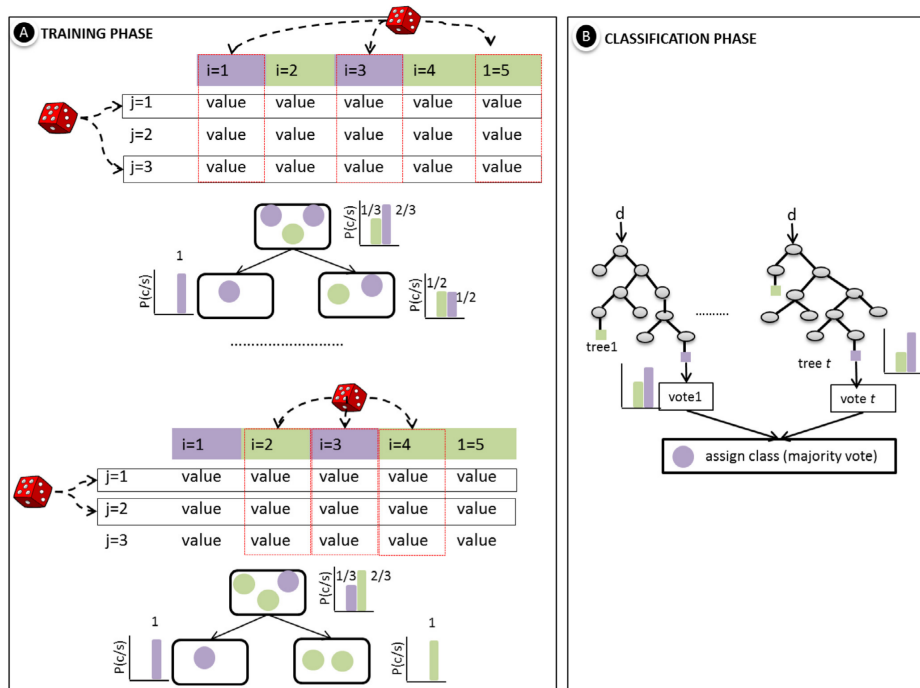


Figure 4.2: Phases of the random forest classification model: samples, variables, probabilities, classes, data, tree counts, and input data are indicated by the letters i, j, p, c, s, t, and d, respectively. [Source: Belgiu and Drăguț (2016)]

4.2 Soil suitability assessment

4.2.1 Soil data collection

Soil is one of the most precious resource required for agriculture. Soil controls the pattern and type of crop in any particular region. Therefore, understanding the soil properties is essential for efficient agriculture policy formulation for better yield. The coastal tract of Odisha is the home of nearly 8 million population and most of them (about 60%) relay on agriculture. Soil data available for this region, are old and lack detailed informations which are required to set-up models to improve agriculture.

Allocation of sampling locations

Conventional method of sampling relies on mental predictive model of soil occurrence and is subjective to surveyors (McBratney et al., 2000). On the other hand digital soil mapping is based on statistical modelling of soil attributes and covariates with the goal to optimize the accuracy of the models and minimize the errors without losing data quality (Scull et al., 2003). A scheme was prepared to collect soil samples from the main Mahanadi delta region for efficient soil mapping. The rest of the delta was not considered due to time constrain. The method utilised multivariate covariate gradients and was based on a stratified version of a random sampling approach (Osterholz et al., 2020; Yang et al., 2007). The covariates used for the stratification are The NDVI, LST, CTI, and DEM. The gradients was obtained by using principle component analysis of the selected covariates, along with K-means clustering of resulted components for the final stratification. Within this scheme, the sampling points were randomly generated within each individual strata (Fig. 4.3). The estimation error is lower than what would be obtained from a purely random sample of the same size due to the method used here.

Collection of soil samples

A network analysis was carried out to efficiently collect the samples from ground. The Open Street Map (OSM) data was extracted and ingested into a postgresql

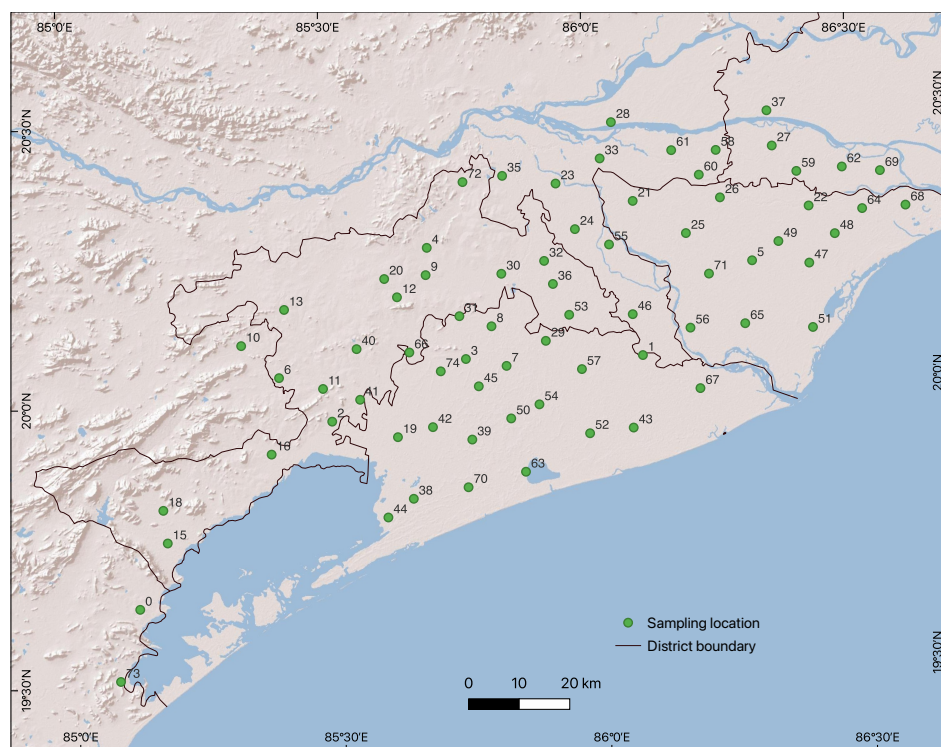


Figure 4.3: Distribution of soil sampling locations

database to run the vehicle routing problem (VRP) solver from PostGIS network analysis module `vrpRouting` ([vrpRouting Contributors, 2018](#)). A minimum stop time of 30 minutes was considered for the collection of soil samples. The solver returned 15 best routes which were used to visit the sampling locations (Fig. 4.4). The samples were collected in April 2018. The GPS track of the routes is given as annex B

4.2.2 Soil data analysis

Soil texture

The relative amounts of sand, slits, and clay in the mineral soil constitute the soil's texture. Various techniques are used to determine the quantity of these particles in the soil. The percentages of different soil minerals, such as sand, silt, and clay, are referred to as soil texture. Different methods are employed to determine the amount these particles in the soil ([Essington, 2015](#)). The method proposed by

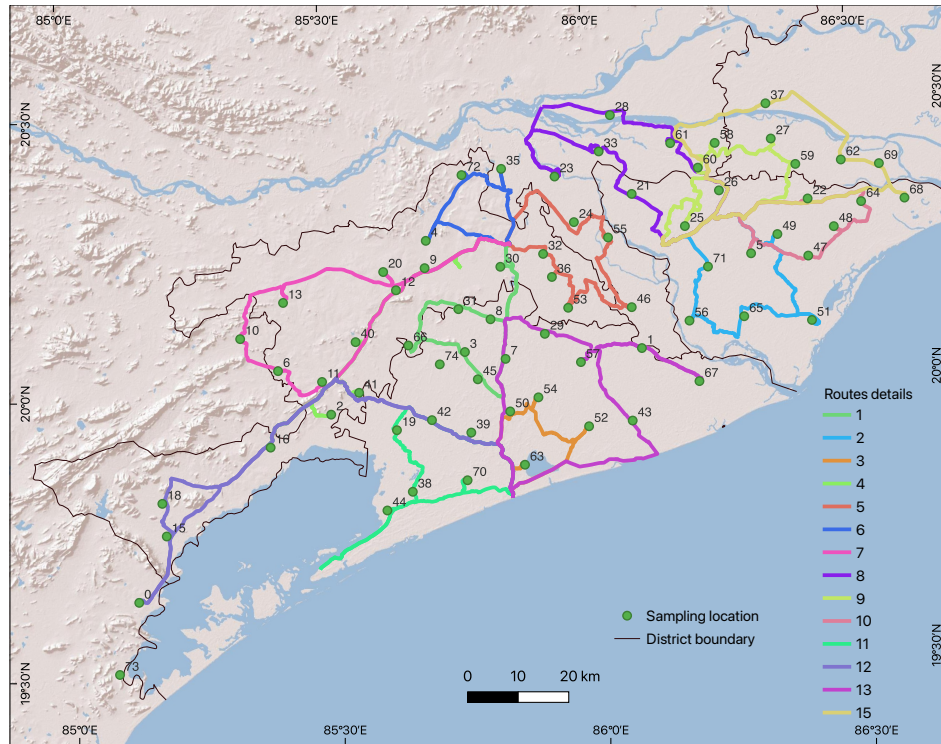


Figure 4.4: Route map used to visit the sampling locations

[Bouyoucos \(1962\)](#) was used to analyse the 72 samples collected from the agricultural in the Delta. Stoke's law serves as the foundation for this method (Eq. 4.3).

$$v = \frac{2gr^2(D - d)}{9n}, \quad (4.3)$$

where v is the rate at which the particles fall ($cm \ sec^{-1}$), g is the gravitational acceleration, r is the radius of the particles, D denotes particles density, d is the density of the liquid, and n is the absolute viscosity of the liquid. A hydrometer is used to measure the density of the soil suspension at different time intervals to estimate the size of the particles ([Gee and Or, 2002](#)). The size of the solids in the suspension is estimated from the density of the soil suspension. The steps followed to estimate the soil texture are listed below ([Rayment et al., 1992](#); [Van Reeuwijk, ed.](#)):

- ① A dispersing solution was created by dissolving 50 g of sodium hexameta-phosphate $Na(PO_3)_6$ in one litre of deionized water and then diluting the

solution to one litre., 5%.

- ② In a cylinder having a capacity of 1000 ml, a blank was made by combining 100 ml of the dispersion solution with 880 ml of deionized water. The remaining 20 ml represent the volume that was taken up by the 50 g of soil.
- ③ 50 g soil was weighted and transferred to a dispersing cup.
- ④ 100 ml of 5% dispersion solution was added.
- ⑤ The cup was attached to a shaker for 30-40 sec.
- ⑥ The suspension was quantitatively transferred to 1000 ml cylinder.
- ⑦ Deionized water was added to fill upto 1000 ml and kept overnight to equilibrate with room temperature.
- ⑧ Hydrometer reading was taken from the blank and room temperature was recorded.
- ⑨ A plunger was inserted into the suspension to mix it properly.
- ⑩ Hydrometer reading was taken after 40 sec. Sand particles need this time to settle to the bottom.
- ⑪ Hydrometer reading was again recorded after 6 hrs 52 min. Silt particles need this time to settle to the bottom.
- ⑫ Influence of temperature was corrected using Equation 4.4.
- ⑬ Equations 4.5, 4.6 and 4.7 were used to calculate the sand, silt and clay percentages.

$$\text{Correction factor (CF)} = (\text{Actual room temperature in } ^\circ\text{F} - 68) \times 0.2 \quad (4.4)$$

$$\%silt + \%clay = \frac{(S - B) + CF}{W} \times 100, \quad (4.5)$$

where B denotes blank readings, W denotes sample weight in g, and S is a sample reading taken at 40 seconds.

$$\%clay = \frac{(S - B) + CF}{W} \times 100, \quad (4.6)$$

where B denotes blank readings, W denotes sample weight in g, and S is a sample reading taken after 6 hours 52 minutes.

$$\%sand = 100 - (\%silt + \%clay). \quad (4.7)$$

Soil pH and electric conductivity

The pH and salinity (electric conductivity) of the soil were determined in a 1:2.5 soil-to-water (pH-H₂O) solution (Van Reeuwijk, ed.). A summary of the steps taken to measure the pH and EC are given below (Rayment et al., 1992).

- ① For the purpose of calibrating the pH metre, buffer solutions with pH values of 4.0, 7.0, and 9.00 were prepared.
- ② The pH metre was adjusted with the help of the buffer solutions.
- ③ The conductivity meter was calibrated using a standard solution of 0.01 M KCl.
- ④ 20 g fine soil was weighted into a 100 ml polythene beaker.
- ⑤ After adding 50 ml of water to the beaker, it was then shaken for a total of two hours.
- ⑥ The electrode probe was immersed in the upper part of suspension.
- ⑦ Stabilized reading was recorded after at an accuracy of 0.1 unit.
- ⑧ The temperature was recorded and set in the conductivity meter to compensate the temperature at 25°C.
- ⑨ The dip cell of the conductivity meter was immersed in the upper part of suspension.
- ⑩ The reading of conductivity was recorded.

Cation Exchange Capacity (CEC)

Soil CEC is considered as an indicator for the retention and supply capacity of soil fertilizer (Khaledian et al., 2017).

An ammonium acetate-based method was used to estimate the CEC (Chapman, 1965). The summary of the steps followed to measure the CEC for all the samples:

385 g NH_4OAc

- ① 385 g NH_4OAc was dissolved in 5 l water to make 1M ammonium acetate solution.
- ② A 250 ml beaker was filled with 10 g of air-dried soil that had been grounded to less than 2 mm in size.
- ③ 25 ml of NH_4OAc was mixed with the soil in the beaker.
- ④ For each sample, A 7 cm Buchner funnel was made by putting a 7 cm piece of Whatman 42 filter paper in it. The filter was wetted with a tiny quantity of NH_4OAc . A 250 ml suction flask was fitted with the funnel. The vacuum pump was adjusted to pressurise the soaked filter. The mixture of soil and NH_4OAc was thoroughly mixed and passed to the filter.
- ⑤ Around 75 mL NH_4OAc of each sample was poured into an individual plastic squirt bottle. About 10 ml of the NH_4OAc was added to the bottle in order to transport the entire soil sample to the Buchner funnel.
- ⑥ A 7.0 cm Whatman #1 filter paper was used to cover soil to keep it moist between leaching.
- ⑦ Five to seven leachings, each with 10 to 15 ml of NH_4OAc , were conducted without allowing the soil to dry completely in between.
- ⑧ After transferring the leachate to a 250 ml volumetric flask, 1 M NH_4OAc was added to get the final volume up to 250 ml.
- ⑨ An atomic absorption spectrophotometer (AAS) was used to measure Ca, Mg, K, and Na from the solution.

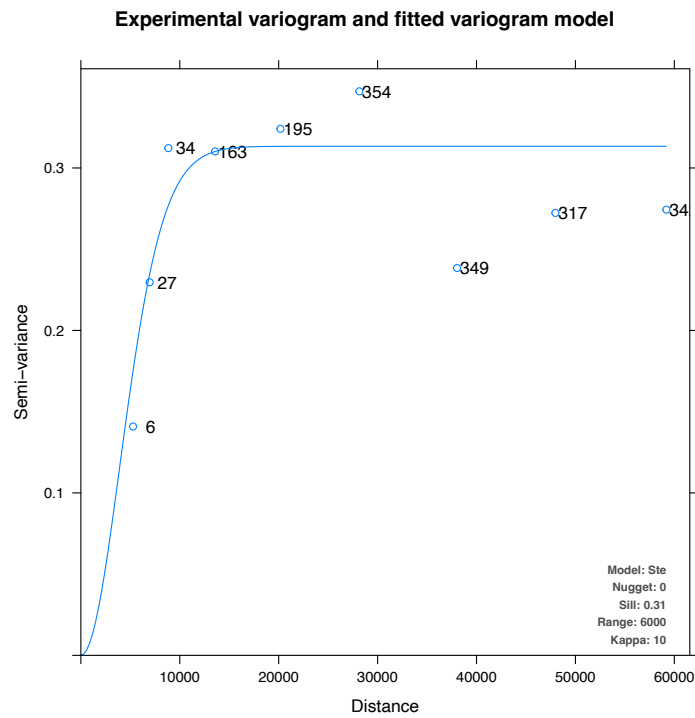


Figure 4.5: Experimental and fitted variogram for the pH samples

- ⑩ $\text{NH}_4\text{-N}$ was quantified in the leachate to measure the CEC (cmol_c/kg) of each sample (Eq. 4.8).

$$\text{CEC} = \left(\frac{\text{mg NH}_4\text{-N}}{\text{L}} \right) \left(\frac{0.25\text{L}}{10\text{ g soil}} \right) \left(\frac{1\text{ meq NH}_4\text{-N}}{14\text{ mg NH}_4\text{-N}} \right) \times 100 \quad (4.8)$$

4.2.3 Spatial interpolation of soil properties

Spatial interpolation was performed to predict all the soils parameters would be distributed over the space. Ordinary kriging method was applied after fitting the variogram model (Pebesma, 2004; Baxter and Oliver, 2005; Lark, 2002; Zhang and Li, 2007). Fig. 4.5 shows the autofitted variogram for pH samples pairs located within 60 km.

4.2.4 Suitability assessment

Soil data was used to prepare a multi-crop suitability map. A rating based system was used to assess the suitability of the soil for the major crops in the delta . The total soil ratings are classified into four groups based on the weight of the soil rating group. (Sys et al., 1991). The ratings were collected from the Global Agro-ecological Zone's database (Fischer et al., 2021). This method uses four constrain categories, these are

- So denotes no constraint with a rating of 100,
- S1 represents slight constraint with a reduced rating of 90,
- S2 denotes the moderate group with rating of 60,
- The severe constraint is represented by S3 with low rating - 40, and
- N stands for not suitable and rating is 10.

The final rating, SR_{int} was calculated using Eq. 4.9.

$$SR_{int}. = 0.5 \times (SQ1 + SQ2) \times SQ3 \times fSR(SQ4, SQ5, SQ6, SQ7), \quad (4.9)$$

where, SQ1 is the nutrient availability (OM, and low pH), SQ2 is the nutrient retention (CEC, base saturation), SQ3 is the rooting conditions (soil depth), SQ4 is the oxygen availability (soil drainage), SQ5 is salinity/sodicity (EC, Na) related quality, SQ6 is lime or gypsum based quality and SQ7 is the workability (soil phase).

4.3 Assessment of crop water requirements

4.3.1 Climate data preparation

CNRM-CM5 model was selected to extract the projected climate data for delta region by considering the overall mean values of rainfall as well as less bias in retrospective values (Fig. 4.6). Downscaled data from the RCPs (4.5 and 8.5) were selected. A summary of the comparisons among the models highlighted in Fig. 4.6 in terms of rainfall, average temperature, number of rainy days and reference

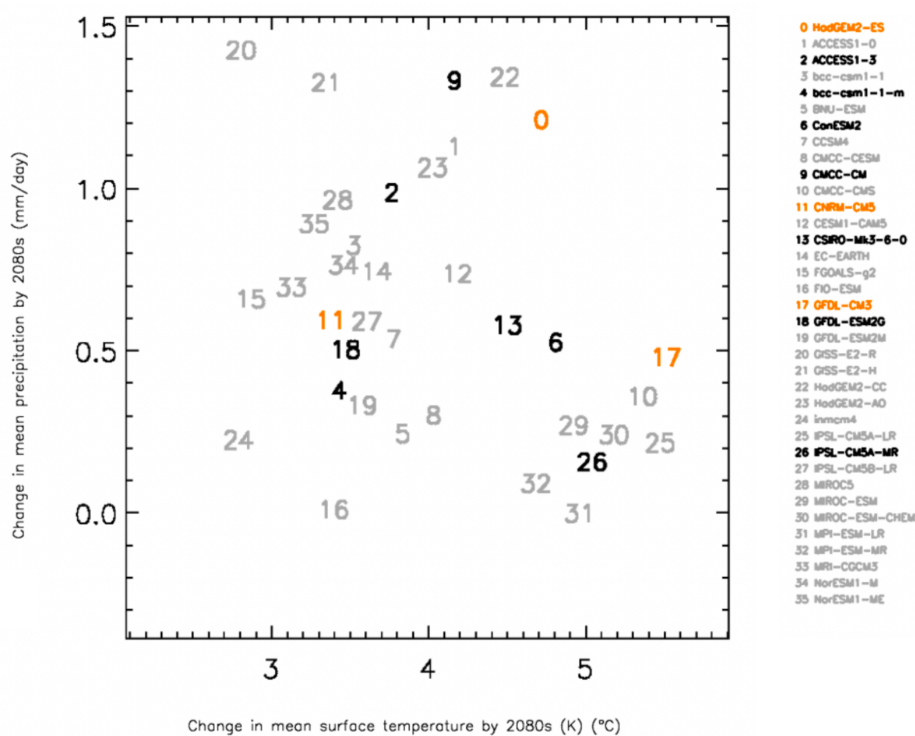


Figure 4.6: Comparisons of different climate models [source: [Janes and Macadam \(2017\)](#)]

evapotranspiration are given in Tables 4.2, 4.3, 4.4 and 4.5 respectively for the RCP 8.5. Aside from the frequency of rainy days, all other indicators are on the rise.

Table 4.2: Comparisons of average total annual precipitation (mm) from different models

Domain	81-10	2020s			2050s			2080s		
	Hist	CNRM-CM5	GFDL-CM3	HadGEM2-ES	CNRM-CM5	GFDL-CM3	HadGEM2-ES	CNRM-CM5	GFDL-CM3	HadGEM2-ES
Study area	1581	1597	1551	1719	1608	1687	1685	1725	1821	1920
Odisha	1504	1507	1485	1709	1591	1666	1620	1703	1866	1876

Table 4.3: Comparisons of average mean annual temperature (°C) from different models

Domain	81-10	2020s			2050s			2080s		
	Hist	CNRM-CM5	GFDL-CM3	HadGEM2-ES	CNRM-CM5	GFDL-CM3	HadGEM2-ES	CNRM-CM5	GFDL-CM3	HadGEM2-ES
Study area	27.3	28	28.68	28.11	29.03	30.48	29.68	30.54	32.32	31.57
Odisha	25.97	26.82	27.63	27.14	28.02	29.63	28.95	29.72	31.82	31.19

Table 4.4: Comparisons of total days per year with rainfall > 1mm from different models

Domain	81-10	2020s			2050s			2080s		
	Hist	CNRM-CM5	GFDL-CM3	HadGEM2-ES	CNRM-CM5	GFDL-CM3	HadGEM2-ES	CNRM-CM5	GFDL-CM3	HadGEM2-ES
Study area	170	132	130	114	132	130	120	131	131	123
Odisha	155	120	119	105	124	120	106	123	123	113

Table 4.5: Comparisons of Average annual reference potential evapotranspiration (mm/m) from different models

Domain	81-10	2020s			2050s			2080s		
	Hist	CNRM-CM5	GFDL-CM3	HadGEM2-ES	CNRM-CM5	GFDL-CM3	HadGEM2-ES	CNRM-CM5	GFDL-CM3	HadGEM2-ES
Study area	1585	1617	1650	1602	1656	1753	1655	1732	1790	1713
Odisha	1551	1579	1611	1571	1617	1707	1640	1695	1761	1716

Table 4.6: Lookup table to convert De Martonne Aridity index values to climate type

Climate type	Aridity index
Arid	0-10
Semi-arid	10-20
Mediterranean	20-24
Semi-humid	24-28
Humid	28-35
Very humid	35-55
Extremely humid	>55

4.3.2 Agro-climatic zone and hydrological regime

De Martonne Aridity index, I_M (Eq. 4.10) was used to assess the type agro-climatic zone (Solomon et al., 2007).

$$I_M = \frac{P}{T + 10}, \quad (4.10)$$

where, P is the mean rainfall in mm per year, T is the annual mean temperature in °C. Table 4.6 was used to convert the index value to climate type information.

The hydrological regime was assessed by dividing the climate data into four different time periods: i) historical, ii) 2020s, iii) 2050s and iv) 2080s.

4.3.3 Assessment of crop water needs and the effects of climate change on agriculture

The yield of crops and the amount of water needed for irrigation were analysed using an aquacrop simulation. It simulates the yield and water requirement on a daily basis. The baseline period and three other future climate scenarios were taken into consideration to analyse the impacts. The Climate information (rainfall, min. temperature, max. temperature, solar radiation), Soil profile data were provided for paddy, wheat, black grams, green grams and groundnut.

Results and Discussion

5.1 Impacts of extreme events

Flood is one of the most common extreme events in the Mahanadi delta. The delta witnesses at least one event a year. The low laying delta plain along with the meandering river and its flood plain determine the location and pattern of inundation extent. There are two distinct flood zones in the delta (Fig. 5.1). One is in the Badrak and Kendapara districts and other in the Puri district. These areas are located within the two to five year flood return period flood events. As the delta is densely populated with huge agrarian people, people in each of the administrative block of the Kendapara district mostly suffered from the flood. A large numbers of people in the Aul block are living in the highly exposed areas (Table 5.1). With the increase in return period, Bhadrak becomes more vulnerable to flood. The reduction in the number of wet days and the intensification of precipitation will increase the frequency of flooding in the future.

The risk map show the flood hotspot in the delta. It shows the same patterns, but not always. The percentage of cropland area is also high in this region. Therefore probable damages of crops in these area are also very high. Administrative block like Tihidi, Dhamnagar, Chandabali, Rajkanika, Aul, Kanas, Delenga are at higher risk prone zone (Fig. 5.2). Nearly 70% of the population dependent directly or indirectly on agriculture. At 100 year return period flood events 418 km² of crop land is flooded in Chandabali block, 298 km² in Basudebpur, 290 km² in Mahakalpara, 251 km² in Rajnagar, 212 km² in Tihidi, 211 km² in Ersama, 206 km² in Pattamundai block. Other most affected blocks in terms of flooding of cropland are Gop, Rajkanika, Nimapada, Dhamnagar, Balikuda, Kendapara, Bhadrak, Aul etc.

Table 5.1: Block wise flood affected population at various return period

Block	District	100 year	50 year	25 year	10 year	5 year	2 year
Bant		87597	63411	19801	1855	0	0
Basudebpur		156334	130919	83249	52945	25131	6295
Bhadrak		109699	75417	23874	6031	1088	42
Bhandaripokhari	Bhadrak	87979	69136	28085	6617	1085	0
Chandabali		221761	202826	153686	114068	66393	22165
Dhamanagar		154779	127959	89255	65995	42922	16847
Tihidi		155185	138316	104412	79149	47953	15882
Balikuda		117035	85524	43187	23119	5295	39
Biridi		42042	26229	10544	4530	650	0
Ersama		119865	107600	79168	53642	20320	1363
Jagatsinghapur (P)	Jagatsinghpur	74978	49863	19962	7887	894	0
Kujang		122650	89230	46966	24095	7208	526
Naugaon		51473	37587	19976	11781	4155	244
Raghunathpur		36042	23181	11597	5996	677	5
Tirtol		95997	69684	36498	18407	3979	100
Aul		129068	115470	94521	76567	52131	17537
Derabisi		83342	55452	25063	12789	4675	593
Garadpur		73404	53627	26911	12225	3389	28
Kendrapara		119687	92925	48164	25111	5465	36
Mahakalapada	Kendrapara	162042	133964	82157	52602	26767	6306
Marsaghai		89710	63478	29072	16703	7968	1821
Pattamundai		143545	122608	89642	65232	32389	9110
Rajkanika		120288	109378	82696	60718	35661	10109
Rajnagar		123865	108592	75285	50954	20062	1790
Balianta		48424	31429	8558	1399	63	0
Balipatna		55168	36689	15666	4979	246	0
Banapur		16865	2324	0	0	0	0
Begunia		49810	31777	16222	9070	5029	2104
Bhubaneswar	Khoorda	43753	25215	7140	2852	177	0
Bolagad		35959	16042	754	31	0	0
Chilika		11617	3347	694	378	1	0
Jatani		50934	31671	9963	5247	2535	862
Khordha		59403	39765	20291	14467	10529	6736
Tangi		46653	23807	8615	4906	2126	252
Astaranga		38272	22571	7747	1896	2	0
Bramhagiri		93391	86184	71233	58796	37780	11770
Delanga		93533	78017	51133	33921	16923	3028
Gop		131612	100545	56829	31662	6540	16
Kakatpur		53397	29215	9677	3908	216	0
Kanas	Puri	141114	131931	109464	92137	66600	28633
Krushnaprasad		16723	7558	1198	646	0	0
Nimapada		135132	95366	45924	19018	1839	0
Pipili		82633	54061	17285	5960	990	326
Puri		121477	102544	71864	48829	22677	2798
Satyabadi		88039	73733	51914	36616	18085	4338

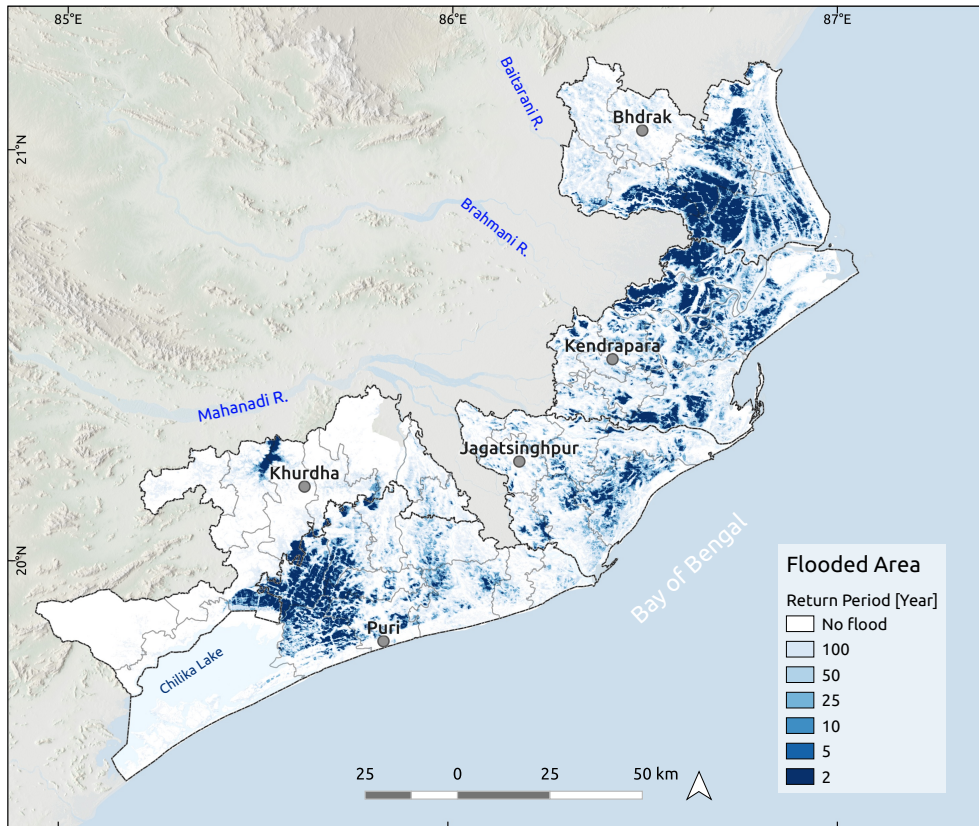


Figure 5.1: Extent of inundated areas at various return periods

Storm surge flooding also very common in the delta during cyclonic events due to low laying flat terrain in the northern part of delta (Fig. 5.3). Chandabali , Mahakalpara, Basudebpur, Rajnagar are highly vulnerable administrative blocks followed by Rajkanika, Pattamundai, Kujang, Tihidi, Aul, Ersama, Kendapara and Khurshanprasad. The amount of cropland impacted by storm surge induced flood is ver high in these blocks. For example, 421 km² in Chandabali, 280 km² in Mahakalpara, 263 km² in Rajnagar, 256 in km² in Basudebpur, 183 km² in Rajkanika, 176 km² in Tihidi, 152 km² in Pattamundai, 148 km² in Ersama. Sea level rise may poses addition risk factor by increasing the extent of surge inundation in future that. Flooding due to storm surge increase the soil salinity that decrease the production of crops. The adaptive measures like shoreline protection, mangrove plantation can prevent the propagation of storm surge water in the mainland area.

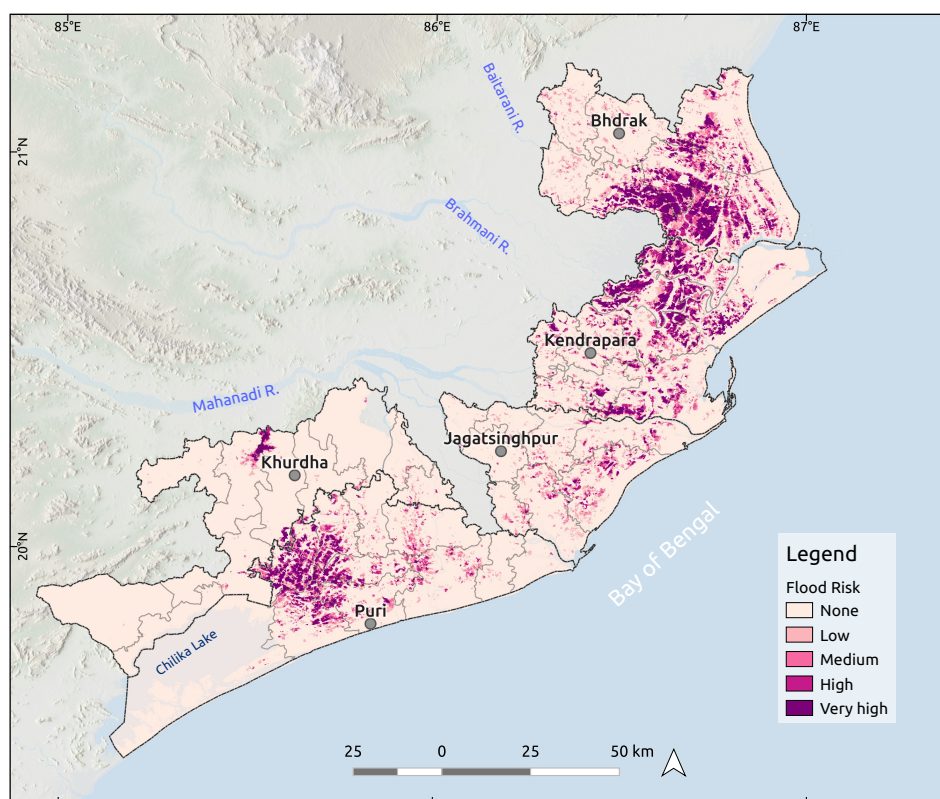


Figure 5.2: Flood risk map of the delta

Cyclone wind is the most destructive force Mahanadi delta often witnessed. Fig. 5.4 shows gust wind simulated using TCRM model for various return periods. In 100 year return period the gust wind reaches at about 50 m/s that is devastating in nature. Mahanadi has been suffered from various devastating cyclone mostly in the month of September-November throughout the last century. In 1885 more that 5,000 human lives was lost, another in 1931 which killed about 20,000 people, more that 1000 people died in 1971 cyclone, in 2013 category 5 on the Saffir-Simpson scale cyclone struck the delta. However, reported human loss was very few beside huge infrastructural damages. The northern part of the delta is more susceptible to high wind speed, hence, are at high risk.

The northern part of the delta experience nearly every extreme events like flooding, storm surge, high cyclonic wind speed as well as heavy rainfall. Therefore, adaptation activities should be prioritized in the blocks which fall under high

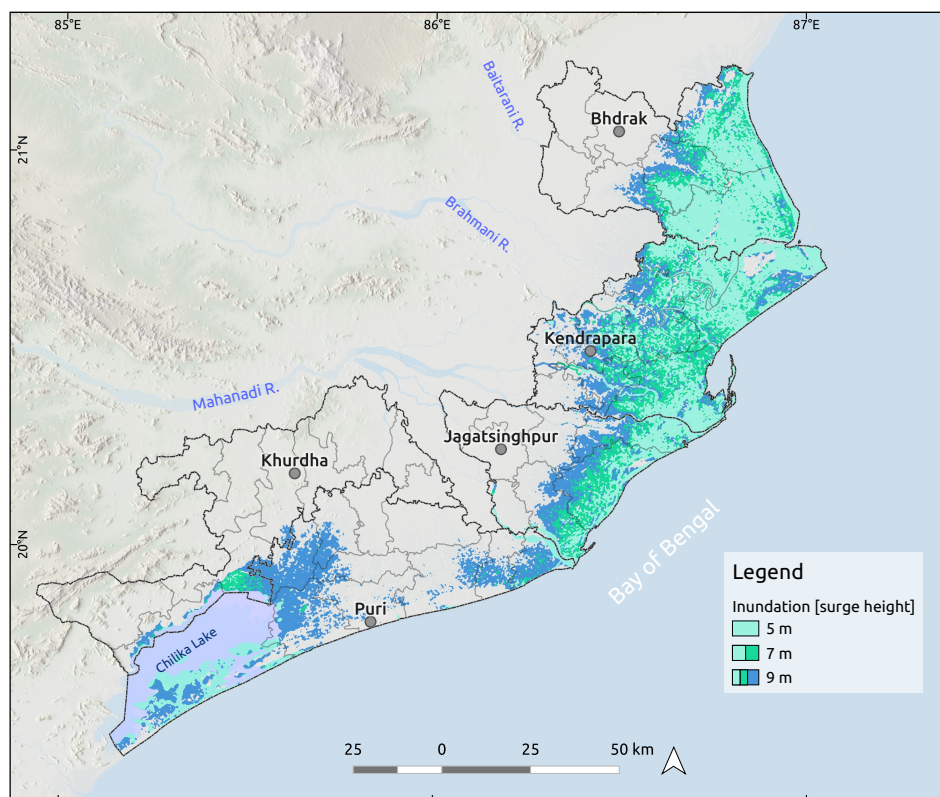


Figure 5.3: Inundation due to storm surge

risk categories.

The risk of cyclone is very in the northern part of the delta due to the poor infrastructure, mainly high percentage of earthen house. Dhamanagar, Tihidi, Rajnagar, Marsaghai, Mahakalpara are the very high risk prone block in the delta.

Fig. 5.7 depicts the overall effects of extreme weather events on rice crop yields.

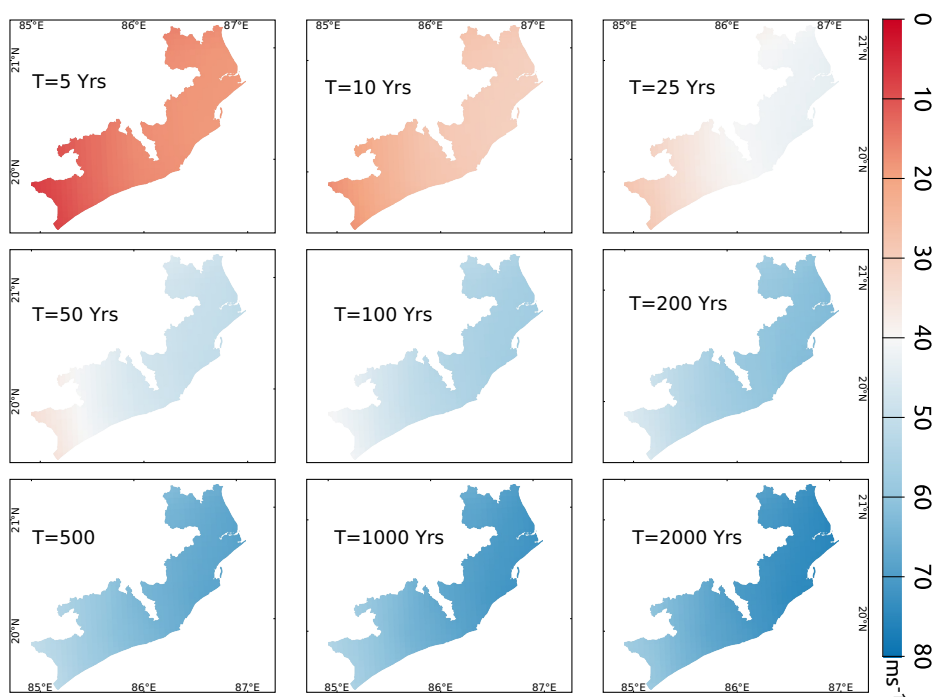


Figure 5.4: Gust wind of storms at various return periods

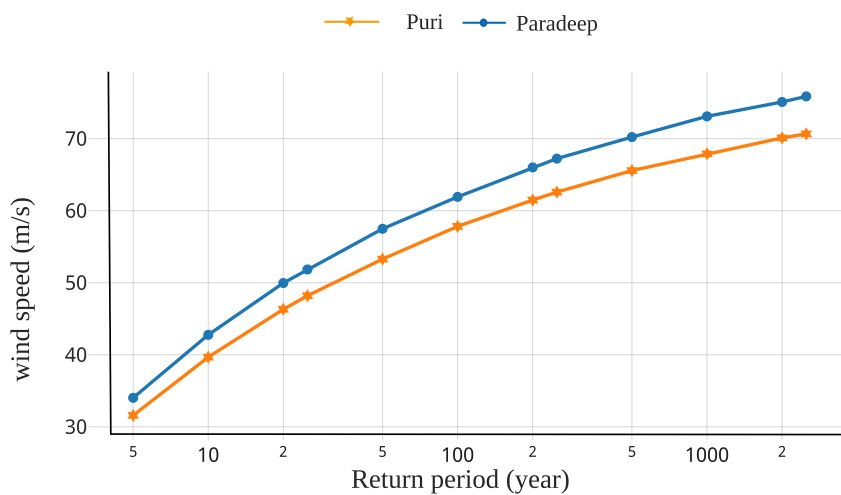


Figure 5.5: Wind profile of storm at various return period at Paradeep and Puri

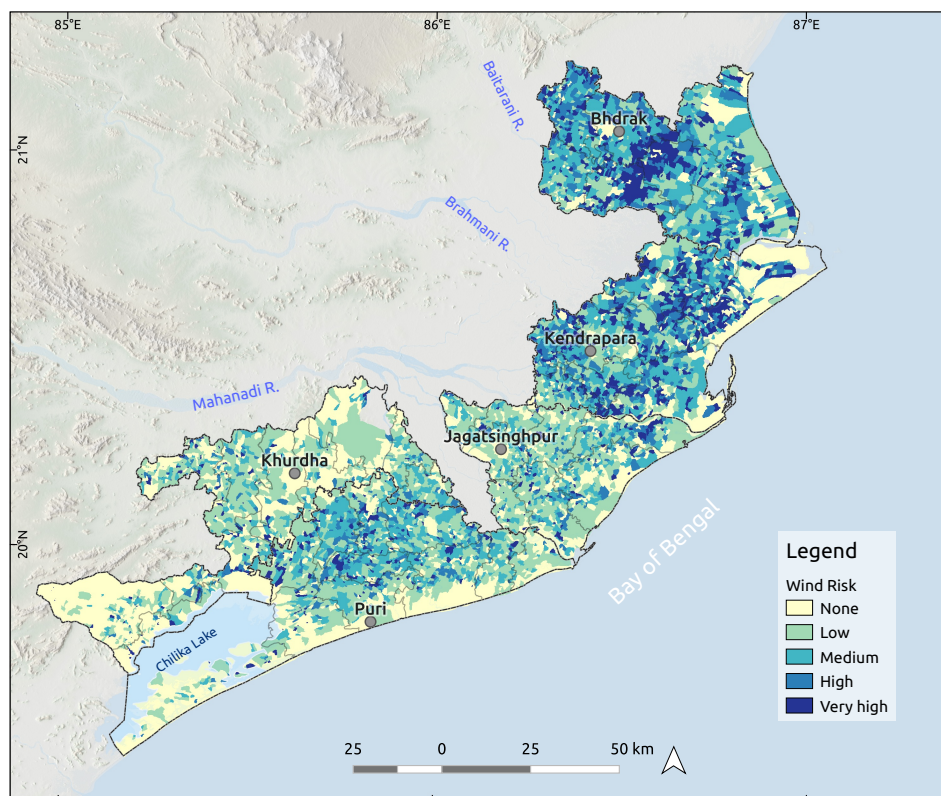


Figure 5.6: Wind risk map of the delta

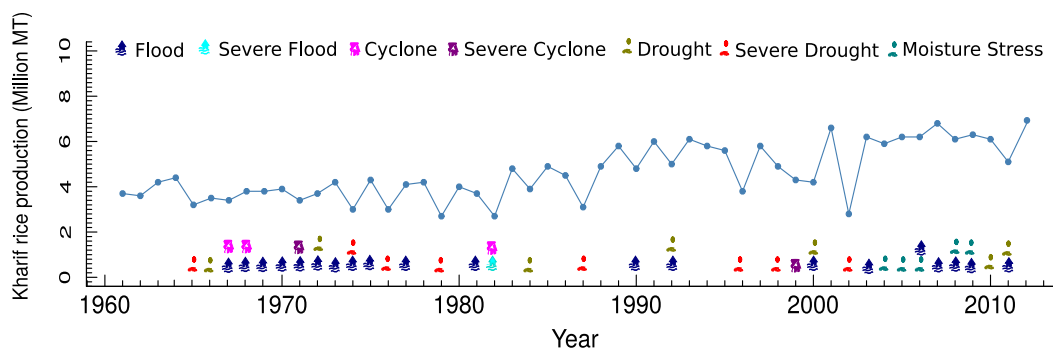


Figure 5.7: Effects of extreme climatic events on Kharif rice production in Odisha

5.2 Soil analysis

5.2.1 Soil data and ratings

All the soil data were interpolated to fill the spatial cell designed to represent the study area. The resulted maps are presented in Figs. 5.8, 5.9, 5.10, 5.11, 5.12, 5.13, 5.14, 5.15 and 5.16.

Table 5.2: Suitability rating for nutrient retention capacity based on the cation exchange capacity (cmol/kg) [after Fischer et al. (2021)]

Crops	I CECs 100	I CECs 90	I CECs 70	II CECs 50	I CECs 30	I CECs 10
Wheat	10	8	4	2	0	999
Rice (wetland)	8	6	3	2	0	999
Rice (dryland)	8	6	3	2	0	999
Maize	10	8	4	2	0	999
Potato (white)	9	7	4	2	0	999
Potato (sweet)	10	8	4	2	0	999
Sugarcane	10	8	4	2	0	999
Gram	10	8	4	2	0	999
Groundnut	8	6	3	2	0	999
Sunflower	10	6	3	2	0	999
Rape	10	8	4	2	0	999
Cabbage	10	8	4	2	0	999
Carrot	10	8	4	2	0	999
Onion	10	8	4	2	0	999
Tomato	10	8	4	2	0	999

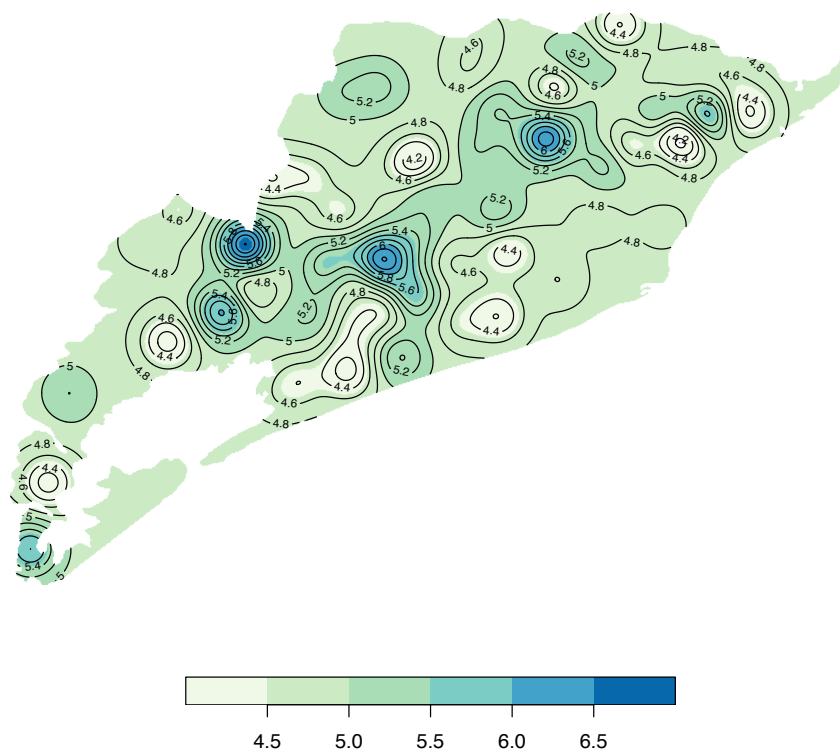


Figure 5.8: Spatial distribution of soil pH in the study area

Table 5.3: Suitability rating based on the exchangeable sodium percentage - ESP (%) [after Fischer et al. (2021)]

Crops	H+I+L ESP 100	H+I+L ESP 90	H+I+L ESP 70	H+I+L ESP 50	H+I+L ESP 30	H+I+L ESP 10
Wheat	15	20	35	45	999	100
Rice (wetland)	10	20	30	40	999	100
Rice (dryland)	10	20	30	40	999	100
Maize	8	15	20	25	999	100
Potato (white)	15	25	35	45	999	100
Potato (sweet)	8	15	20	25	999	100
Sugarcane	5	10	15	20	999	100
Gram	8	15	20	25	999	100
Groundnut	8	10	15	20	999	100
Sunflower	8	15	20	25	999	100
Rape	8	15	20	25	999	100
Cabbage	8	15	20	25	999	100
Carrot	10	20	35	50	999	999
Onion	10	20	35	50	999	100
Tomato	8	15	25	35	999	100

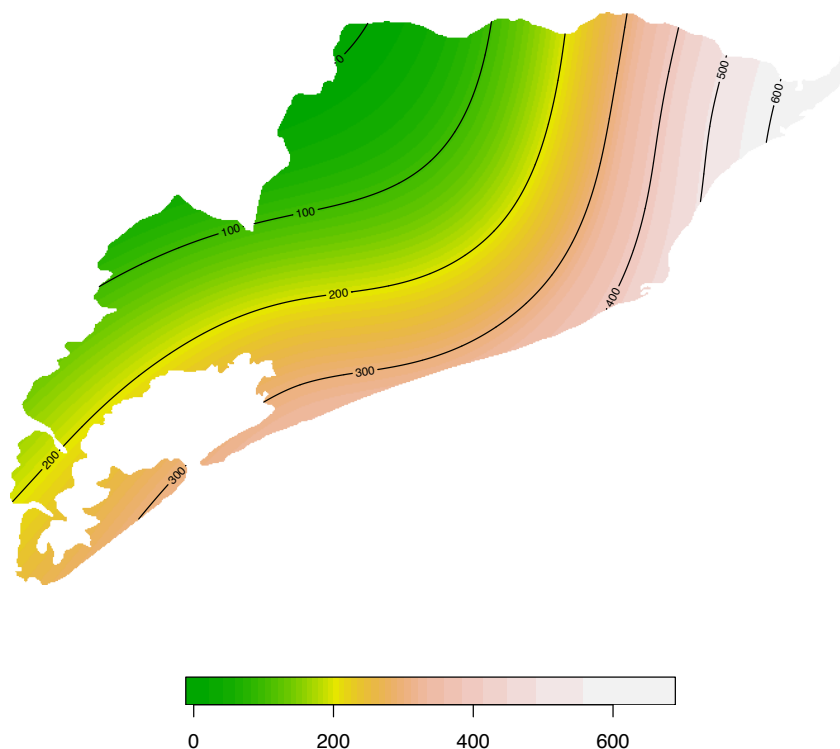


Figure 5.9: Spatial distribution of soil electric conductivity (salinity $\mu\text{S}/\text{cm}$) in the study area

Table 5.4: Suitability rating based on electric conductivity (dS/m), presence of salinity [after Fischer et al. (2021)]

Crops	H+I+L EC 100	H+I+L EC 90	H+I+L EC 70	H+I+L EC 50	H+I+L EC 30	H+I+L EC 10
Wheat	1	3	5	6	10	100
Rice (wetland)	1	2	4	6	12	100
Rice (dryland)	1	2	4	6	12	100
Maize	2	4	6	8	12	100
Potato (white)	1	3	5	6	10	100
Potato (sweet)	1	3	6	10	999	100
Sugarcane	2	5	8	10	14	100
Gram	2	3	5	7	999	100
Groundnut	2	4	6	8	12	100
Sunflower	2	4	9	12	999	100
Rape	1	2	4	6	999	100
Cabbage	3	4.5	7	10	999	100
Carrot	1	1.5	4.5	7	999	999
Onion	1	2	3	5	999	100
Tomato	3	5	8	10	999	100

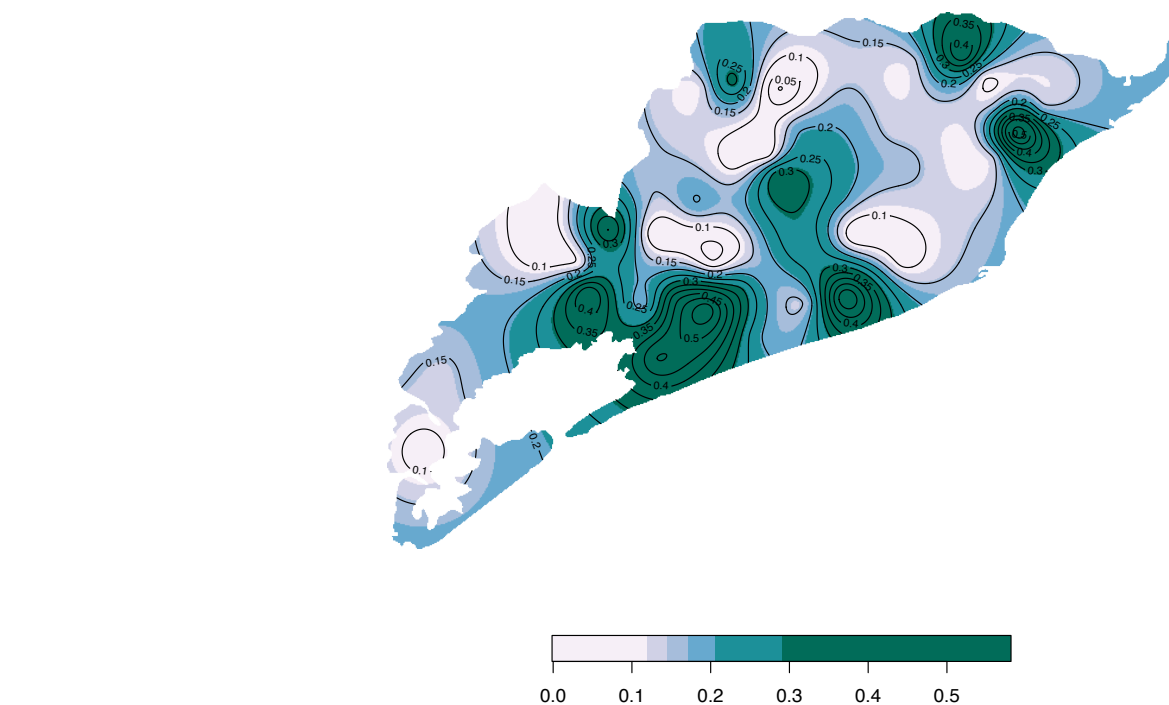


Figure 5.10: Spatial distribution of soil potassium in the study area

Table 5.5: Suitability rating based on soil depth (cm) [after Fischer et al. (2021)]

Crops	I+L RC 100	I+L RC 90	I+L RC 70	I+L RC 50	I+L RC 30	I+L RC 10
Wheat	70	35	999	20	10	0
Rice (wetland)	85	70	999	35	20	0
Rice (dryland)	90	70	999	35	20	0
Maize	85	70	999	35	20	0
Potato (white)	75	60	999	30	20	0
Potato (sweet)	85	70	999	35	20	0
Sugarcane	90	70	999	40	25	0
Gram	75	70	999	35	20	0
Groundnut	85	70	999	40	25	0
Sunflower	100	85	999	70	50	0
Rape	85	70	999	35	20	0
Cabbage	85	70	999	35	20	0
Carrot	85	70	999	50	35	0
Onion	85	70	999	25	20	0
Tomato	85	70	999	50	35	0

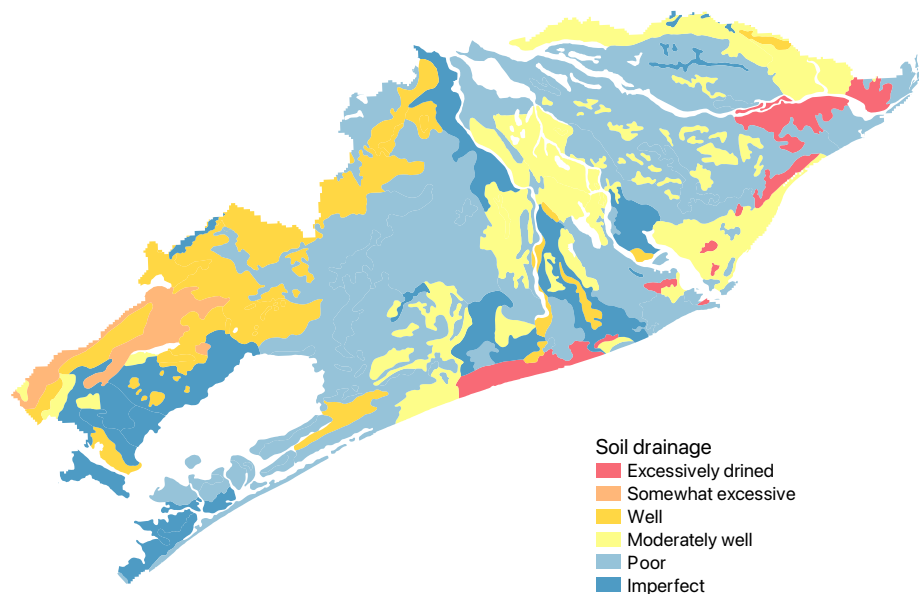


Figure 5.11: Spatial distribution of soil drainage class in the study area

Table 5.6: Suitability rating based total exchangeable bases (cmol/kg) [after Fischer et al. (2021)]

Crops	I+L TEB 100	I+L TEB 90	I+L TEB 70	I+L TEB 50	I+L TEB 30	I+L TEB 10
Wheat	8	5	3.5	2	0	999
Rice (wetland)	6.5	4	2.8	1.6	0	999
Rice (dryland)	4	2.8	1.6	0	999	999
Maize	8	5	3.5	2	0	999
Potato (white)	5	3.5	2	0	999	999
Potato (sweet)	5	3.5	2	0	999	999
Sugarcane	8	5	3.5	2	0	999
Gram	5	3.5	2	0	999	999
Groundnut	4	2.8	1.6	0	999	999
Sunflower	4	2.8	1.6	0	999	999
Rape	5	3.5	2	0	999	999
Cabbage	5	3.5	2	0	999	999
Carrot	4	2.8	1.6	0	999	999
Onion	5	3.5	2	0	999	999
Tomato	5	3.5	2	0	999	999

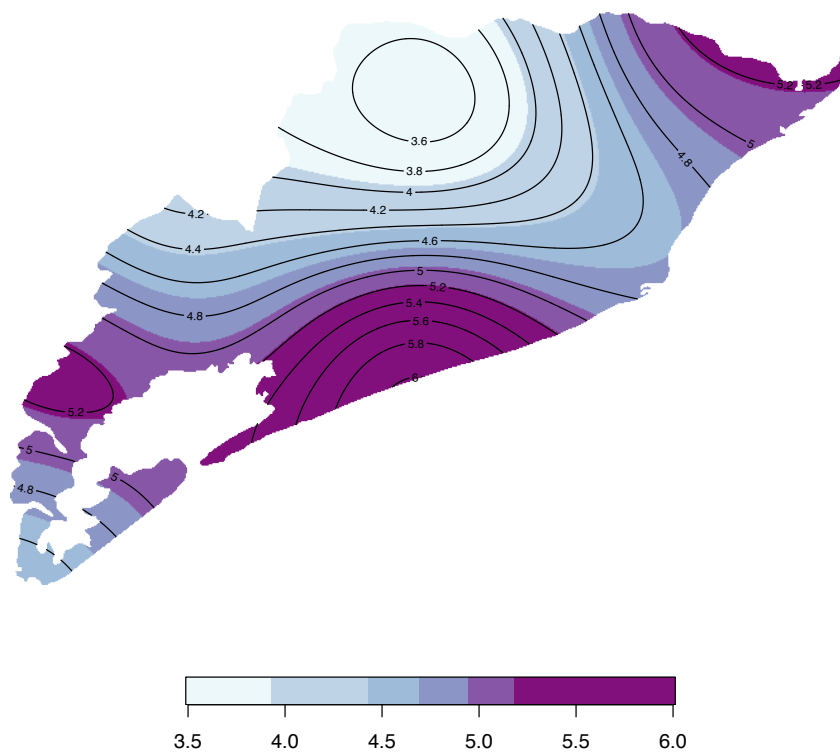


Figure 5.12: Spatial distribution of soil calcium in the study area

Table 5.7: Suitability rating based soil pH [after Fischer et al. (2021)]

Crops	I+L pH 100	I+L pH 90	I+L pH 70	I+L pH 50	I+L pH 30	I+L pH 10
Wheat	6.5	6	5.6	5.2	4.7	4.2
Rice (wetland)	6	5.5	5	4.5	4.1	3.6
Rice (dryland)	6	5.5	5	4.5	4.1	3.6
Maize	6.2	5.8	5.5	5.2	4.7	4.2
Potato (white)	6	5.6	5.2	4.8	4.3	3.8
Potato (sweet)	6	5.2	4.8	4.5	4.1	3.6
Sugarcane	6	5.5	5	4.5	4.1	3.6
Gram	6	5.5	5.4	5.2	4.7	4.2
Groundnut	6.5	6	5.6	5.4	4.9	4.3
Sunflower	6.2	6	5.5	5	4.5	4.0
Rape	6	5.6	5.2	4.8	4.3	3.8
Cabbage	6.2	6	5.8	5.5	5.0	4.4
Carrot	6.2	6	5.7	5.2	5	4.4
Onion	6.2	6	5.8	5.5	5.0	4.4
Tomato	6.2	6	5.5	5	4.5	4.0

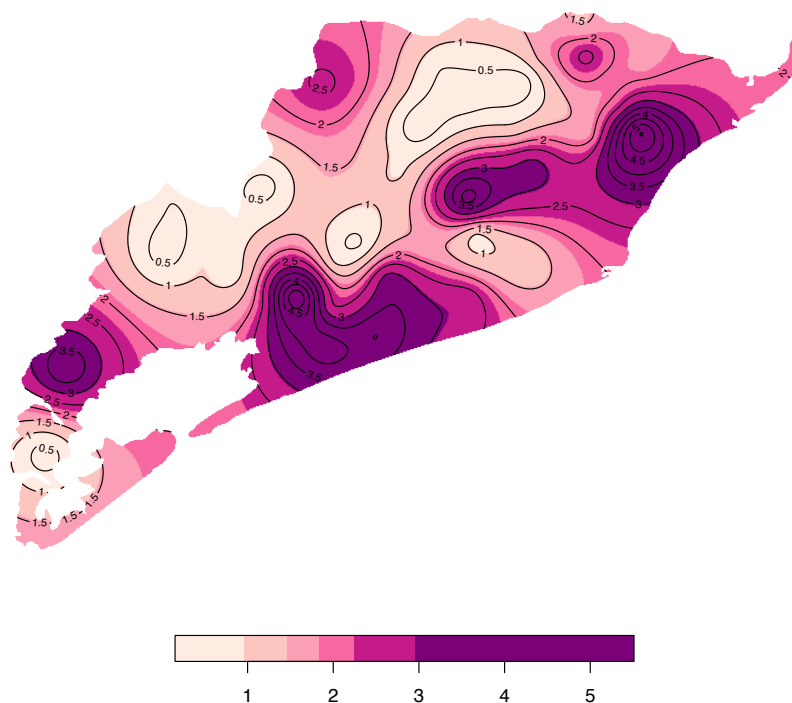


Figure 5.13: Spatial distribution of soil magnesium in the study area

Table 5.8: Suitability rating based on soil texture class [after Fischer et al. (2021)]

Crops	Clay, silt, clay loam, silt, silt loam, loam, sandy clay loam	Sandy loam	Loamy sand	Sand	I+L pH 10
Wheat	100	90	70	30	4.2
Rice (wetland)	100	90	50	30	3.6
Rice (dryland)	100	90	70	30	3.6
Maize	100	90	70	30	4.2
Barley	100	90	70	30	3.8
Sugarcane	100	90	70	30	3.6
Gram	100	90	70	50	3.6
Groundnut	100	90	70	50	4.2
Sunflower	100	90	70	30	4.3
Rape	100	90	70	30	4.0
Cabbage	100	90	70	30	3.8
Carrot	100	90	70	30	4.4
Onion	100	90	70	30	4.4
Tomato	100	90	70	30	4.4

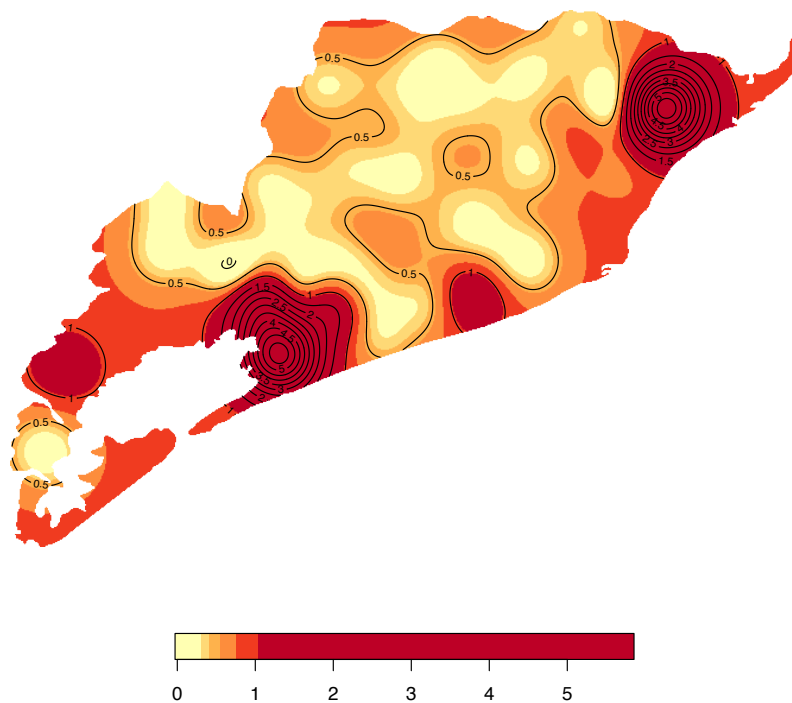


Figure 5.14: Spatial distribution of soil sodium in the study area

Table 5.9: Suitability rating based on soil drainage [after Fischer et al. (2021)]

Crops	Very Poor	Poor	Imperfectly	Moderately well	Well	Somewhat excessive	Excessive
Wheat	10	50	90	100	100	100	100
Rice (wetland)	50	90	100	100	100	70	10
Rice (dryland)	10	50	90	100	100	100	100
Potato (white)	10	30	70	90	100	100	100
Potato (sweet)	10	30	70	90	100	100	100
Sugarcane	30	70	90	100	100	100	100
Gram	10	50	90	100	100	100	100
Sunflower	10	50	90	100	100	100	100
Rape	10	50	90	100	100	100	100
Cabbage	10	30	70	90	100	100	100
Carrot	10	30	70	90	100	100	100
Onion	10	30	70	90	100	100	100
Tomato	10	30	70	90	100	100	100
Tomato	100	90	70	30	4.4		

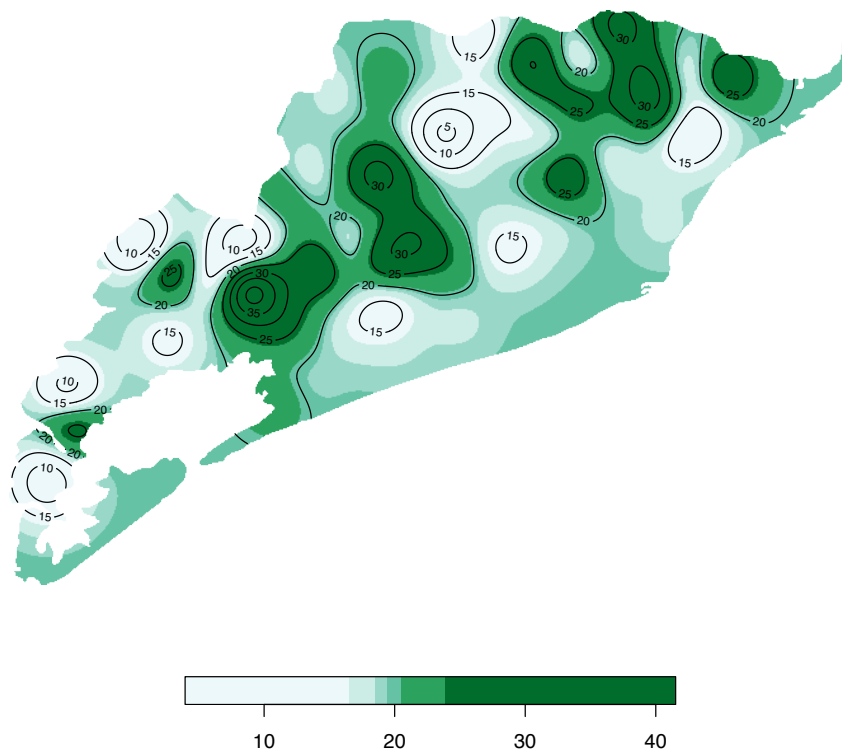


Figure 5.15: Spatial distribution of proportion of silt (%) in the study area

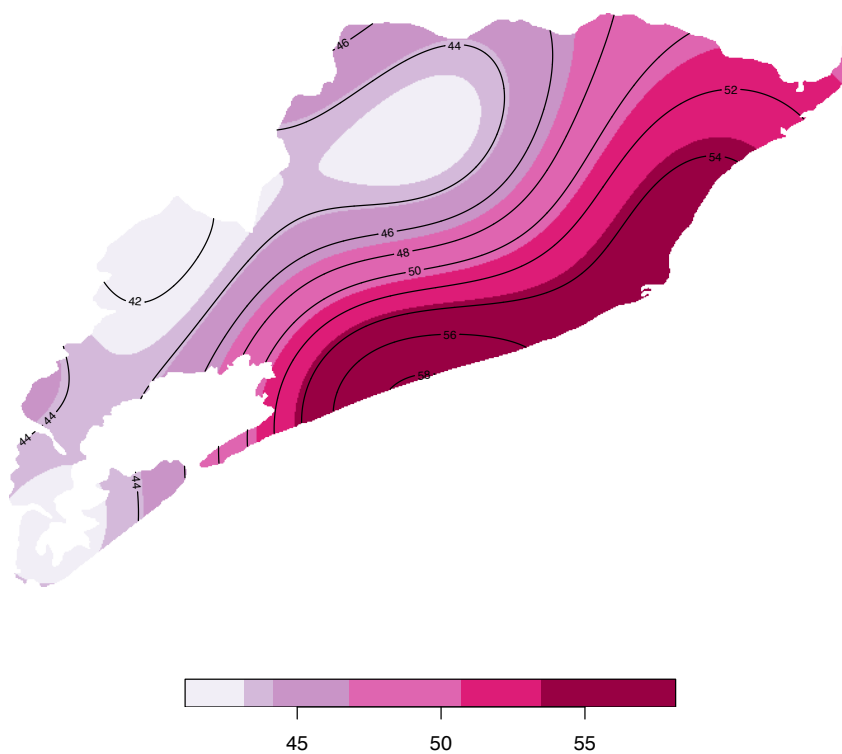


Figure 5.16: Spatial distribution of proportion of clay (%) in the study area

5.2.2 Soil suitability

The delta is suitable for most the common crops. The rating used to derived the suitability map are given in Tables 5.2, 5.3, 5.4, 5.5, 5.6, 5.7, 5.8 and 5.9. Most marginally and not suitable areas are located across the shore line due to the high salinity in these area. A small patch of marginally suitable area is located near the Khoorda area. The drainage condition in this area is poor.

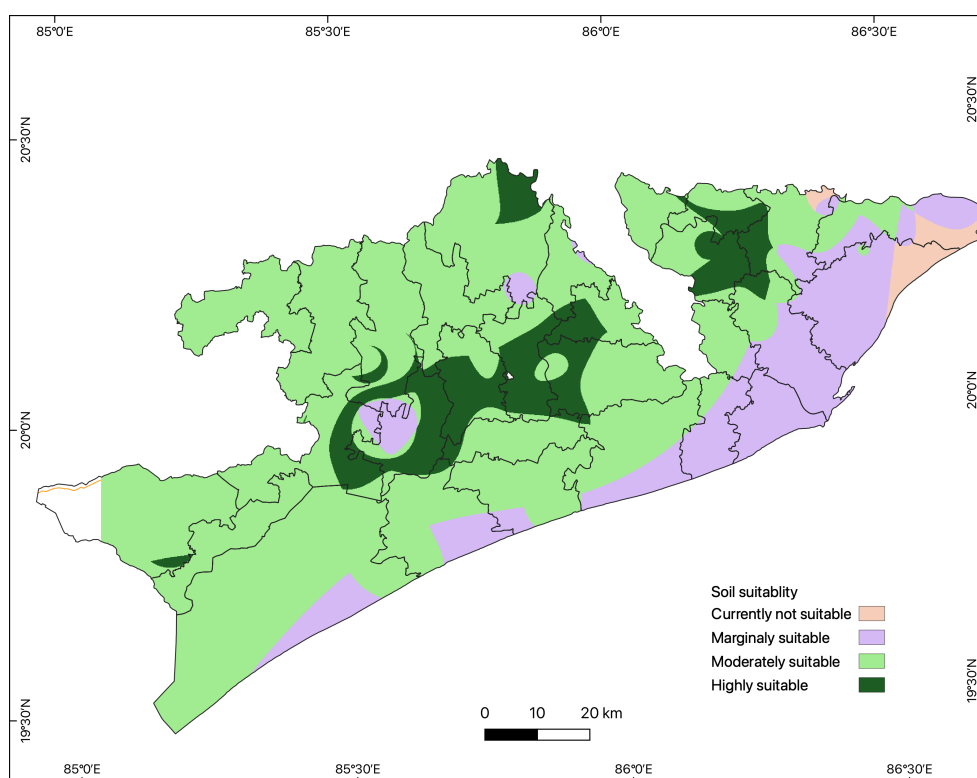


Figure 5.17: Spatial distribution of multi-crop suitability in the study area

5.3 Water requirement and yield response to climate change

The Mahanadi delta experiences we humid climate according to the De Martonne Aridity index. Fig. 5.18, Fig. 5.19 and Fig. 5.20 portray hydrological regime in the

Table 5.10: Areal distribution of suitability categories in the study area

Suitability class	Area (km ²)	Area (%)
Currently not suitable	145.78	1.89
Marginally suitable	1376.27	17.88
Moderately suitable	5210.20	67.70
Highly suitable	963.72	12.52
Total	7695.96	100.00

delta. These figure show that there is an increasing trend in the three climate variables.

Water requirement and yield response to climate change analysi were performed on the five commomn crops in the delta these are: i) Paddy, ii) Wheat, iii) Black gram, iv) Green gram and v) groundnut

5.3.1 Paddy

Paddy is the common crop in the entire delta, particularity in the Kharif season. There are some double and triple cropping cropland that are used to cultivate paddy. The result of the simulations show that there is an increase in yield in the far future in both the climate scenarios with an increasing uncertainty as well. Whereas, the irrigation require is less than that of the historical period with variability. The variability of yield rate is higher in the RCP 8.5 in the period between 2061 and 2080 (Fig. 5.21).

5.3.2 Wheat

Wheat is also an import crop in the delta, cultivated mostly in the mainland of the delta. The yield response is similar to paddy, i.e, comparatively higher yield in the far future. The irrigation requirement is less than that of the baseline period. The variability of irrigation demand is higher after 2040 and the variability of yield rate is higher in RCP8.5 (Fig. 5.22).

5.3.3 Black and green grams

Black and green gram are shown in the residual moisture in this region. The delta produces a considerable amount of black and green gram in the Rabi season. The result of the simulation for grams crops show a higher yield rate in the far future, particularly after 2040 in RCP4.5. Irrigation demand is lower than that of the baseline condition (Fig. 5.23).

5.3.4 Groundnut

Groundnut is also an important crop in the Rabi and zaid seasons. The results of the simulations show that there is an increasing trend in the yield of ground in the region. Irrigation requirement is almost constant in all the periods and RCPs (Fig. 5.24).

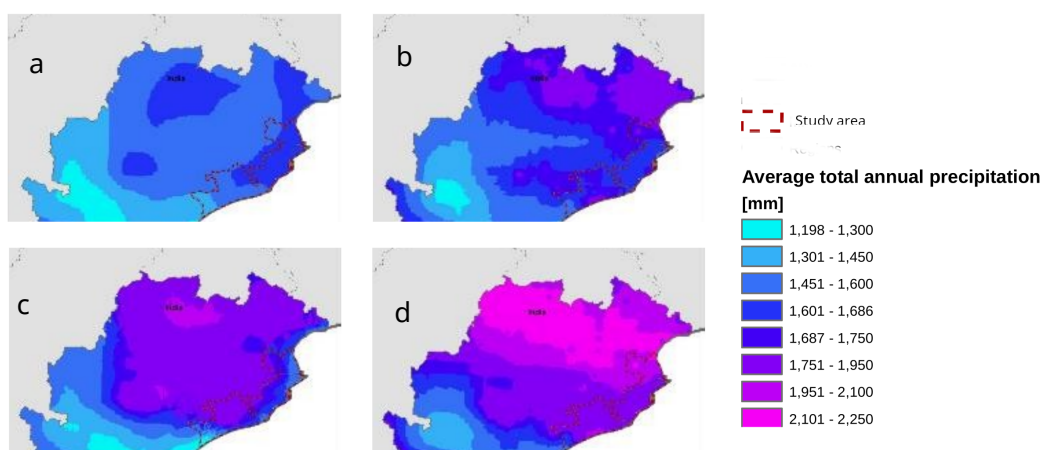


Figure 5.18: Average annual rainfall distribution in the study area, a) historical, b) 2020s, c) 2050s, d) 2080s

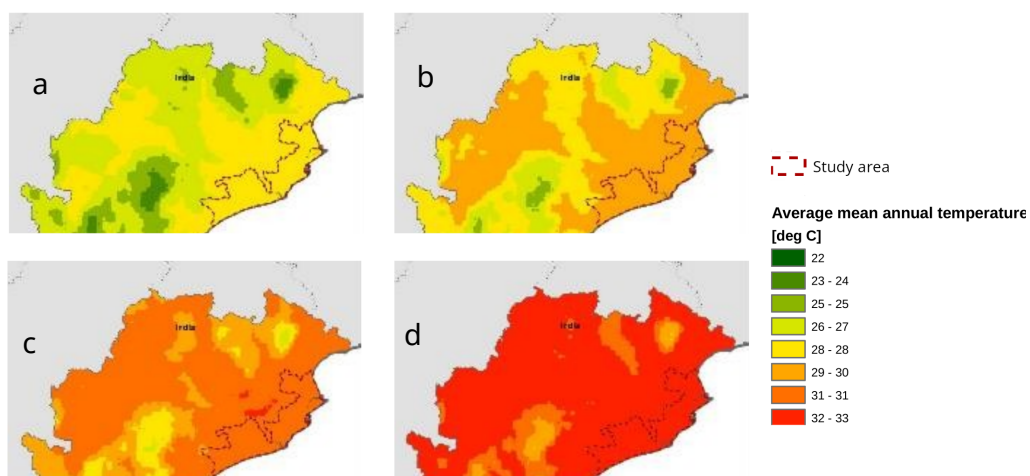


Figure 5.19: Average mean temperature distribution in the study area, a) historical, b)2020s, c) 2050s, d) 2080s

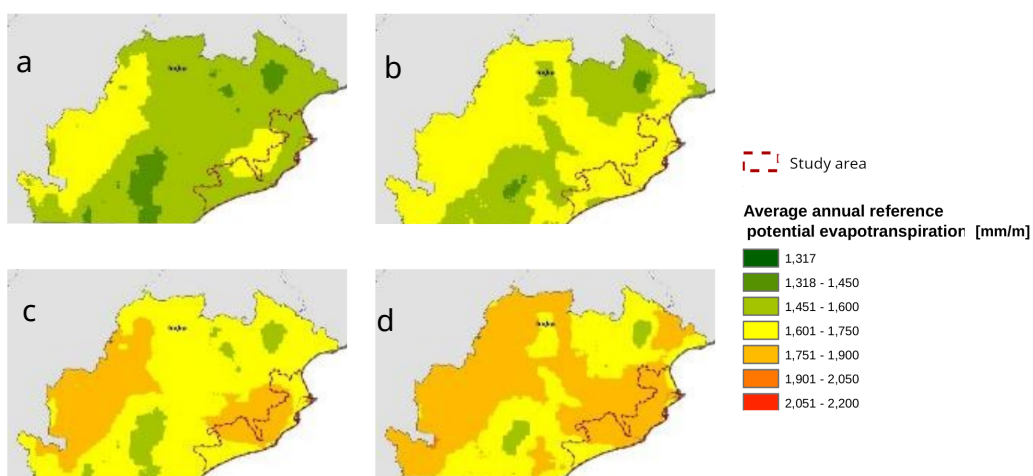


Figure 5.20: Average reference evapotranspiration distribution in the study area, a) historical, b)2020s, c) 2050s, d) 2080s

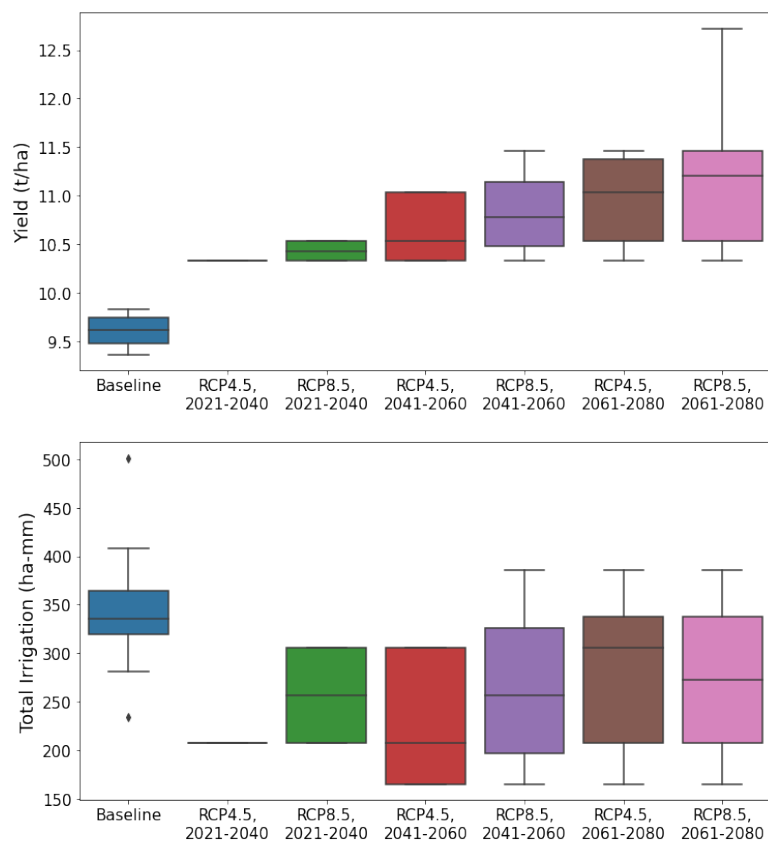


Figure 5.21: Yield response and irrigation requirement for the paddy in the baseline and future scenarios

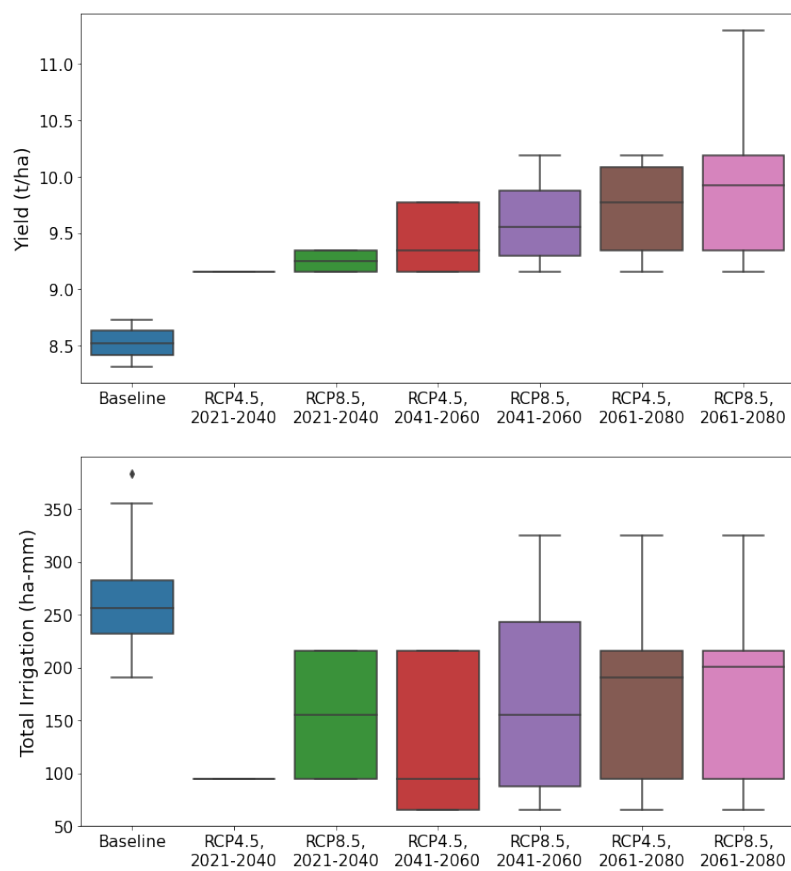


Figure 5.22: Yield response and irrigation requirement for the wheat in the baseline and future scenarios

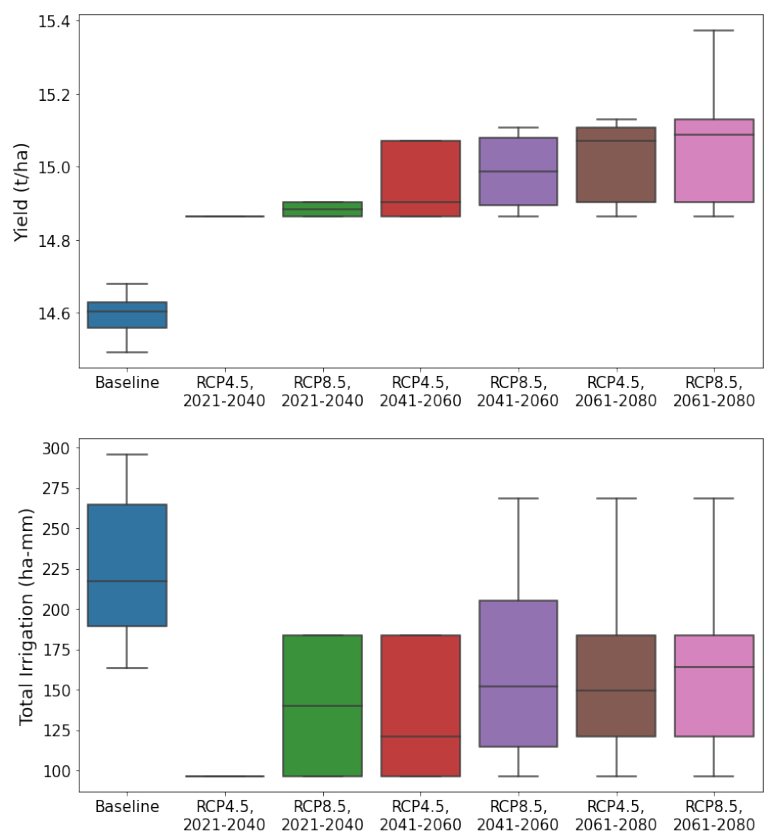


Figure 5.23: Yield response and irrigation requirement for black and green grams in the baseline and future scenarios

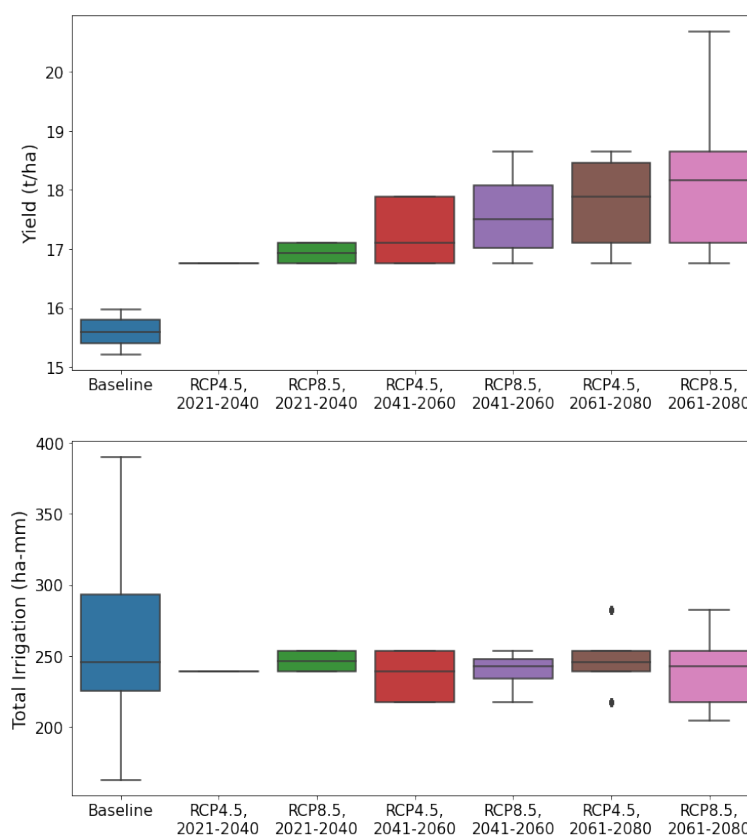


Figure 5.24: Yield response and irrigation requirement for potato in the baseline and future scenarios

5.4 Decadal occurrences of dry spells

Numerous climate-related factors are profoundly impacted by variations in precipitation's intensity and duration. The monsoonal peak flood at the delta apex (Naraj) has been delayed by nearly 20 days, as depicted in Fig. ???. A dry spell is one of the many factors that directly affect crop production. It is a stretch of time during which the weather has been unusually dry. Compared to a drought, a dry spell is less severe and lasts for a shorter time (Wilhite and Glantz, 1985). However, different threshold levels and definitions of dry spell have been utilised by various authors (Usman and Reason, 2004; Ceballos et al., 2004; Peiris, 2008). Understanding the future water needs requires an understanding of the dry periods.

During the *kharif* season, the two selected climate scenarios' longest and most frequent dry spells were evaluated. The average and longest dry spell durations in the 2020s are longer in RCP 4.5 than in RCP 8.5. The Khordha and Puri districts have slightly higher values (Figs. 5.26, 5.27, 5.27 and 5.29). When dry spells extend more than a particular number of days in well-drained locations, it is essential to supply supplemental irrigation. According to crop water requirement research, the value persists for approximately fifteen days on average.

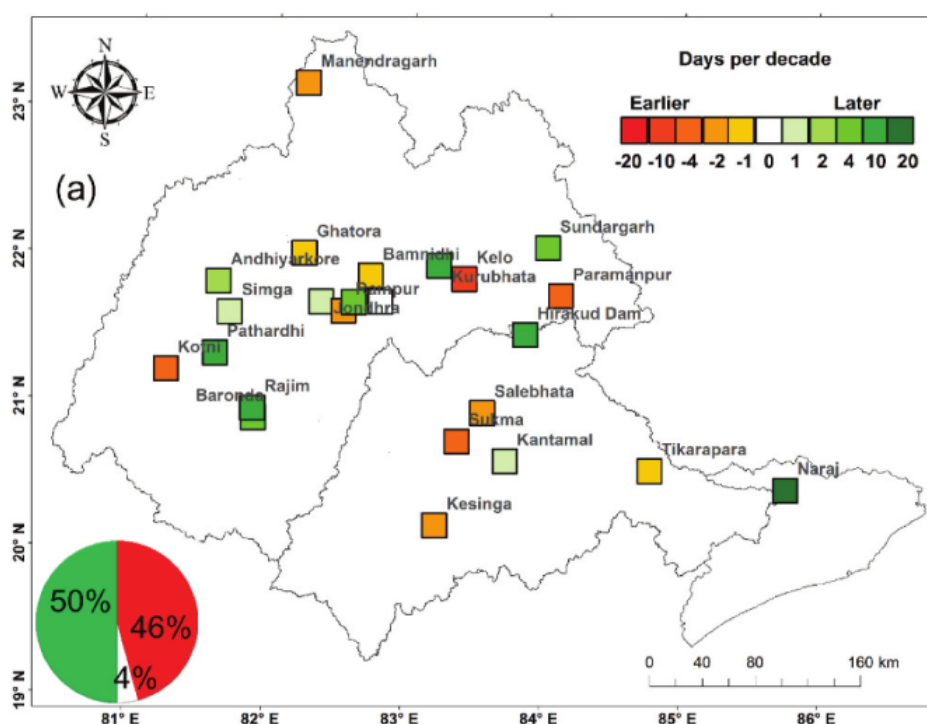


Figure 5.25: Variations in flood timing trends across the Mahanadi basin [Source: Ganguli et al. (2022)]

For both the average and longest dry spell scenarios in the 2030s, the dry spell durations under RCP 4.5 are almost comparable to those under RCP 8.5. With the heaviest dry spell, this is the situation. The values are marginally lower in the district of Khordha, while marginally higher in the districts of Bhadrak, Kendapara, and Jagatsinghpur (Figs. 5.30, 5.31, 5.31 and 5.33). Well-drained areas require supplementary irrigation when dry spells last more than 15 days.

In the 2040s, the lengths of dry spells are almost identical in RCP 4.5 and RCP 8.5 in both the average and longest dry spell cases. This holds true for both the

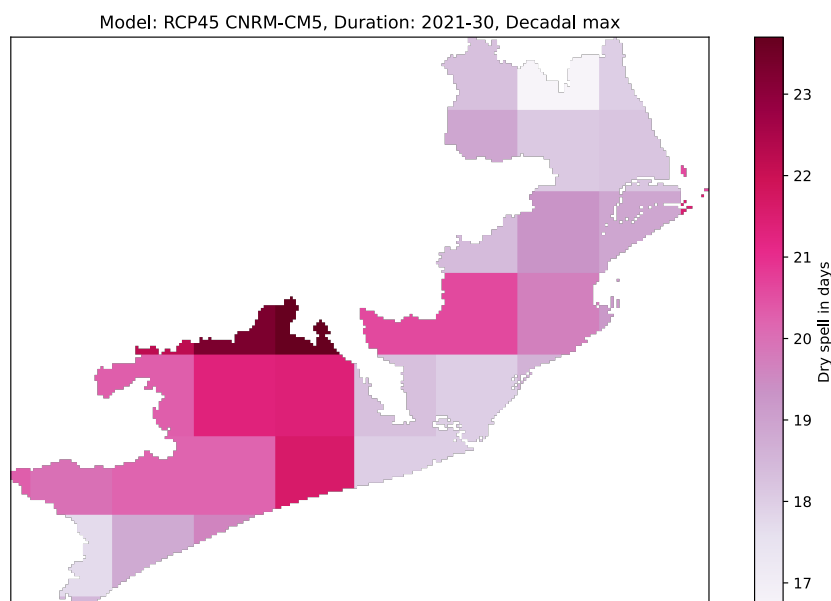


Figure 5.26: Predicted longest dry spell days from 2021 to 2030 for the RCP 4.5 emission scenario using CNRM's CM5 model

average and longest dry spell cases. The Khordha district and certain areas of the Bhadrak district have slightly higher averages of dry spells than the rest of the district (Figs. 5.34, 5.35, 5.35 and 5.37). Nearly 17 days is the lowest value among all situations. Therefore, additional irrigation is needed in districts with well-drained areas where moisture deficits may emerge over this decade.

In the middle of the century, the shorter durations of dry spells are projected in RCP 4.5 compared to RCP 8.5 for both the average and longest dry spell cases. In RCP 4.5, the values for the average and longest dry spell durations fluctuate around 15 days, whereas in RCP 8.5, the values range anywhere from 12 to 20 days. Because of this, the spatial variability of the RCP 8.5 scenario is noticeably higher than that of the RCP 4.5 scenario. It is also abundantly clear that the values of dry spells in the districts of Khordha and Puri are higher in comparison to those in the other districts that make up RCP 8.5 (Figs. 5.38, 5.39, 5.39 and 5.41). The Khurada and Puri districts have the highest values of dry spells, which indicates that supplemental irrigation is necessary in the well-drained regions of districts where moisture deficits could occur during this decade.

In the 2060s, RCP 8.5 predicted shorter dry spell durations than RCP 4.5 for

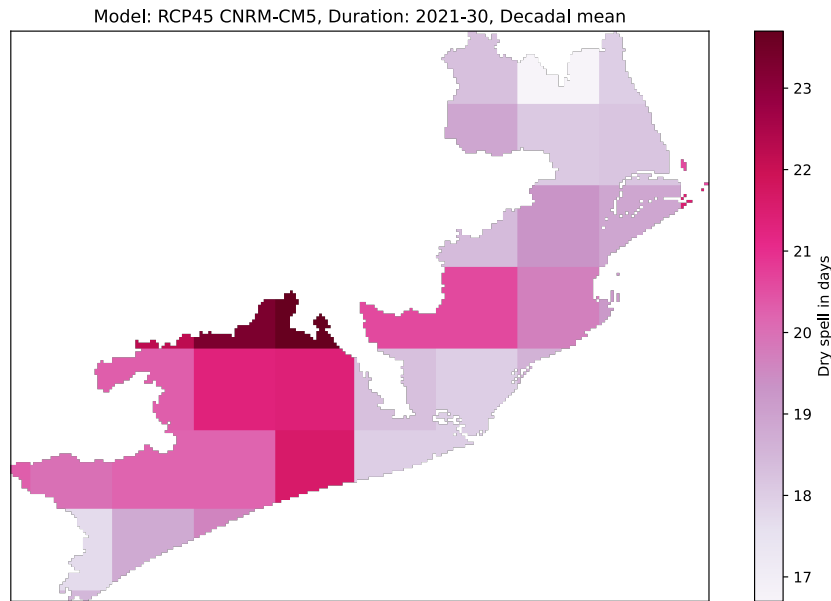


Figure 5.27: Predicted average dry spell days from 2021 to 2030 for RCP 4.5 emission scenario using CNRM's CM5 model

both the average and longest dry spell situations. The average and longest lengths of dry spells in RCP 8.5 range between 15 and 17 days, whereas the corresponding values in RCP 4.5 range between 13 and 18 days. Consequently, the spatial variability of RCP 4.5 is considerably greater than that of RCP 8.5. The higher dry spell high spell zone will be relocated to the districts of Bhadrak and Kendapara during this decade. It is also evident that the values of dry periods in the districts of Bhadrak and Kendapara are more than those of the other districts in RCP 4.5 (Figs. 5.42, 5.43, 5.43 and 5.45). The highest values for dry spells in Bhadrak and Kendapara districts over the this decade indicate that supplemental irrigation is required in well-drained districts where moisture deficiencies may occur.

In the 2070s, both the average and longest dry spell cases are predicted to be shorter in RCP 8.5 in comparison to RCP 4.5. RCP 8.5 has values for both the average and longest dry period duration of 15–23 days, while RCP 4.5 has values of 15–19 days. For this reason, RCP 4.5 and RCP 8.5 share analogues in terms of both regional variability and zonation. In this decade, the Puri and Khordha districts will once again be part of the upper dry spell high spell zone. Similarly, in both RCP 4.5 and 8.5, the values of dry spells in the Puri and Khordha districts

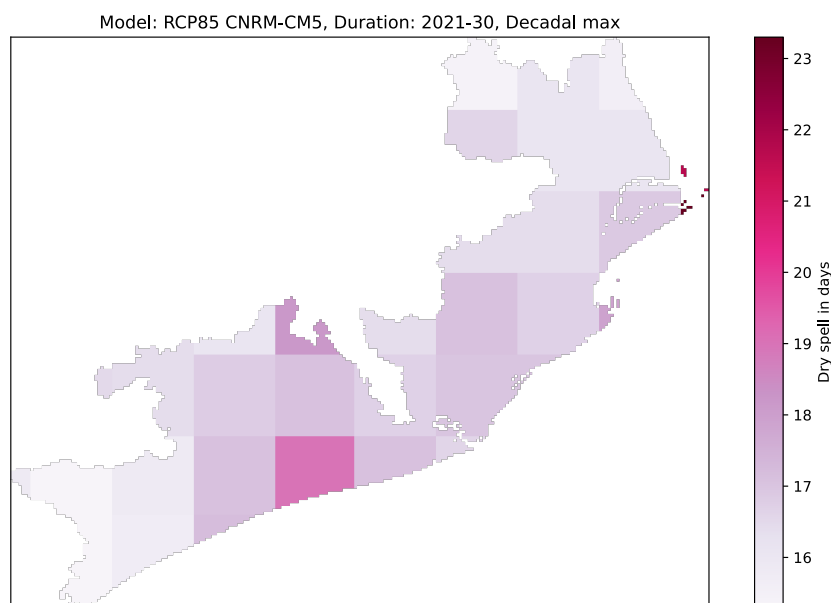


Figure 5.28: Predicted longest dry spell days from 2021 to 2030 for RCP 8.5 emission scenario using CNRM's CM5 model

are clearly higher than in the other districts (Figs. 5.46, 5.47, 5.47 and 5.49). As a result, in districts where moisture deficits could occur due to such long dry spells, supplementary irrigation is required in the well-drained regions.

There is very little spatial variation in the RCPs for both the average and longest dry spell cases in the 2080s. As well as low-lying areas with high values, both RCPs have a few places where the values are relatively high. RCP 8.5 has average and maximum dry spell durations of 17–23 days, while RCP 4.5 has values of 16–20 days. For this reason, RCP 4.5 and RCP 8.5 share analogues in terms of both spatial variability and zonation. For this decade, under RCP 8.5, the slightly higher dry spell high spell zone would return to the Bhadrak and Kendapara districts. Dry spell values in RCP 4.5 and 8.5 show a clear variation between 17 and 28 days (Figs. 5.50, 5.51, 5.51 and 5.53). Supplementary irrigation is still required in the well drained regions of districts where moisture deficit could occur due to such long dry spells despite the fact that the spatial variation is almost same.

In the 2090s, the average and longest dry spell cases, as well as the RCPs, all have shorter durations than the preceding decades. Comparatively, RCP 4.5

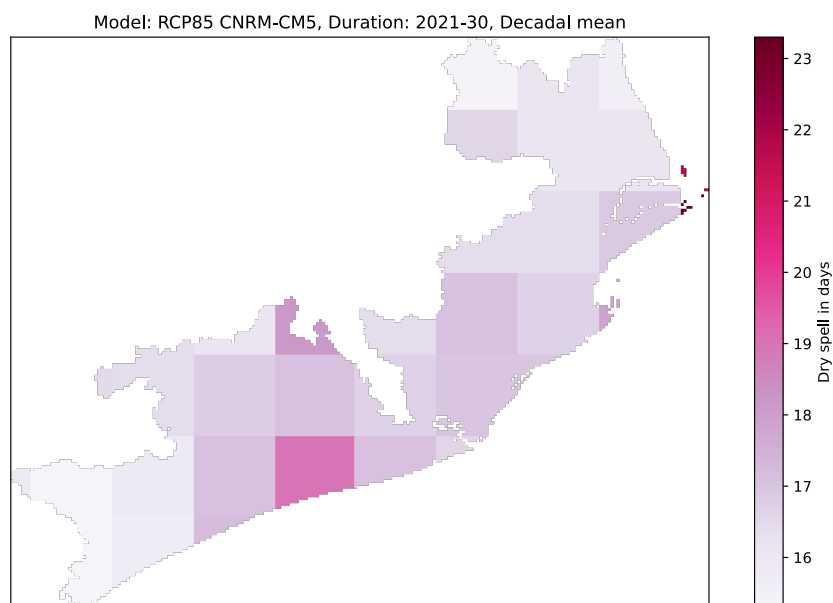


Figure 5.29: Predicted average dry spell days from 2021 to 2030 for RCP 8.5 emission scenario using CNRM's CM5 model

predicts an average and maximum dry spell duration of 15 to 18 days, while RCP 8.5 predicts 13 to 15 days (Figs. 5-54, 5-55, 5-55 and 5-57). In RCP 4.5, the values are slightly greater in the Khordha district. In some areas of the Khordha district, supplemental irrigation may be required during this decade.

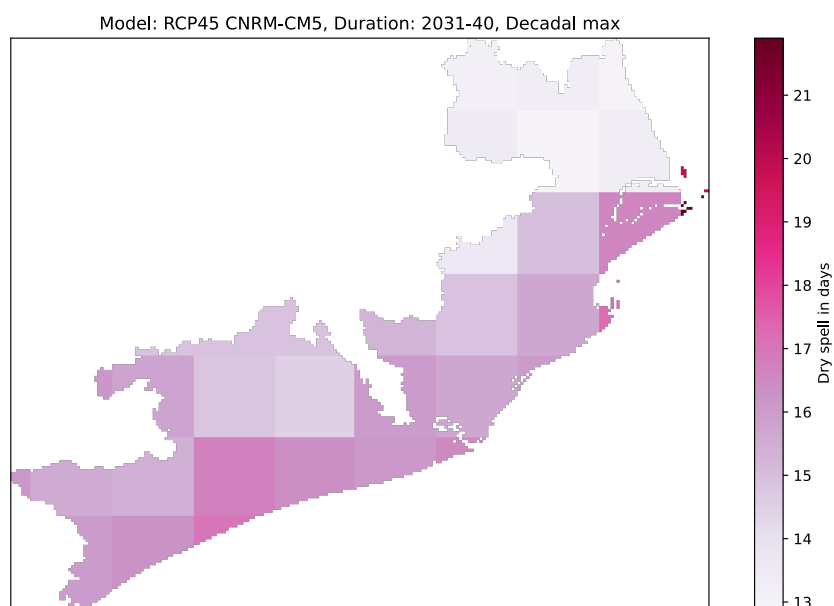


Figure 5.30: Predicted longest dry spell days from 2031 to 2040 for RCP 4.5 emission scenario using CNRM's CM5 model

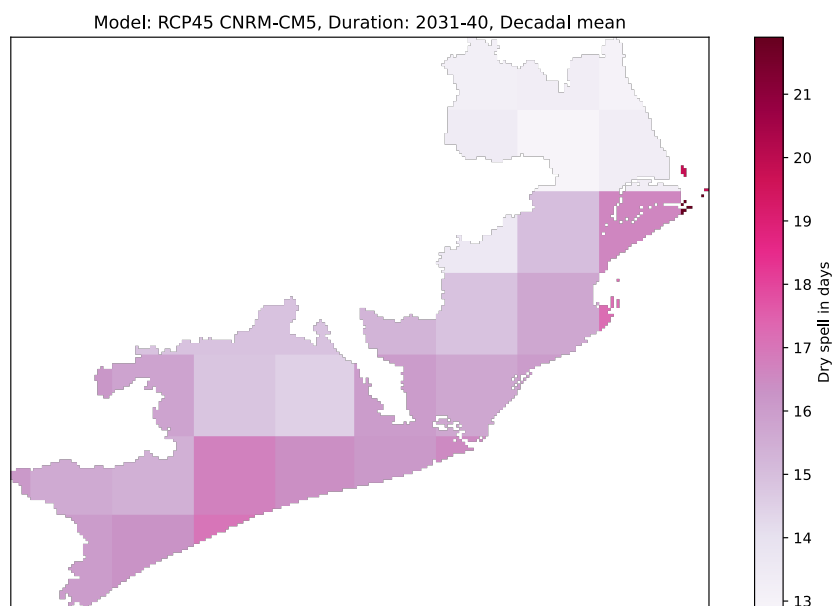


Figure 5.31: Predicted average dry spell days from 2031 to 2040 for RCP 4.5 emission scenario using CNRM's CM5 model

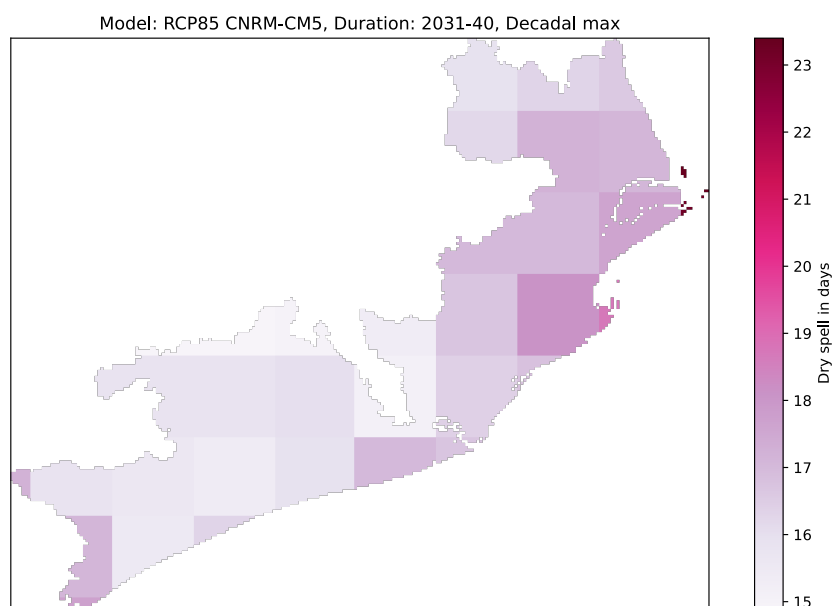


Figure 5.32: Predicted longest dry spell days from 2031 to 2040 for RCP 8.5 emission scenario using CNRM's CM5 model

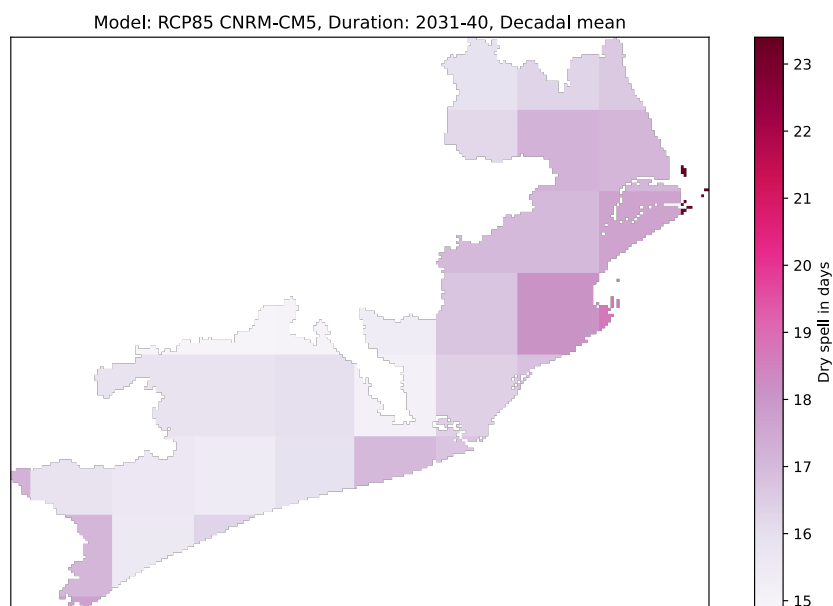


Figure 5.33: Predicted average dry spell days from 2031 to 2040 for RCP 8.5 emission scenario using CNRM's CM5 model

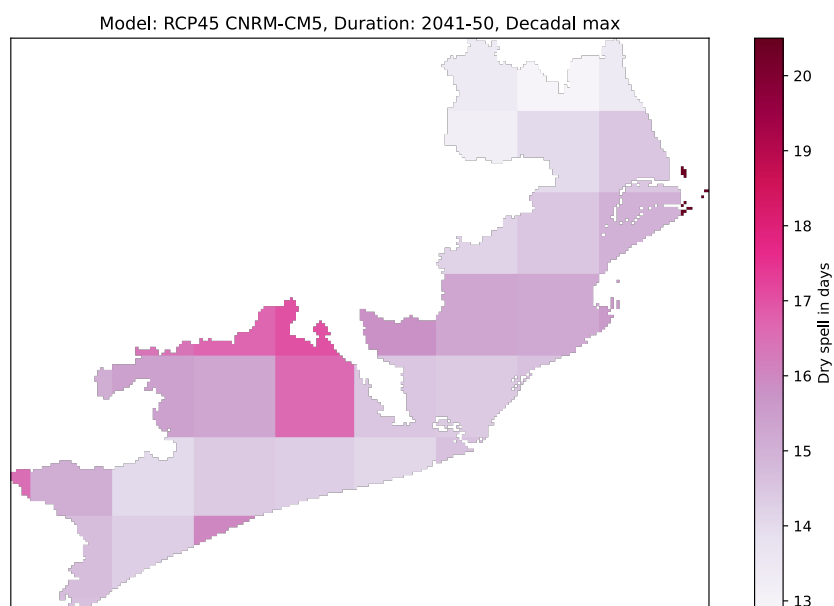


Figure 5.34: Predicted longest dry spell days from 2041 to 2050 for RCP 4.5 emission scenario using CNRM's CM5 model

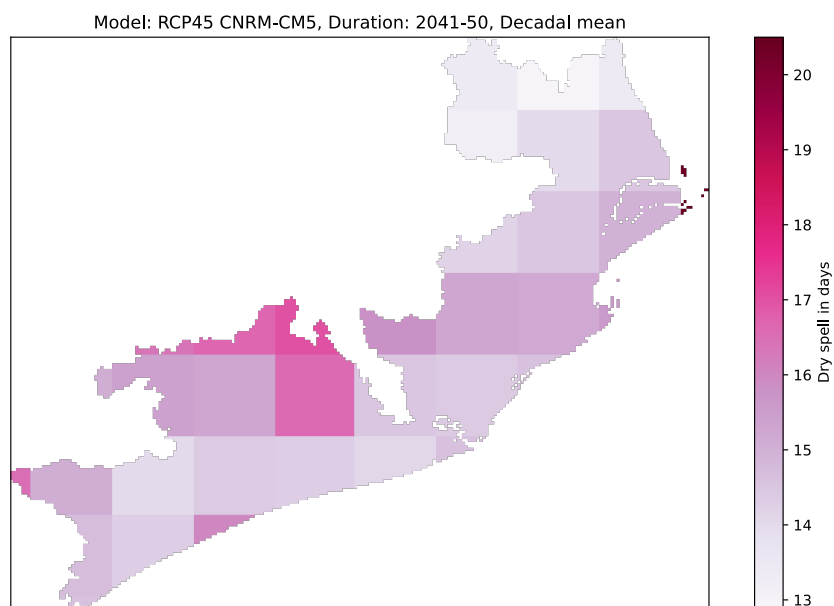


Figure 5.35: Predicted average dry spell days from 2041 to 2050 for RCP 4.5 emission scenario using CNRM's CM5 model

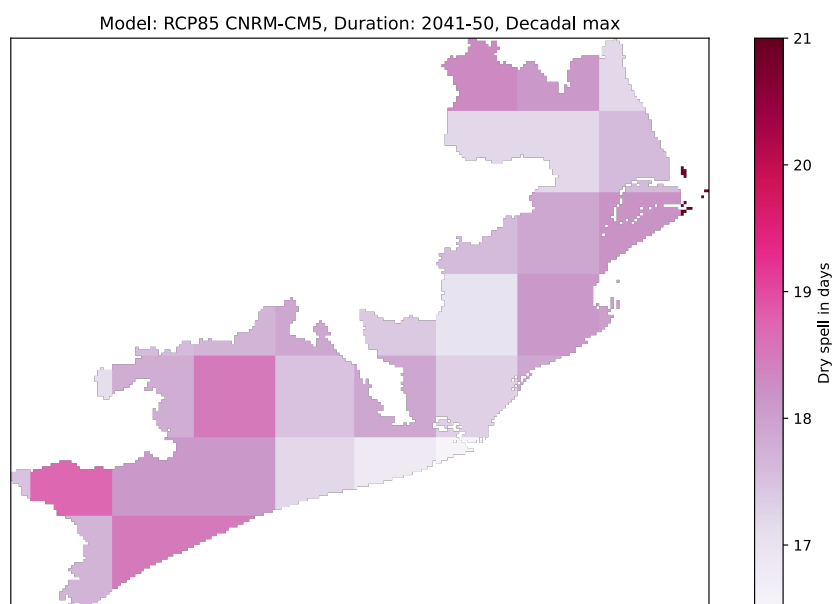


Figure 5.36: Predicted longest dry spell days from 2041 to 2050 for RCP 8.5 emission scenario using CNRM's CM5 model

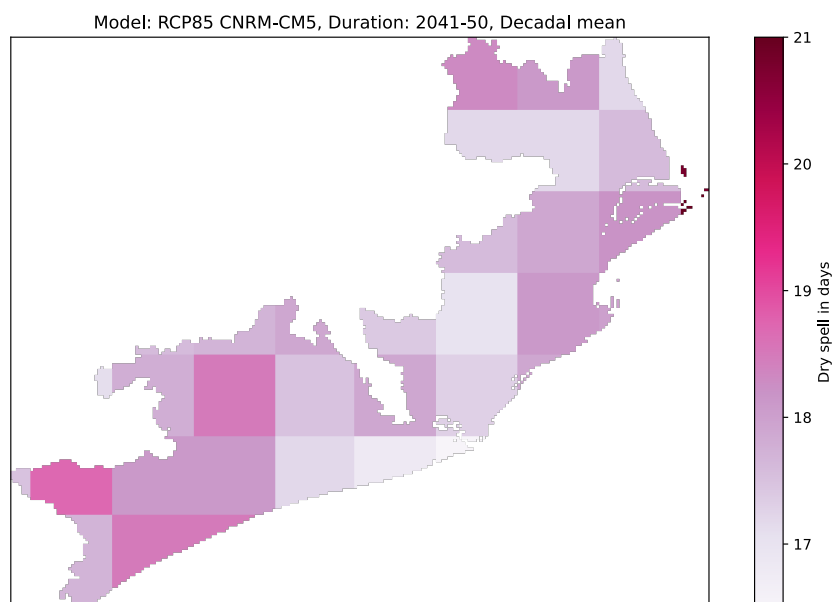


Figure 5.37: predicted average dry spell days from 2041 to 2050 for RCP 8.5 emission scenario using CNRM's CM5 model

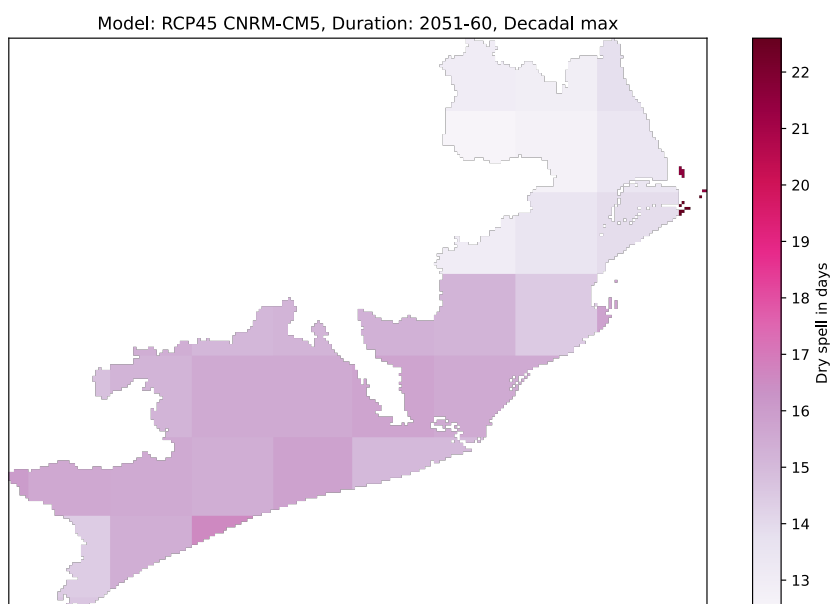


Figure 5.38: Predicted longest dry spell days from 2051 to 2060 for RCP 4.5 emission scenario using CNRM's CM5 model

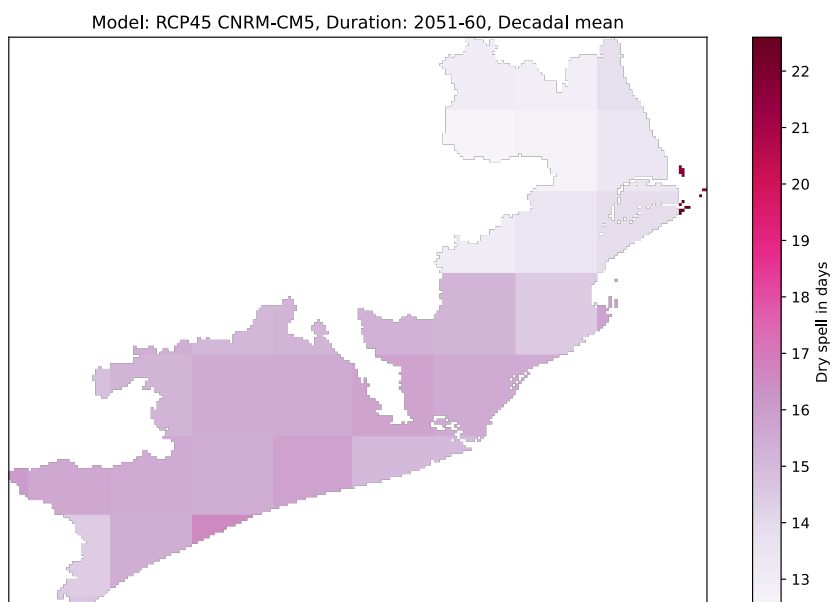


Figure 5.39: Predicted average dry spell days from 2051 to 2060 for RCP 4.5 emission scenario using CNRM's CM5 model

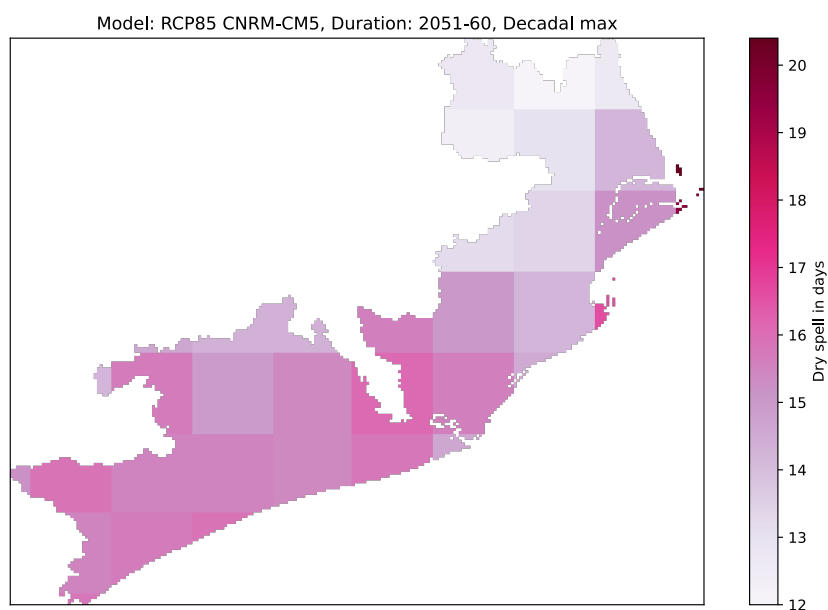


Figure 5.40: Predicted longest dry spell days from 2051 to 2060 for RCP 8.5 emission scenario using CNRM's CM5 model

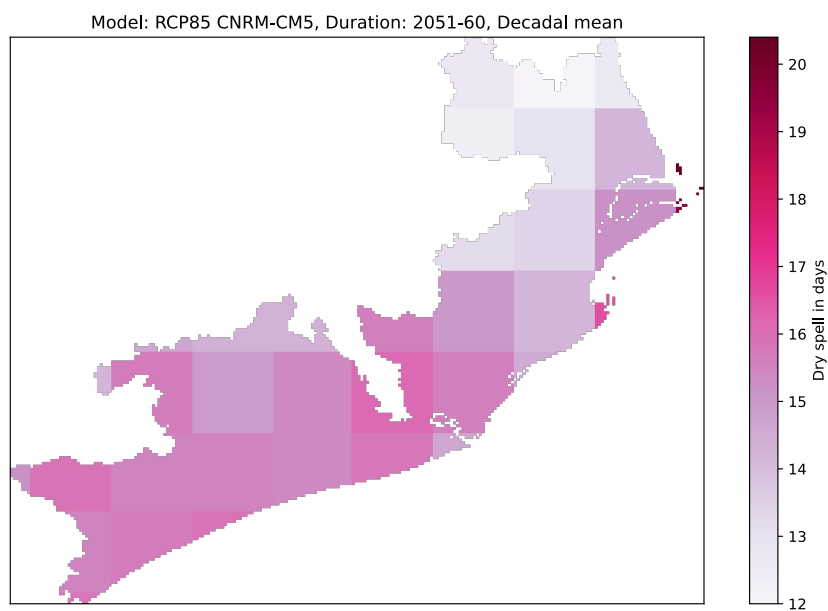


Figure 5.41: Predicted average dry spell days from 2051 to 2060 for RCP 8.5 emission scenario using CNRM's CM5 model

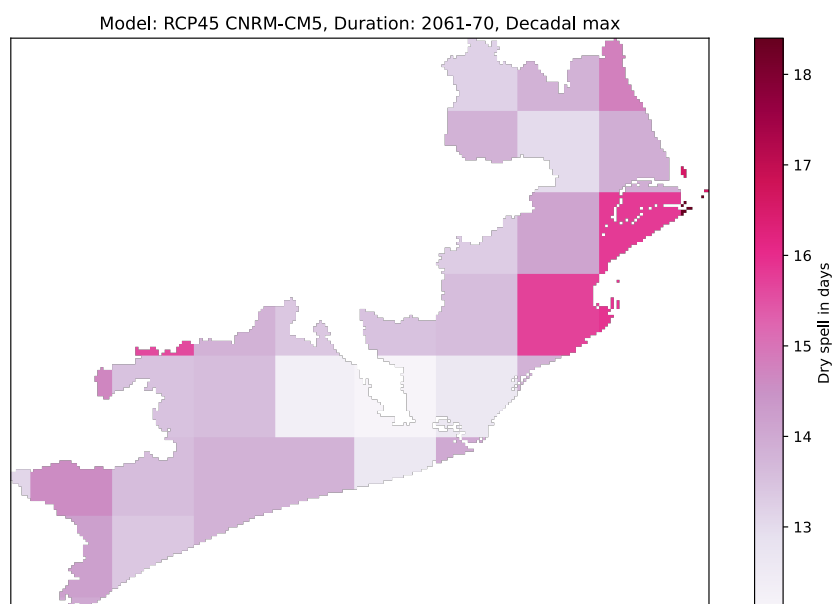


Figure 5.42: Rredicted longest dry spell days from 2061 to 2070 for RCP 4.5 emis-
sion scenario using CNRM's CM5 model

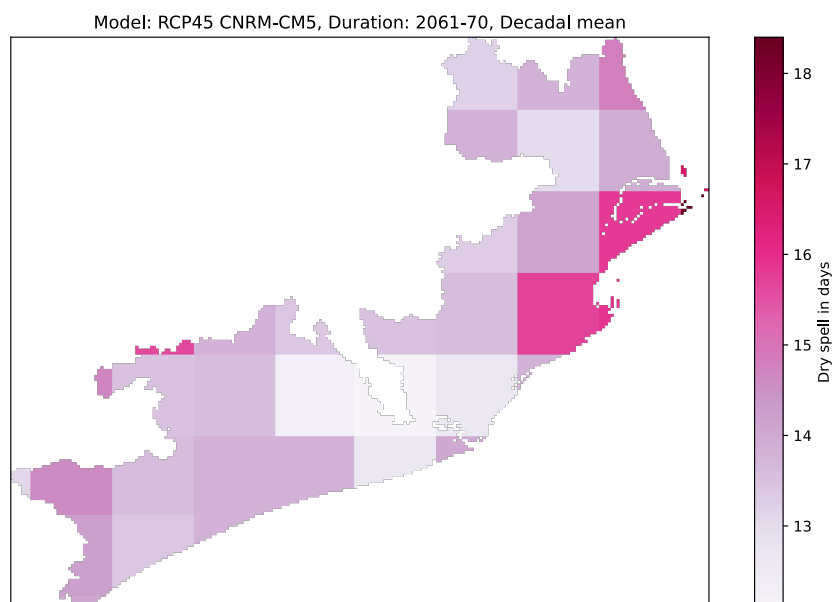


Figure 5.43: Predicted average dry spell days from 2061 to 2070 for RCP 4.5 emis-
sion scenario using CNRM's CM5 model

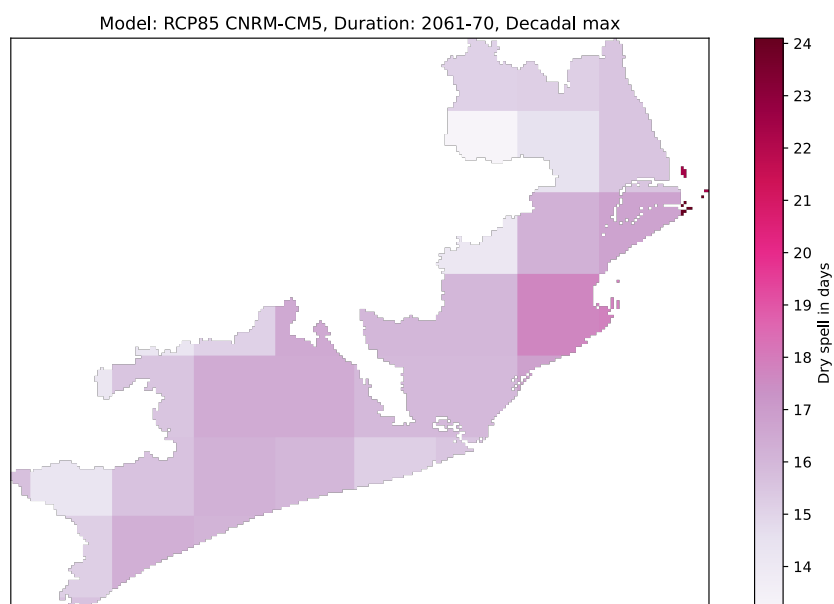


Figure 5.44: Predicted longest dry spell days from 2061 to 2070 for RCP 8.5 emission scenario using CNRM's CM5 model

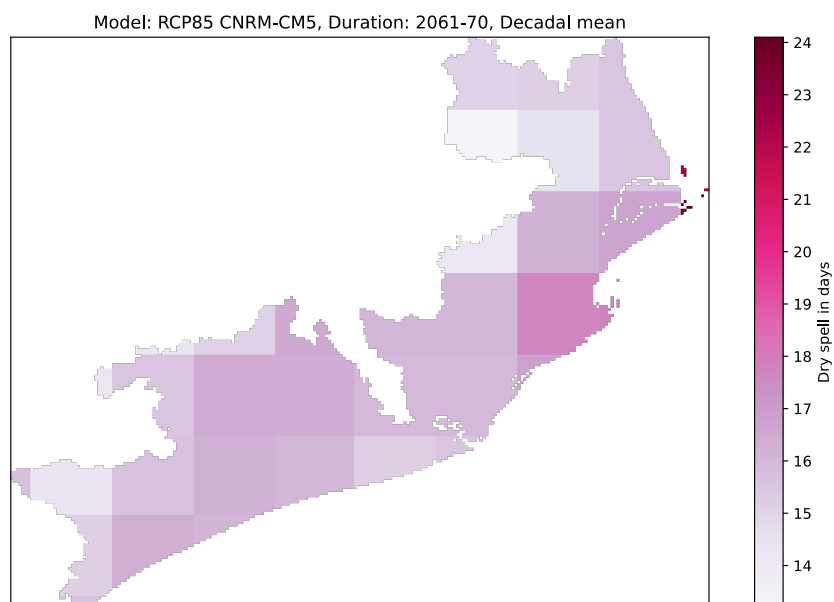


Figure 5.45: Predicted average dry spell days from 2061 to 2070 for RCP 8.5 emission scenario using CNRM's CM5 model

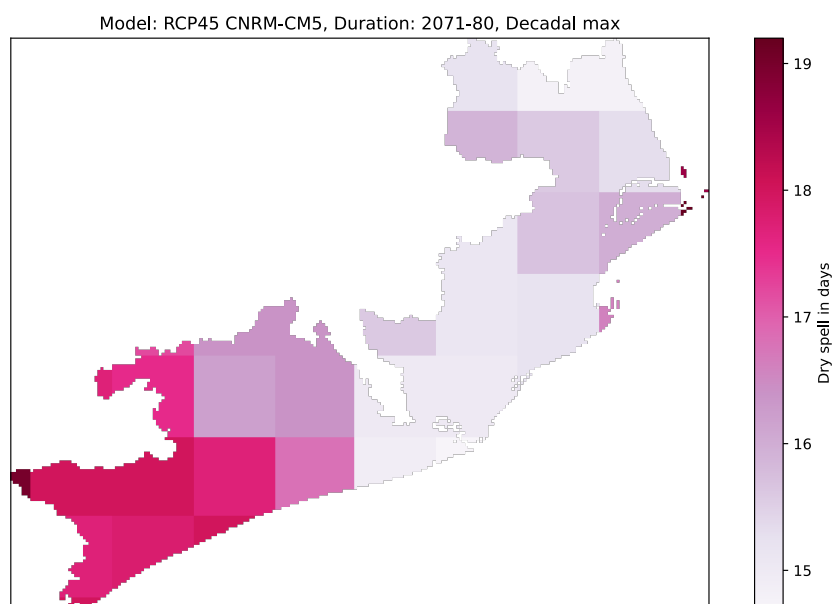


Figure 5.46: Predicted longest dry spell days from 2071 to 2080 for RCP 4.5 emission scenario using CNRM's CM5 model

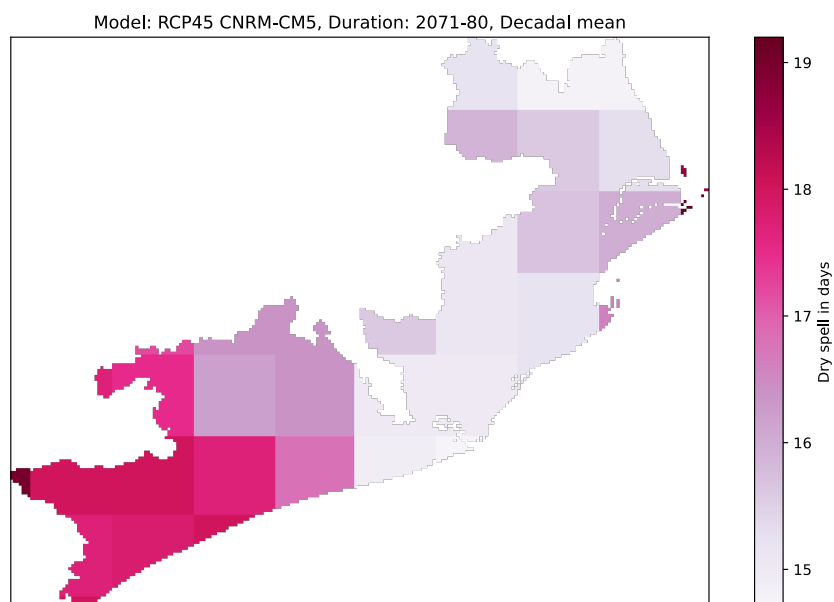


Figure 5.47: Predicted average dry spell days from 2071 to 2080 for RCP 4.5 emission scenario using CNRM's CM5 model

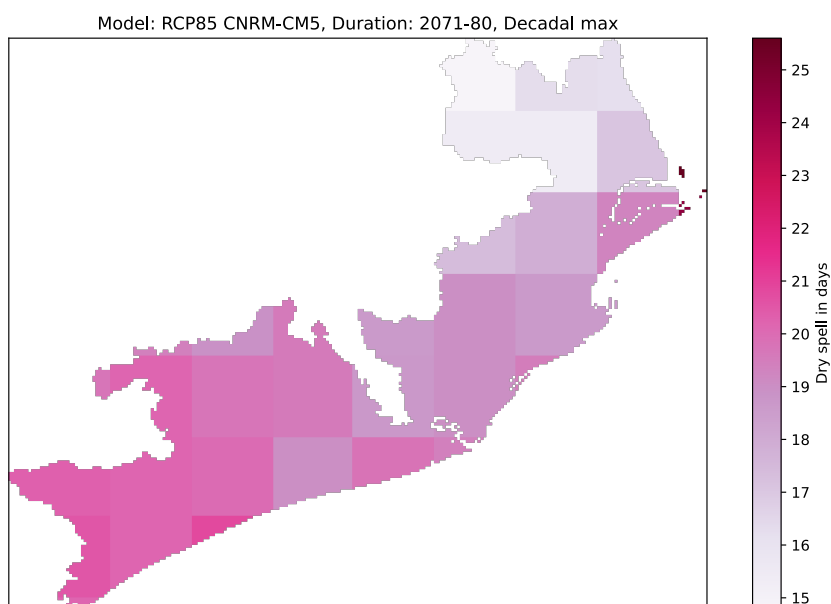


Figure 5.48: Predicted longest dry spell days from 2071 to 2080 for RCP 8.5 emission scenario using CNRM's CM5 model

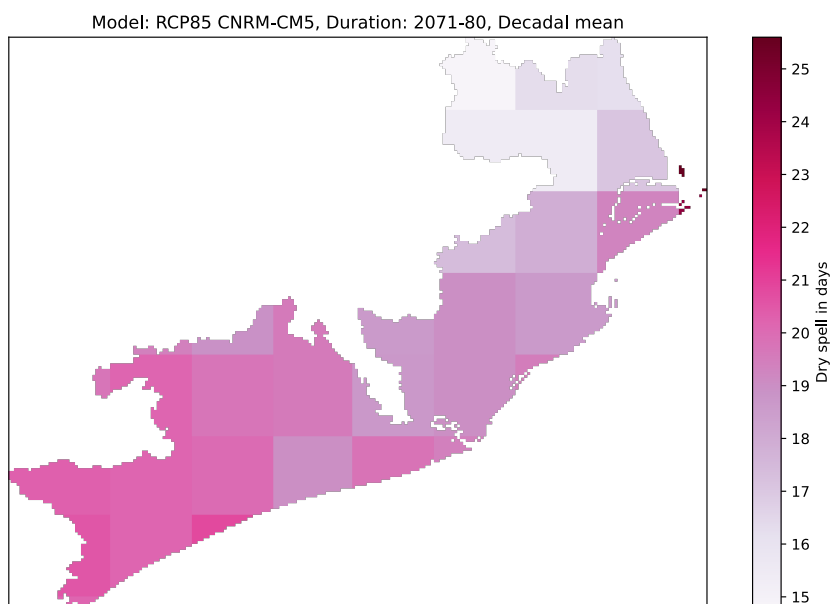


Figure 5.49: Predicted average dry spell days from 2071 to 2080 for RCP 8.5 emission scenario using CNRM's CM5 model

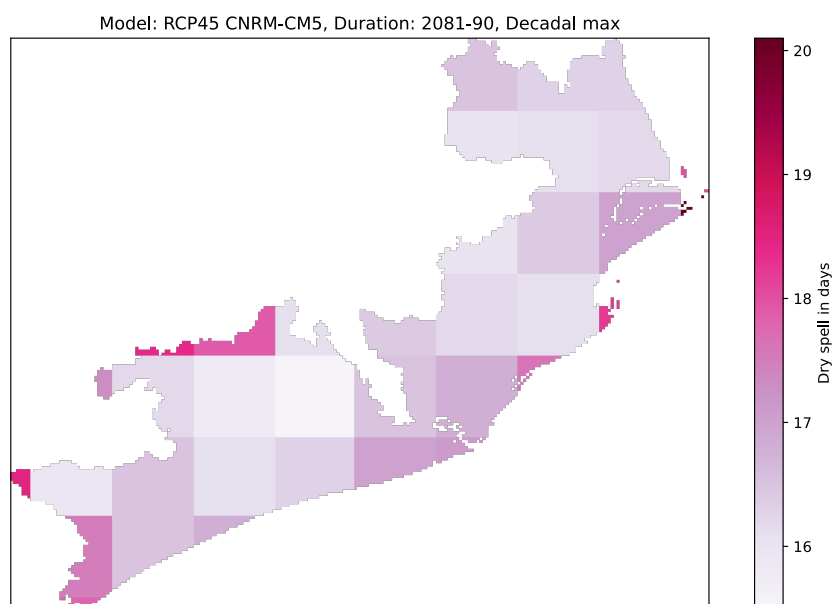


Figure 5.50: Predicted longest dry spell days from 2081 to 2090 for RCP 4.5 emission scenario using CNRM's CM5 model

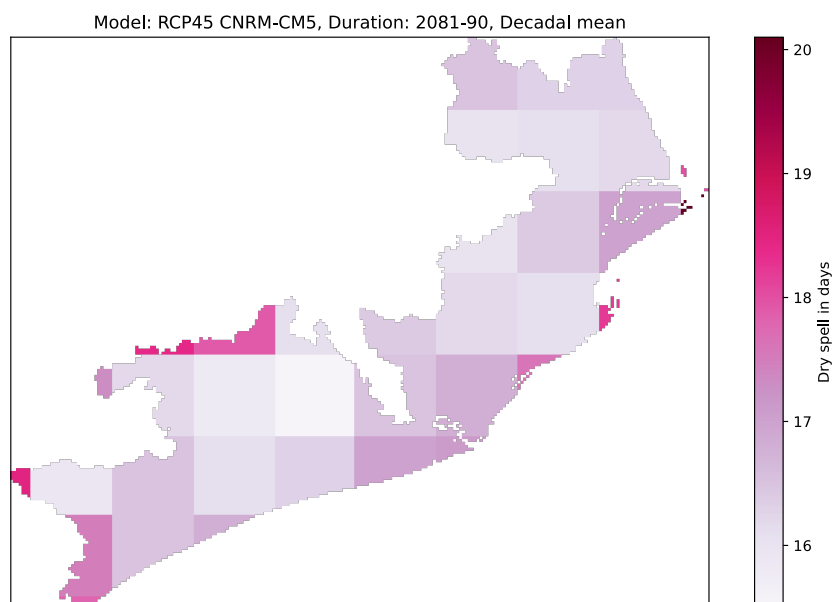


Figure 5.51: Predicted average dry spell days from 2081 to 2090 for RCP 4.5 emission scenario using CNRM's CM5 model

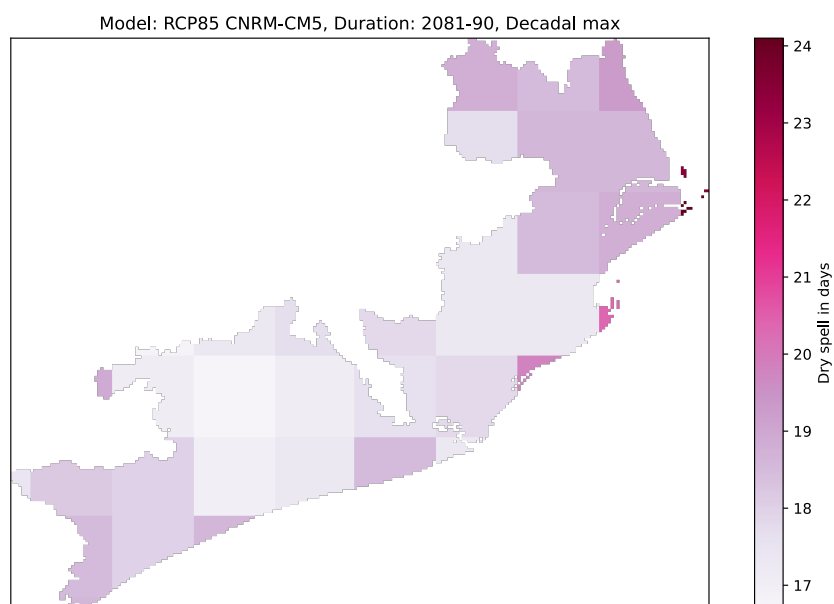


Figure 5.52: Predicted longest dry spell days from 2081 to 2090 for RCP 8.5 emission scenario using CNRM's CM5 model

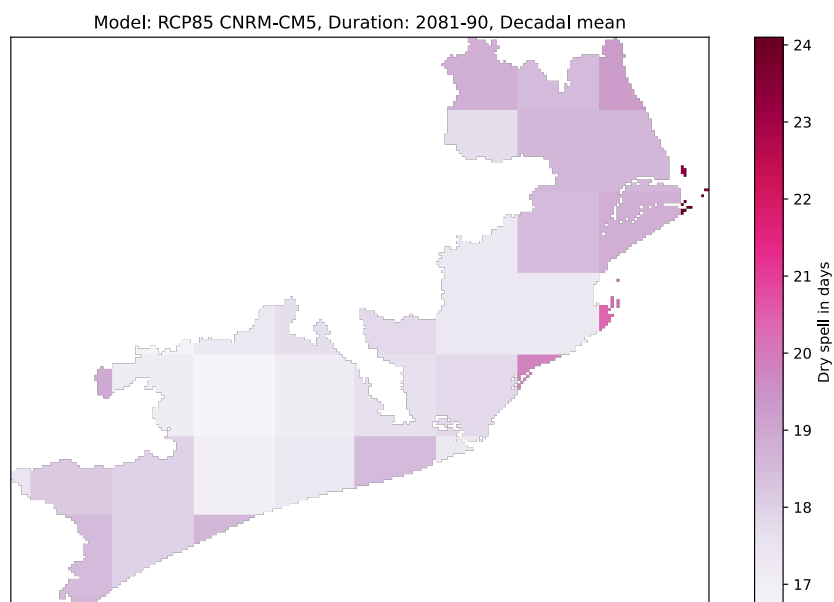


Figure 5.53: Predicted average dry spell days from 2081 to 2090 for RCP 8.5 emission scenario using CNRM's CM5 model

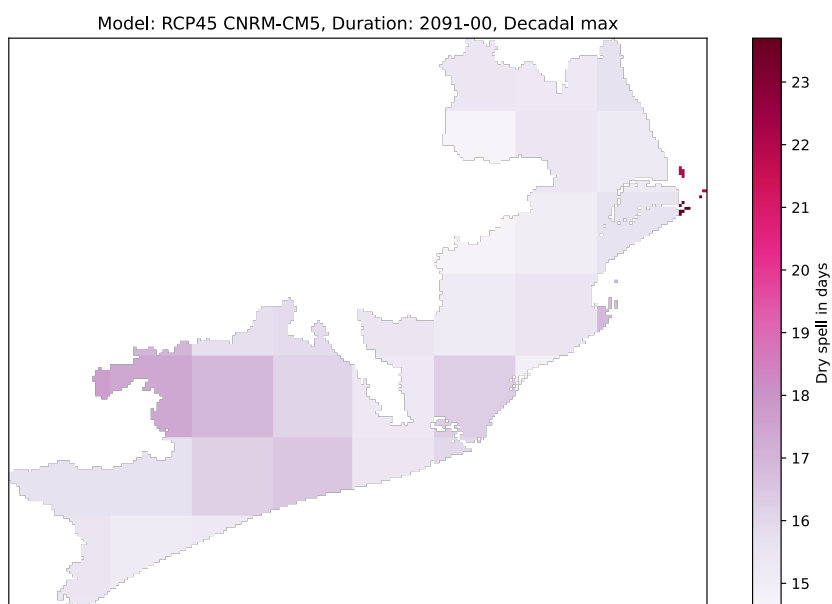


Figure 5.54: Predicted longest dry spell days from 2091 to 2100 for RCP 4.5 emission scenario using CNRM's CM5 model

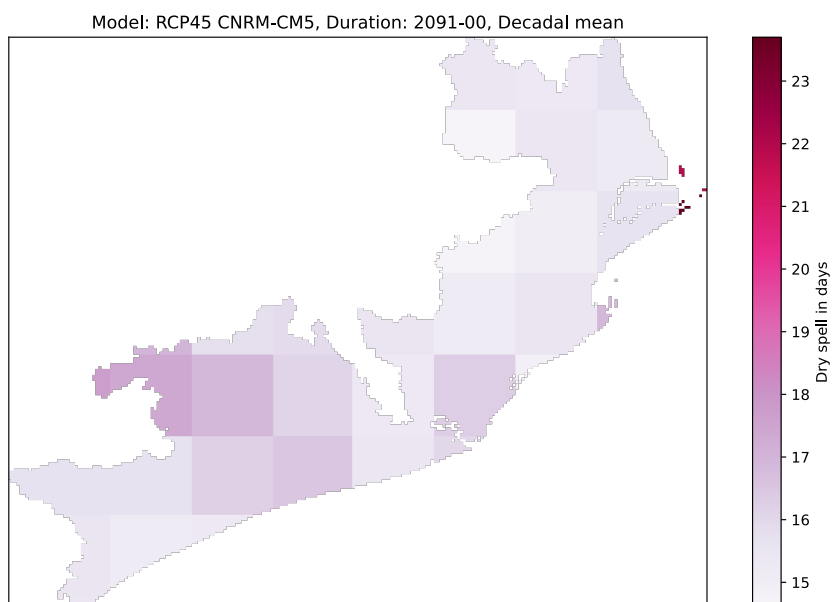


Figure 5.55: Predicted average dry spell days from 2091 to 2100 for RCP 4.5 emission scenario using CNRM's CM5 model

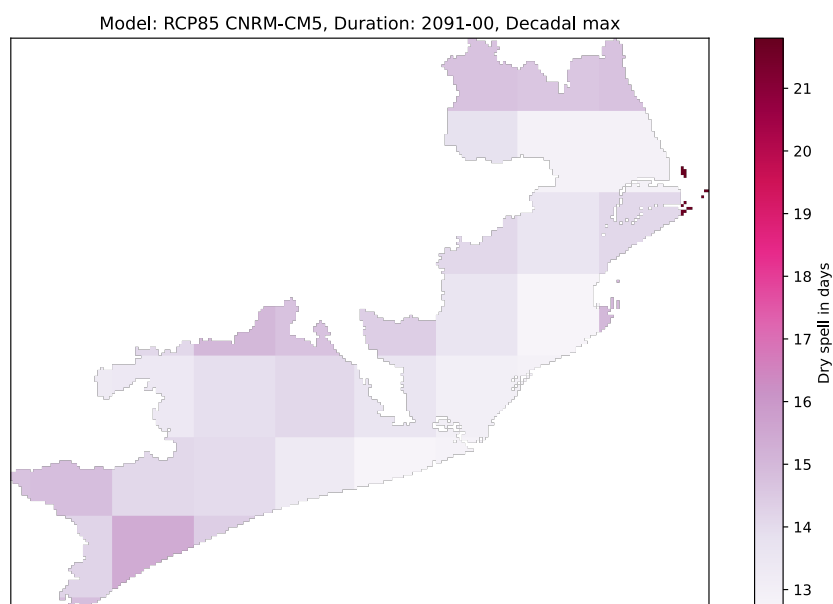


Figure 5.56: Predicted longest dry spell days from 2091 to 2100 for RCP 8.5 emission scenario using CNRM's CM5 model

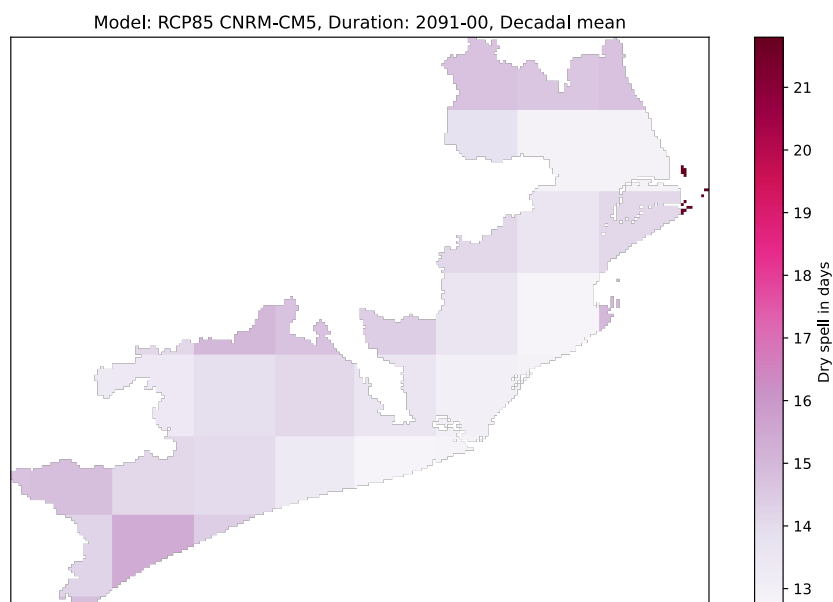


Figure 5.57: Predicted average dry spell days from 2091 to 2100 for RCP 8.5 emission scenario using CNRM's CM5 model

Conclusion and recommendations

Climate change is steadily becoming a common occurrence and its manifestations and impacts are becoming more pervasive. Scientists, researchers and policy makers are not as sceptical as they used to be. Even the general populace is becoming more cognizant of the impacts of climate change on the differing behaviour of precipitation and temperature and their different manifestation. Climate change poses a significant threat to the world's low-lying coastal regions, such as the major deltas, due to rising sea levels and an increase in the frequency of cyclones. The Mahanadi delta is a significant delta on the eastern coast of India that faces the same difficulties.

The findings indicate that the northern portion of the Delta, including administrative blocks such as Chandabali, Basudebpur, Mahakalpara, Rajnagar, Tihidi, Ersama, Pattamundai, Aul, and Kujang, is in an extremely high-risk zone and requires immediate risk reduction and adaptation initiatives due to the high occurrences of extreme events.

A 100-year flood and a 7-meter storm surge are likely to impact approximately 88% of the cultivated land. In addition, a 7 m surge would affect 80 percent of residents in certain areas, including Chandabali, Mahakalpara, and Rajnagar. Agriculture provides a living for somewhat more than two-thirds of the people making them more vulnerable to extreme events and their damaging effects on agriculture, food security, and livelihood security. Coastal erosion caused by a rise in sea level can also increase the risk of storm surge in these areas. Bhadrak and Jagatsinghpur are identified as the districts with the highest risk of extreme events. Khordha just happened to be the least affected. Implementing adaptation strategies, such as the creation of early warning systems, the building of sufficient dikes and mangrove plantations on open beaches, the creation of crop varieties resis-

tant to flooding and sea level rise, salinization, and other infrastructure upgrades, is the typical response to these challenges. However, implementing adaptation strategies should consider all factors concerning the local bio-physical and socio-economic environment. For example, the magnitude and scope of the risk of climate extremes must be taken into account for adaptations to be effective.

Due to the extensive coastline and alluvium, the Mahanadi Delta region is one of the best farming regions in the country. According to the analysis of soil suitability, the majority of the delta is appropriate for all of the major crops.

However, variations in temperature and precipitation can lower the yield and production of the current crop varieties. In these circumstances, additional irrigation is required due to the higher temperatures that contributed to the prolonged dry spells. Adopting alternative crops is a popularly recommended adaptation strategy to cope with climatic change and variation. Based on projected climate changes, suitable crop rotation and cropping patterns can be adopted. However, food habits and dietary patterns are important factors to consider when proposing an alternative crop. For example, [Auffhammer \(2018\)](#) proposed a simple model for crop choice and profit in the short and long run based only on economic activity (Fig. 6.1).

Modeling alternative crop choices also requires field data on soil, climate, terrain, and socioeconomics. Adjustment of the crop model with local field specific wetting points, crop coefficients, and harvest information could improve the results of the projections. The availability of water for irrigation is another essential component to consider. For instance, in all of the climate scenarios examined, wheat has a very high yield potential. However, due to the low need for irrigation, green and black gram are more widely grown crops in the delta during the rabi season. Since the Delta has a very good canal network and nearly 85% of the area is covered by major and minor irrigation commands, the irrigation system can be improved by renovating the current canal system. To figure out how climate change affects water availability, crop yield, crop water productivity, and soil water balance, it is important to use crop simulation models and climate change scenarios with higher spatial and temporal resolution. Downscaling ensembles of projected climate data is important for projecting any changes and providing recommendations based on that fact because, for example, GCM and RCM are based

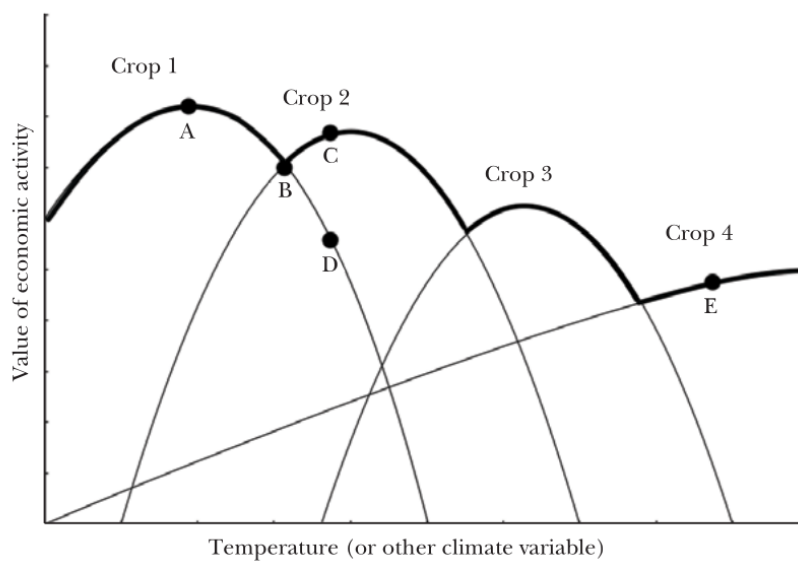


Figure 6.1: Crop choice model based on the value of economic activity by [Auffhammer \(2018\)](#). The best crops are those with thick curves based on the value of economic activity.

on global land cover data for land surface balance calculations, which may not reflect local conditions. Moreover, participation from all of the relevant stakeholder groups is essential in order to modernize the agricultural system in the Delta and make it more resistant to the effects of climate change.

References

- Jr. Allen, L.H., K.J. Boote, J.W. Jones, P.H. Jones, R.R. Valle, B. Acock, H.H. Rogers, and R.C. Dahlman. Response of vegetation to rising carbon dioxide: Photosynthesis, biomass, and seed yield of soybean. *Global Biogeochemical Cycles*, 1(1):1–14, 1987. doi: 10.1029/GBoo11001p00001. URL <https://doi.org/10.1029/GBoo11001p00001>. Cited on p. 2.
- Richard G Allen, Luis S Pereira, Dirk Raes, Martin Smith, et al. Fao irrigation and drainage paper no. 56. *Rome: Food and Agriculture Organization of the United Nations*, 56(97):e156, 1998. Cited on p. 16.
- Abbas Amini Fasakhodi, Seyed Hedayatollah Nouri, and Manouchehr Amini. Water resources sustainability and optimal cropping pattern in farming systems; a multi-objective fractional goal programming approach. *Water resources management*, 24(15):4639–4657, 2010. doi: 10.1007/s11269-010-9683-z. URL <https://doi.org/10.1007/s11269-010-9683-z>. Cited on p. 2.
- Muhuddin Rajin Anwar, Garry O’Leary, David McNeil, Hemayet Hossain, and Roger Nelson. Climate change impact on rainfed wheat in south-eastern australia. *Field crops research*, 104(1-3):139–147, 2007. Cited on p. 14.
- Craig Arthur, Anthony Schofield, and Bob Cechet. Assessing the impacts of tropical cyclones. *The Australian Journal of Emergency Management*, 23(4): 14–20, 2008. ISSN 1324-1540. doi: 10.3316/ielapa.609161450367363. URL <https://search.informit.org/doi/10.3316/ielapa.609161450367363>. Cited on p. 32.
- Maximilian Auffhammer. Quantifying economic damages from climate change. *Journal of Economic Perspectives*, 32(4):33–52, 2018. Cited on pp. x, 89, and 90.

- Fakira Bastia and Sk Md Equeenuddin. Spatio-temporal variation of water flow and sediment discharge in the mahanadi river, india. *Global and Planetary Change*, 144:51–66, 2016. Cited on p. 19.
- S.J. Baxter and M.A. Oliver. The spatial prediction of soil mineral n and potentially available n using elevation. *Geoderma*, 128(3):325–339, 2005. ISSN 0016-7061. doi: 10.1016/j.geoderma.2005.04.013. URL <https://www.sciencedirect.com/science/article/pii/S0016706105001011>. Pedometrics 2003. Cited on p. 40.
- Satyapriya Behera, Deepak Khare, Prabhash Kumar Mishra, and Sangitarani Sahoo. Impact of climate change on crop water requirement for sunei medium irrigationproject, odisha, india. *Int. J. Eng. Trends and Technol.(IJETT)*, 34(8): 358–367, 2016. Cited on p. 19.
- Mariana Belgiu and Lucian Drăguț. Random forest in remote sensing: A review of applications and future directions. *ISPRS journal of photogrammetry and remote sensing*, 114:24–31, 2016. Cited on pp. vii and 33.
- Devananda Beura. Floods in mahanadi river, odisha, india: its causes and management. *International Journal of Engineering and Applied Sciences*, 2(2):257992, 2015. Cited on p. 22.
- J Bouma. Land evaluation for landscape units. In *Handbook of soil science*, pages E393–E412. CRC Press, 1999. Cited on pp. vi, 16, and 17.
- George John Bouyoucos. Hydrometer method improved for making particle size analyses of soils¹. *Agronomy Journal*, 54(5):464–465, 1962. doi: 10.2134/agronj1962.00021962005400050028x. URL <https://acsess.onlinelibrary.wiley.com/doi/abs/10.2134/agronj1962.00021962005400050028x>. Cited on p. 36.
- Leo Breiman. Random forests. *Machine learning*, 45(1):5–32, 2001. Cited on p. 33.
- Antonio Ceballos, José Martínez-Fernández, and Miguel Ángel Luengo-Ugidos. Analysis of rainfall trends and dry periods on a pluviometric gradient representative of mediterranean climate in the duero basin, spain. *Journal of Arid Environments*, 58(2):215–233, 2004. Cited on p. 68.

- Govind Joseph Chakrapani and V Subramanian. Factors controlling sediment discharge in the mahanadi river basin, india. *Journal of Hydrology*, 117(1-4):169–185, 1990. Cited on p. 21.
- Avoiding Dangerous Climate Change, Tony Blair, Rajendra K Pachauri, and Rajendra Pachauri. *Avoiding dangerous climate change*. Cambridge University Press, 2006. Cited on pp. vi, 6, and 7.
- H.D. Chapman. *Cation-Exchange Capacity*, chapter 57, pages 891–901. John Wiley and Sons, Ltd, 1965. ISBN 9780891182047. doi: 10.2134/agronmonogr9.2.c6. URL <https://access.onlinelibrary.wiley.com/doi/abs/10.2134/agronmonogr9.2.c6>. Cited on p. 39.
- Alessia Cogato, Franco Meggio, Massimiliano De Antoni Migliorati, and Francesco Marinello. Extreme weather events in agriculture: A systematic review. *Sustainability*, 11(9):2547, 2019. doi: 10.3390/su11092547. URL <https://www.mdpi.com/2071-1050/11/9/2547>. Cited on pp. 2 and 14.
- James M Coleman. *Deltas: Processes of deposition & models for exploration*. Burgess Publishing Company, CEPCO Division, 1981. Cited on p. 2.
- William R Cotton and Roger A Pielke Sr. *Human impacts on weather and climate*. Cambridge University Press, 2007. Cited on p. 9.
- Wolfgang P. Cramer and Rik Leemans. *Assessing Impacts of Climate Change on Vegetation Using Climate Classification Systems*, pages 190–217. Springer US, Boston, MA, 1993. ISBN 978-1-4615-2816-6. doi: 10.1007/978-1-4615-2816-6_10. URL https://doi.org/10.1007/978-1-4615-2816-6_10. Cited on p. 4.
- Isha Das, Valentina Lauria, Susan Kay, Ignacio Cazcarro, Iñaki Arto, Jose A Fernandes, and Sugata Hazra. Effects of climate change and management policies on marine fisheries productivity in the north-east coast of india. *Science of the Total Environment*, 724:138082, 2020. Cited on p. 19.
- Manoj Kumar Das and Padmaja Mishra. Vulnerability of agriculture to climate shocks in odisha, india. *International Journal of African and Asian Studie*, 40: 27–35, 2017. Cited on p. 20.

- Stephen Devereux. The impact of droughts and floods on food security and policy options to alleviate negative effects. *Agricultural Economics*, 37(s1):47–58, 2007. doi: <https://doi.org/10.1111/j.1574-0862.2007.00234.x>. URL <https://onlinelibrary.wiley.com/doi/abs/10.1111/j.1574-0862.2007.00234.x>. Cited on p. 14.
- Antonio Di Gregorio. *Land cover classification system: classification concepts and user manual: LCCS*, volume 2. Food and Agriculture Organization, 2005. Cited on p. 33.
- J Doorenbos and AH Kassam. Yield response to water. *Irrigation and drainage paper*, 33:257, 1979. Cited on p. 17.
- SK Dube, Indu Jain, AD Rao, and TS Murty. Storm surge modelling for the bay of bengal and arabian sea. *Natural Hazards*, 51(1):3–27, 2009. doi: 10.1007/s11069-009-9397-9. URL <https://doi.org/10.1007/s11069-009-9397-9>. Cited on pp. 31 and 32.
- John Duncan, Emma Tompkins, Jadunandan Dash, and Basundhara Tripathy. Resilience to hazards: rice farmers in the mahanadi delta, india. *Ecology and Society*, 22(4), 2017. Cited on p. 20.
- Alaa E Eissa and Manal M Zaki. The impact of global climatic changes on the aquatic environment. *Procedia Environmental Sciences*, 4:251–259, 2011. Cited on p. 4.
- J Eitzinger, M Štastná, Z Žalud, and M Dubrovský. A simulation study of the effect of soil water balance and water stress on winter wheat production under different climate change scenarios. *Agricultural Water Management*, 61(3):195–217, 2003. Cited on p. 14.
- Michael E Essington. *Soil and water chemistry: an integrative approach*. CRC press, 2015. Cited on p. 35.
- Pingzhi Fang, Gengjiao Ye, and Hui Yu. A parametric wind field model and its application in simulating historical typhoons in the western north pacific ocean. *Journal of Wind Engineering and Industrial Aerodynamics*, 199:104131,

2020. ISSN 0167-6105. doi: <https://doi.org/10.1016/j.jweia.2020.104131>. URL <https://www.sciencedirect.com/science/article/pii/S0167610520300416>. Cited on p. 32.
- Günther Fischer, Freddy O Nachtergaele, H van Velthuizen, F Chiozza, G Francheschini, M Henry, D Muchoney, and S Tramberend. Global agro-ecological zones (GAEZv4)-model documentation. Technical report, FAO & IIASA, 2021. URL <https://gaez.fao.org>. Cited on pp. xii, xiii, 41, 52, 53, 54, 55, 56, 57, 58, and 59.
- Christoph Frei, Regina Schöll, Sophie Fukutome, Jürg Schmidli, and Pier Luigi Vidale. Future change of precipitation extremes in europe: Intercomparison of scenarios from regional climate models. *Journal of Geophysical Research: Atmospheres*, 111(D6), 2006. Cited on p. 14.
- Yoichi Fujihara, Kenji Tanaka, Tsugihiko Watanabe, Takanori Nagano, and Toshiharu Kojiri. Assessing the impacts of climate change on the water resources of the seyhan river basin in turkey: Use of dynamically downscaled data for hydrologic simulations. *Journal of Hydrology*, 353(1-2):33–48, 2008. Cited on p. 14.
- Poulomi Ganguli, Yamini Rama Nandamuri, and Chandranath Chatterjee. Understanding flood regime changes of the mahanadi river. *ISH Journal of Hydraulic Engineering*, pages 1–14, 2022. Cited on pp. viii and 69.
- Glendon W Gee and Dani Or. 2.4 particle-size analysis. In Jacob H. Dane and Clarke G. Topp, editors, *Methods of soil analysis: Part 4 physical methods*, volume 5, pages 255–293. Wiley, 2002. ISBN 978-0-891-18893-3. doi: 10.2136/sssabookser5.4. URL <https://doi.org/10.2136/sssabookser5.4.c12>. Cited on p. 36.
- Subimal Ghosh, Deepashree Raje, and PP Mujumdar. Mahanadi streamflow: climate change impact assessment and adaptive strategies. *Current Science*, pages 1084–1091, 2010. Cited on p. 22.

- AK Gosain, Sandhya Rao, and Debajit Basuray. Climate change impact assessment on hydrology of indian river basins. *Current science*, pages 346–353, 2006. Cited on p. 22.
- Govt. of India. Primary census abstract (PCA), 2011. URL <https://censusindia.gov.in>. Cited on pp. xii, 22, and 28.
- Govt. of Odisha. District statistical handbook- bhadrak, 2011a. URL <http://desorissa.nic.in>. Cited on pp. xii and 25.
- Govt. of Odisha. District statistical handbook- jagatsinghpur, 2011b. URL <http://desorissa.nic.in>. Cited on pp. xii and 25.
- Govt. of Odisha. District statistical handbook- kendrapara, 2011c. URL <http://desorissa.nic.in>. Cited on pp. xii and 25.
- Govt. of Odisha. District statistical handbook- khordha, 2011d. URL <http://desorissa.nic.in>. Cited on pp. xii and 25.
- Govt. of Odisha. District statistical handbook- puri, 2011e. URL <http://desorissa.nic.in>. Cited on pp. xii and 25.
- Emil Julius Gumbel. The return period of flood flows. *The annals of mathematical statistics*, 12(2):163–190, 1941. URL <https://www.jstor.org/stable/2235766>. Cited on p. 29.
- Murali Krishna Gumma, Samarendu Mohanty, Andrew Nelson, Rala Arnel, Irshad A Mohammed, and Satya Ranjan Das. Remote sensing based change analysis of rice environments in odisha, india. *Journal of environmental management*, 148:31–41, 2015. Cited on p. 19.
- Jingpeng Guo, Kebiao Mao, Yinghui Zhao, Zhong Lu, and Xiaoping Lu. Impact of climate on food security in mainland china: A new perspective based on characteristics of major agricultural natural disasters and grain loss. *Sustainability*, 11(3), 2019. ISSN 2071-1050. doi: 10.3390/su11030869. URL <https://www.mdpi.com/2071-1050/11/3/869>. Cited on p. 14.
- Kazuyo Hirose, Yuichi Maruyama, Quy Do Van, Makoto Tsukada, and Yuichi Shiokawa. Visualization of flood monitoring in the lower reaches of the mekong

- river. In *Paper presented at the 22nd Asian Conference on Remote Sensing*, volume 5, page 9, 2001. Cited on p. 29.
- J. R. M. Hosking. L-moments: Analysis and estimation of distributions using linear combinations of order statistics. *Journal of the Royal Statistical Society: Series B (Methodological)*, 52(1):105–124, 1990. doi: <https://doi.org/10.1111/j.2517-6161.1990.tb01775.x>. URL <https://rss.onlinelibrary.wiley.com/doi/abs/10.1111/j.2517-6161.1990.tb01775.x>. Cited on p. 32.
- IPCC. *Climate change 2001: impacts, adaptation, and vulnerability: contribution of Working Group II to the third assessment report of the Intergovernmental Panel on Climate Change* [McCarthy, James J and Canziani, Osvaldo F and Leary, Neil A and Dokken, David J and White, Kasey S eds.], volume 2. Cambridge University Press, 2001. Cited on pp. vi and 12.
- IPCC. *Climate change 2007: synthesis report*. IPCC Geneva, Switzerland, 2007. Cited on pp. 1, 3, 6, 7, 9, 13, and 14.
- IPCC. *Climate change 2007-impacts, adaptation and vulnerability: Working group II contribution to the fourth assessment report of the IPCC*, volume 4. Cambridge University Press, 2007. Cited on p. 3.
- IPCC. *Climate Change 2013: The physical Science Basis. Contribution of Working Group I to the Fifth Assessment Report of the Intergovernmental Panel on Climate Change*, [T.F. Stocker and D. Qin and G.-K. Plattner and M. Tignor and S.K. Allen and J. Boschung and A. Nauels and Y. Xia (eds.)]. Cambridge University Press, Cambridge, United Kingdom and New York, NY, USA, 2013. ISBN 978-1-107-66182-0. URL <https://www.ipcc.ch/report/ar5/wg1/>. Cited on pp. vi, xii, 1, 3, 11, and 13.
- IPCC. *Climate Change 2021: The Physical Science Basis. the Working Group I contribution to the Sixth Assessment Report of the Intergovernmental Panel on Climate Change*, [Masson-Delmotte, V., P. Zhai, A. Pirani, S.L. Connors, C. Péan, S. Berger, N. Caud, Y. Chen, L. Goldfarb, M.I. Gomis, M. Huang, K. Leitzell, E. Lonnoy, J.B.R. Matthews, T.K. Maycock, T. Waterfield, O. Yelekçi, R. Yu, and B. Zhou (eds.)]. Cambridge University Press, 2021. doi: 10.1017/9781009157896. URL <https://dx.doi.org/10.1017/9781009157896>. Cited on p. 1.

- T Janes and I Macadam. Selection of climate model simulations for the decma project. Technical report, IDRC, 2017. URL www.deccma.com. Cited on pp. vii and 42.
- Prachi Pratyasha Jena, Chandranath Chatterjee, Gourirani Pradhan, and Ashok Mishra. Are recent frequent high floods in mahanadi basin in eastern india due to increase in extreme rainfalls? *Journal of Hydrology*, 517:847–862, 2014. Cited on p. 19.
- Pragnya Paramita Jena. Climate change and its worst effect on coastal odisha: An overview of its impact in jagatsinghpur district. *IOSR Journal of Humanities and Social Science*, 23(1):1–15, 2018. Cited on p. 19.
- Li Jin, Paul G Whitehead, Harvey Rodda, Ian Macadam, and Sananda Sarkar. Simulating climate change and socio-economic change impacts on flows and water quality in the mahanadi river system, india. *Science of the Total Environment*, 637:907–917, 2018. Cited on p. 19.
- James W Jones, Gerrit Hoogenboom, Cheryl H Porter, Ken J Boote, William D Batchelor, LA Hunt, Paul W Wilkens, Upendra Singh, Arjan J Gijssman, and Joe T Ritchie. The dssat cropping system model. *European journal of agronomy*, 18(3-4):235–265, 2003. Cited on p. 18.
- Anil Kumar Kar, Anil Kumar Lohani, Narendra Kumar Goel, and Gopal Prasad Roy. Development of flood forecasting system using statistical and ann techniques in the downstream catchment of mahanadi basin, india. *Journal of Water Resource and Protection*, 2(10):880, 2010. Cited on p. 22.
- Thomas R Karl and Kevin E Trenberth. Modern global climate change. *science*, 302(5651):1719–1723, 2003. doi: 10.1126/science.1090228. URL <https://www.science.org/doi/abs/10.1126/science.1090228>. Cited on pp. vi, 6, and 9.
- Thomas R Karl, Jerry M Melillo, Thomas C Peterson, and Susan J Hassol. *Global climate change impacts in the United States*. Cambridge University Press, 2009. ISBN 9780521144070. URL <https://www.cambridge.org/in/academic/subjects/earth-and-environmental-science/climatology-and-climate-change/global->

[climate-change-impacts-united-states?format=PB&isbn=9780521144070](#).

Cited on p. 2.

Jeff Kepert. The dynamics of boundary layer jets within the tropical cyclone core. part i: Linear theory. *Journal of the Atmospheric Sciences*, 58 (17):2469 – 2484, 2001. doi: 10.1175/1520-0469(2001)058<2469:TDOBLJ>2.0.CO;2. URL https://journals.ametsoc.org/view/journals/atsc/58/17/1520-0469_2001_058_2469_tdoblj_2.0.co_2.xml. Cited on p. 32.

Yones Khaledian, Eric C. Brevik, Paulo Pereira, Artemi Cerdà, Mohammed A. Fattah, and Hossein Tazikheh. Modeling soil cation exchange capacity in multiple countries. *CATENA*, 158:194–200, 2017. ISSN 0341-8162. doi: <https://doi.org/10.1016/j.catena.2017.07.002>. URL <https://www.sciencedirect.com/science/article/pii/S0341816217302254>. Cited on p. 39.

R Kidson and KS Richards. Flood frequency analysis: assumptions and alternatives. *Progress in Physical Geography*, 29(3):392–410, 2005. doi: 10.1191/0309133305pp454ra. URL <https://doi.org/10.1191/0309133305pp454ra>. Cited on p. 29.

Kenneth R Knapp, Michael C Kruk, David H Levinson, Howard J Diamond, and Charles J Neumann. The international best track archive for climate stewardship (ibtracs) unifying tropical cyclone data. *Bulletin of the American Meteorological Society*, 91(3):363–376, 2010. doi: 10.1175/2009BAMS2755.1. URL https://journals.ametsoc.org/view/journals/bams/91/3/2009bams2755_1.xml. Cited on p. 32.

Claudia Kuenzer and Fabrice G Renaud. Climate and environmental change in river deltas globally: expected impacts, resilience, and adaptation. In *The Mekong Delta System*, pages 7–46. Springer, 2012. Cited on p. 2.

David M Lapola, Joerg A Priess, and Alberte Bondeau. Modeling the land requirements and potential productivity of sugarcane and jatropha in brazil and india using the lpjml dynamic global vegetation model. *Biomass and Bioenergy*, 33 (8):1087–1095, 2009. Cited on p. 19.

- R. M. Lark. Robust estimation of the pseudo cross-variogram for cokriging soil properties. *European Journal of Soil Science*, 53(2):253–270, 2002. doi: 10.1046/j.1365-2389.2002.00456.x. URL <https://bsssjournals.onlinelibrary.wiley.com/doi/abs/10.1046/j.1365-2389.2002.00456.x>. Cited on p. 40.
- Edgar R Lemon. *CO₂ and plants: the response of plants to rising levels of atmospheric carbon dioxide*. CRC Press, 2019. Cited on pp. vi and 15.
- NK Mahalik. Satellite imageries in geological mapping of orissa and geomorphological study of mahanadi-baitarani compound data. *Res Bull Eastern Geographic Soc, Bhubaneswan*, 22:1–12, 1984. Cited on pp. vi and 24.
- Merin Mariam Mathew, K Sreelash, Micky Mathew, P Arulbalaji, and D Padmalal. Spatiotemporal variability of rainfall and its effect on hydrological regime in a tropical monsoon-dominated domain of western ghats, india. *Journal of Hydrology: Regional Studies*, 36:100861, 2021. Cited on p. 15.
- Alex B McBratney, Inakwu OA Odeh, Thomas FA Bishop, Marian S Dunbar, and Tamara M Shatar. An overview of pedometric techniques for use in soil survey. *Geoderma*, 97(3-4):293–327, 2000. doi: 10.1016/S0016-7061(00)00043-4. URL [https://doi.org/10.1016/S0016-7061\(00\)00043-4](https://doi.org/10.1016/S0016-7061(00)00043-4). Cited on p. 34.
- R.L. McCown, G.L. Hammer, J.N.G. Hargreaves, D.P. Holzworth, and D.M. Freebairn. Apsim: a novel software system for model development, model testing and simulation in agricultural systems research. *Agricultural Systems*, 50(3):255–271, 1996. ISSN 0308-521X. doi: [https://doi.org/10.1016/0308-521X\(94\)00055-V](https://doi.org/10.1016/0308-521X(94)00055-V). URL <https://www.sciencedirect.com/science/article/pii/0308521X9400055V>. Cited on p. 18.
- Hans Middelkoop, Karlheinz Daamen, Daniel Gellens, Wolfgang Grabs, Jaap CJ Kwadijk, Herbert Lang, Bart WAH Parmet, Bruno Schadler, J. Schulla, and Klaus Wilke. Impact of climate change on hydrological regimes and water resources management in the rhine basin. *Climatic change*, 49(1):105–128, 2001. doi: 10.1023/A:1010784727448. URL <https://doi.org/10.1023/A:1010784727448>. Cited on pp. 2 and 15.

- Alexey Mikhaylov, Nikita Moiseev, Kirill Aleshin, and Thomas Burkhardt. Global climate change and greenhouse effect. *Entrepreneurship and Sustainability Issues*, 7(4):2897, 2020. Cited on p. 6.
- PK Mishra. Socio-economic impacts of climate change in odisha: issues, challenges and policy options. *Journal of Climate Change*, 3(1):93–107, 2017. Cited on p. 19.
- Siba Prasad Mishra and JG Jena. Analytical study of monsoon rainfall south mahanadi delta and chilika lagoon, odisha. *International Journal of Engineering and Technology (IJET)*, 7:985–996, 2015a. Cited on p. 19.
- Siba Prasad Mishra and JG Jena. Geo-climatic abstractions of south mahanadi delta and chilika lagoon, india: Post anthropogenic interventions. *World Applied Sciences Journal, WASJ*, 33(2):326–335, 2015b. Cited on p. 19.
- SP Mishra and KC Sethi. The imprints of holocene climate and environmental changes in the south mahanadi delta and the chilika lagoon, odisha, india—an overview, in book: *Holocene climate change and environment*, elsvier. 2021; 457-482. Cited on p. 19.
- John FB Mitchell. The “greenhouse” effect and climate change. *Reviews of Geophysics*, 27(1):115–139, 1989. Cited on p. 6.
- Manmohan Mohanti and Manas Ranjan Swain. Mahanadi river delta, east coast of india: an overview on evolution and dynamic processes. *Department of geology. Utkal University, Vani Vihar*, 2005. Cited on p. 21.
- Raymond P Motha. The impact of extreme weather events on agriculture in the united states. In *Challenges and opportunities in agrometeorology*, pages 397–407. Springer, 2011. Cited on p. 2.
- MM Nageswararao, P Sinha, UC Mohanty, RK Panda, and GP Dash. Evaluation of district-level rainfall characteristics over odisha using high-resolution gridded dataset (1901–2013). *SN Applied Sciences*, 1(10):1–24, 2019. Cited on p. 19.
- Nebojsa Nakicenovic. Special report on emissions scenarios /. page 599 p. ;, 2000. URL <http://digitallibrary.un.org/record/466938>. ”A special report of IPCC

- Working Group III of the Intergovernmental Panel on Climate Change". Cited on p. 11.
- Jayanti Mala Nayak, AV Manjunatha, et al. *Risk sources and management strategies of farmers: Evidence from mahanadi river basin of Odisha in India*. Institute for Social and Economic Change, 2019. Cited on p. 20.
- PC Nayak, B Venkatesh, T Thomas, and YR Satyaji Rao. Hydrological impact assessment due to climate change on mahanadi basin in india. Cited on p. 19.
- Dibiat Nibal and Jena Damodar. Trend analysis of climate change indicators in puri district of odisha, india. *Disaster Adv*, 13:43–50, 2020. Cited on p. 19.
- Robert J Nicholls, Frank MJ Hoozemans, and Marcel Marchand. Increasing flood risk and wetland losses due to global sea-level rise: regional and global analyses. *Global Environmental Change*, 9:S69–S87, 1999. Cited on p. 3.
- Rodomiro Ortiz, Kenneth D Sayre, Bram Govaerts, Raj Gupta, GV Subbarao, Tomohiro Ban, David Hodson, John M Dixon, J Iván Ortiz-Monasterio, and Matthew Reynolds. Climate change: can wheat beat the heat? *Agriculture, Ecosystems & Environment*, 126(1-2):46–58, 2008. Cited on p. 14.
- William Osterholz, Kevin King, Mark Williams, Brittany Hanrahan, and Emily Duncan. Stratified soil sampling improves predictions of p concentration in surface runoff and tile discharge. *Soil Systems*, 4(4), 2020. ISSN 2571-8789. doi: 10.3390/soilsystems4040067. URL <https://www.mdpi.com/2571-8789/4/4/67>. Cited on p. 34.
- Dileep K Panda, A Kumar, S Ghosh, and RK Mohanty. Streamflow trends in the mahanadi river basin (india): Linkages to tropical climate variability. *Journal of Hydrology*, 495:135–149, 2013. Cited on p. 22.
- Rabindra K Panda and Gurjeet Singh. Analysis of trend and variability of rainfall in the mid-mahanadi river basin of eastern india. *International Journal of Geological and Environmental Engineering*, 10(6):659–663, 2016. Cited on p. 19.
- Martin L Parry. *Climate change and world agriculture*. Routledge, 1990. Cited on p. 14.

- Surendranath Pasupalak. Climate change and agriculture in orissa. *Orissa Review*, pages 49–52, 2009. Cited on p. 19.
- Unmesh Patnaik and Krishnan Narayanan. Vulnerability and climate change: an analysis of the eastern coastal districts of india. 2009. Cited on p. 19.
- Edzer J Pebesma. Multivariable geostatistics in s: the gstat package. *Computers & Geosciences*, 30(7):683–691, 2004. ISSN 0098-3004. doi: 10.1016/j.cageo.2004.03.012. URL <https://www.sciencedirect.com/science/article/pii/S0098300404000676>. Cited on p. 40.
- T.S.G. Peiris. Assessment of climate variability for coconut and other crops: A statistical approach. *CORD*, 24(1):19, Apr. 2008. doi: 10.37833/cord.v24i1.157. URL <https://journal.coconutcommunity.org/index.php/journalicc/article/view/157>. Cited on p. 68.
- Mark Powell, George Soukup, Steve Cocke, Sneha Gulati, Nirva Morisseau-Leroy, Shahid Hamid, Neal Dorst, and Lizabeth Axe. State of florida hurricane loss projection model: Atmospheric science component. *Journal of Wind Engineering and Industrial Aerodynamics*, 93(8):651–674, 2005. ISSN 0167-6105. doi: <https://doi.org/10.1016/j.jweia.2005.05.008>. URL <https://www.sciencedirect.com/science/article/pii/S0167610505000607>. Cited on p. 32.
- GSLHV Prasada, VUM Rao, and GGSN Rao. *Climate change and agriculture over India*. PHI Learning Pvt. Ltd., 2010. Cited on p. 2.
- Sambit Priyadarshi, SN Ojha, and Arpita Sharma. An assessment of vulnerability of fishers livelihood to climate change in coastal odisha, india. *Current World Environment*, 14(1):60, 2019. Cited on p. 19.
- Stefan Rahmstorf and Dim Coumou. Increase of extreme events in a warming world. *Proceedings of the National Academy of Sciences*, 108(44):17905–17909, 2011. Cited on p. 2.
- Navin Ramankutty, Jonathan A. Foley, John Norman, and Kevin McSweeney. The global distribution of cultivable lands: current patterns and sensitivity to possible climate change. *Global Ecology and Biogeography*, 11(5):377–392,

2002. doi: 10.1046/j.1466-822x.2002.00294.x. URL <https://onlinelibrary.wiley.com/doi/abs/10.1046/j.1466-822x.2002.00294.x>. Cited on p. 6.
- P Govinda Rao. Climatic changes and trends over a major river basin in india. *Climate Research*, pages 215–223, 1993. Cited on p. 22.
- GE Rayment, Francis Ross Higginson, et al. *Australian laboratory handbook of soil and water chemical methods*. Inkata Press Pty Ltd, 1992. Cited on pp. 36 and 38.
- Joeri Rogelj, Malte Meinshausen, and Reto Knutti. Global warming under old and new scenarios using ipcc climate sensitivity range estimates. *Nature climate change*, 2(4):248–253, 2012. Cited on p. 11.
- Janine Rohwer, Dieter Gerten, and Wolfgang Lucht. Development of functional irrigation types for improved global crop modelling. 2007. Cited on p. 19.
- C. Rosenzweig, J.W. Jones, J.L. Hatfield, A.C. Ruane, K.J. Boote, P. Thorburn, J.M. Antle, G.C. Nelson, C. Porter, S. Janssen, S. Asseng, B. Basso, F. Ewert, D. Wallach, G. Baigorria, and J.M. Winter. The agricultural model intercomparison and improvement project (agmip): Protocols and pilot studies. *Agricultural and Forest Meteorology*, 170:166–182, 2013. ISSN 0168-1923. doi: <https://doi.org/10.1016/j.agrformet.2012.09.011>. URL <https://www.sciencedirect.com/science/article/pii/S0168192312002857>. Agricultural prediction using climate model ensembles. Cited on p. 19.
- Cynthia Rosenzweig, Joshua Elliott, Delphine Deryng, Alex C Ruane, Christoph Müller, Almut Arneth, Kenneth J Boote, Christian Folberth, Michael Glotter, Nikolay Khabarov, et al. Assessing agricultural risks of climate change in the 21st century in a global gridded crop model intercomparison. *Proceedings of the national academy of sciences*, 111(9):3268–3273, 2014. Cited on p. 15.
- Naresh Chandra Sahu and Diptimayee Mishra. Analysis of perception and adaptability strategies of the farmers to climate change in odisha, india. *APCBEE procedia*, 5:123–127, 2013. Cited on p. 20.
- Netrananda Sahu, Arpita Panda, Sridhara Nayak, Atul Saini, Manoranjan Mishra, Takahiro Sayama, Limonlisa Sahu, Weili Duan, Ram Avtar, and Swadhin Be-

- hera. Impact of indo-pacific climate variability on high streamflow events in mahanadi river basin, india. *Water*, 12(7):1952, 2020. Cited on p. 19.
- Clare Lizamit Samling, Shouvik Das, and Sugata Hazra. Migration in the indian bengal delta and the mahanadi delta - a review of the literature. 2015. Cited on p. 24.
- Stephen H Schneider. Co 2, climate and society: a brief overview. *Social science research and climate change*, pages 9–15, 1983. Cited on pp. vi and 8.
- P. Scull, J. Franklin, O. A. Chadwick, and D. McArthur. Predictive soil mapping: a review. *Progress in Physical Geography: Earth and Environment*, 27(2): 171–197, 2003. doi: 10.1191/0309133303pp366ra. URL <https://doi.org/10.1191/0309133303pp366ra>. Cited on p. 34.
- Selsis, F., Kasting, J. F., Levrard, B., Paillet, J., Ribas, I., and Delfosse, X. Habitable planets around the star gliese 581? *A&A*, 476(3):1373–1387, 2007. doi: 10.1051/0004-6361:20078091. URL <https://doi.org/10.1051/0004-6361:20078091>. Cited on p. 6.
- Asis Kumar Senapati. Weather effects and their long-term impact on agricultural yields in odisha, east india: Agricultural policy implications using nardl approach. *Journal of Public Affairs*, 22(3):e2498, 2022. Cited on p. 19.
- Asis Kumar Senapati and P Goyari. Effect of climate variability on yields of major crops grown in odisha, india. *Indian J Agric Econ*, 75:186–216, 2020. Cited on p. 20.
- Raj K Singh and Moumita Das. Mahanadi: the great river. In *The Indian Rivers*, pages 309–318. Springer, 2018. Cited on p. 21.
- BN Sinha. *Geography of Orissa*. National Book Trust India, 1999. Cited on p. 21.
- Susan Solomon, Dahe Qin, Martin Manning, Melinda Marquis, Kristen Averyt, M Tignor, H Miller, and Zhenlin Chen. *Climate change 2007: The physical science basis*. New York: Cambridge Univ. Press. Intergovernmental Panel on Climate Change, 2007. Cited on pp. 3 and 44.

- Pasquale Steduto, Theodore C Hsiao, Dirk Raes, and Elias Fereres. Aquacrop—the fao crop model to simulate yield response to water: I. concepts and underlying principles. *Agronomy Journal*, 101(3):426–437, 2009. Cited on pp. vi, 17, and 18.
- Claudio O Stöckle, Marcello Donatelli, and Roger Nelson. Cropsyst, a cropping systems simulation model. *European journal of agronomy*, 18(3-4):289–307, 2003. Cited on p. 18.
- R Suppiah, KJ Hennessy, PH Whetton, K McInnes, I Macadam, J Bathols, J Ricketts, and CM Page. Australian climate change projections derived from simulations performed for the ipcc 4th assessment report. *Australian Meteorological Magazine*, 56(3):131–152, 2007. Cited on pp. xii and 10.
- Sabyasachi Swain. Impact of climate variability over mahanadi river basin. *International Journal of Engineering Research and Technology*, 3(7):938–943, 2014. Cited on p. 19.
- C Sys, E Van Ranst, and J Debaveye. Land evaluation, part ii. methods in land evaluation. *Agricultural Publication*, (7):247, 1991. Cited on p. 41.
- Claudia Teutschbein and Jan Seibert. Regional climate models for hydrological impact studies at the catchment scale: a review of recent modeling strategies. *Geography Compass*, 4(7):834–860, 2010. Cited on p. 9.
- Jagadish Timsina and EJAS Humphreys. Performance of ceres-rice and ceres-wheat models in rice–wheat systems: a review. *Agricultural systems*, 90(1-3): 5–31, 2006. Cited on p. 19.
- Le Anh Tuan and Suppakorn Chinvanno. Climate change in the mekong river delta and key concerns on future climate threats. In Mart A. Stewart and Peter A. Coclanis, editors, *Environmental Change and Agricultural Sustainability in the Mekong Delta*, pages 207–217. Springer Netherlands, Dordrecht, 2011. ISBN 978-94-007-0934-8. doi: 10.1007/978-94-007-0934-8_12. URL https://doi.org/10.1007/978-94-007-0934-8_12. Cited on p. 3.
- UN. World population prospects: The 2006 revision and world urbanization prospects: The 2007 revision. *Population Division of the Department of Economic*

- and Social Affairs of the United Nations Secretariat*. <http://esa.un.org/unup>, 2007. Cited on p. 2.
- AS Unnikrishnan, MR Ramesh Kumar, and B Sindhu. Tropical cyclones in the bay of bengal and extreme sea-level projections along the east coast of india in a future climate scenario. *Current Science*, pages 327–331, 2011. Cited on p. 22.
- Muhammad T Usman and CJC Reason. Dry spell frequencies and their variability over southern africa. *Climate research*, 26(3):199–211, 2004. Cited on p. 68.
- LP Van Reeuwijk (ed.). Procedures for soil analysis. Technical report, ISRIC–World Soil Information Centre, Wageningen, Netherlands, 2006. URL https://www.isric.org/sites/default/files/ISRIC_TechPap09.pdf. Cited on pp. 36 and 38.
- W Verheye, AP Koochafkan, and F Nachtergaele. The fao guidelines for land evaluation. *Encyclopedia of land use, land cover and soil sciences: Land evaluation*, 2:78–100, 2009. Cited on p. 16.
- vrpRouting Contributors. vrprouting - vehicle routing problems on postgresql, 2018. URL <https://vrp.pgrouting.org/latest/en/index.html>. Cited on p. 35.
- Donald A Wilhite and Michael H Glantz. Understanding: the drought phenomenon: the role of definitions. *Water international*, 10(3):111–120, 1985. Cited on p. 68.
- Ralph A Wurbs, Ranjan S Muttiah, and Fabrice Felden. Incorporation of climate change in water availability modeling. *Journal of Hydrologic Engineering*, 10(5):375–385, 2005. doi: 10.1061/(ASCE)1084-0699(2005)10:5(375). URL [https://doi.org/10.1061/\(ASCE\)1084-0699\(2005\)10:5\(375\)](https://doi.org/10.1061/(ASCE)1084-0699(2005)10:5(375)). Cited on p. 2.
- Yasuharu Yamada. Detection of flood-inundated area and relation between the area and micro-geomorphology using SAR and GIS. In *Geoscience and Remote Sensing Symposium, 2001. IGARSS'01. IEEE 2001 International*, volume 7, pages 3282–3284. IEEE, 2001. Cited on p. 29.
- X Yang, GA Chapman, JM Gray, and MA Young. Delineating soil landscape facets from digital elevation models using compound topographic index in a geographic information system. *Soil Research*, 45(8):569–576, 2007. doi: <https://doi>.

- org/10.1071/SR07058. URL <https://www.publish.csiro.au/SR/SR07058>. Cited on p. 34.
- Chuanrong Zhang and Weidong Li. Comparing a fixed-path markov chain geostatistical algorithm with sequential indicator simulation in categorical variable simulation from regular samples. *Giscience & Remote Sensing - GISCI REMOTE SENS*, 44:251–266, 09 2007. doi: 10.2747/1548-1603.44.3.251. URL <https://www.tandfonline.com/doi/abs/10.2747/1548-1603.44.3.251>. Cited on p. 40.
- Donato Zingaro, Ivan Portoghese, and Giacomo Giannoccaro. Modelling crop pattern changes and water resources exploitation: A case study. *Water*, 9(9): 685, 2017. doi: 10.3390/w9090685. URL <https://doi.org/10.3390/w9090685>. Cited on p. 2.

Land cover legend–class diagram

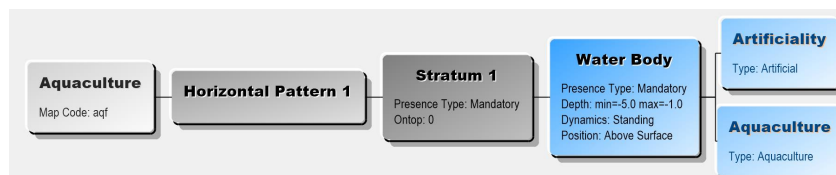


Figure A.1: Aquaculture

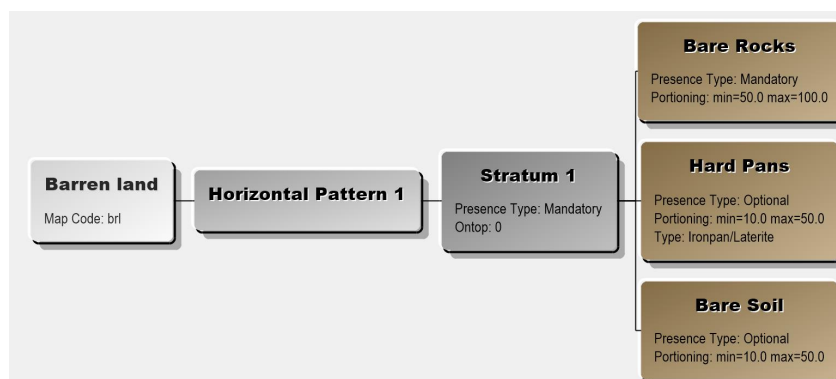


Figure A.2: Bareland



Figure A.3: Mono cropland

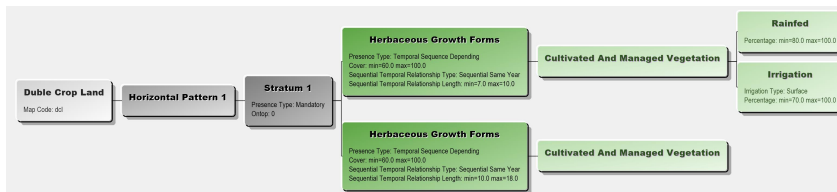


Figure A.4: Double cropland

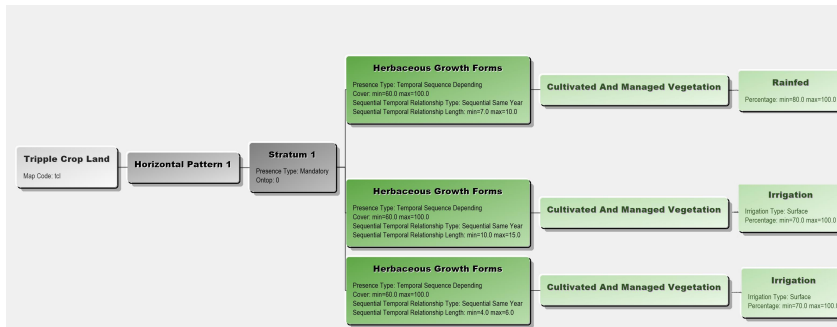


Figure A.5: Tripple cropland

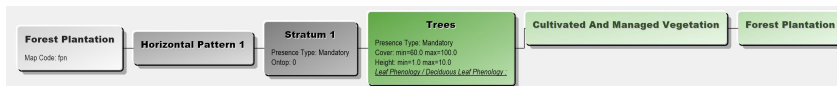


Figure A.6: Forest plantation

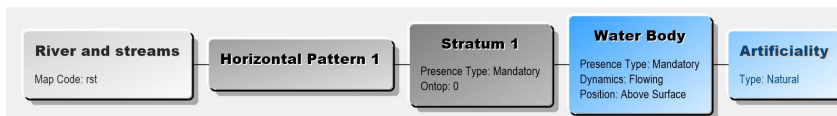


Figure A.7: River and stream class diagram

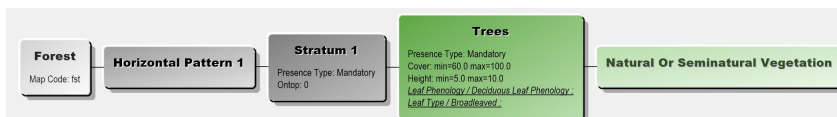


Figure A.8: Forest

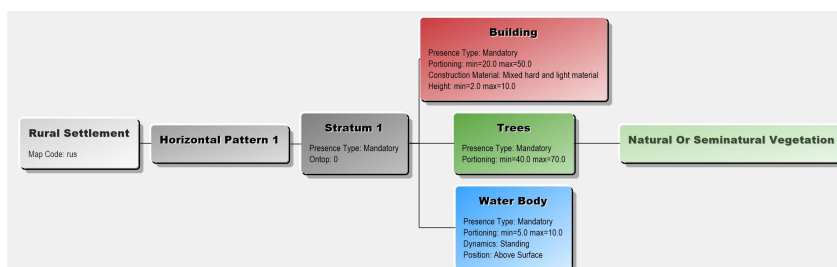


Figure A.9: Rural settlement

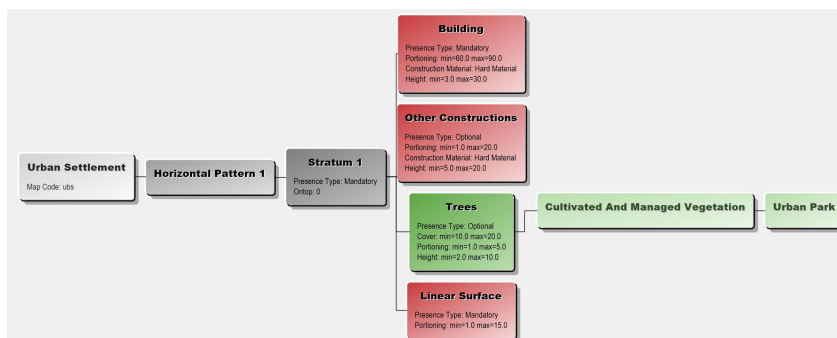


Figure A.10: Urban settlement

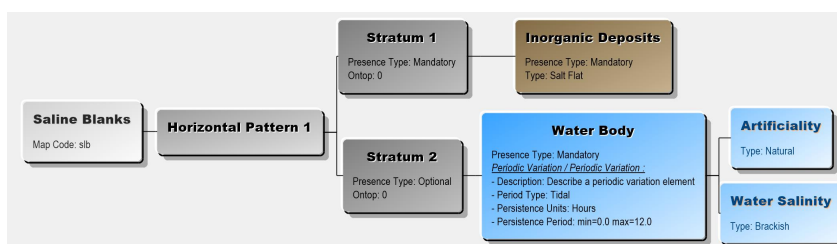


Figure A.11: Scrub land

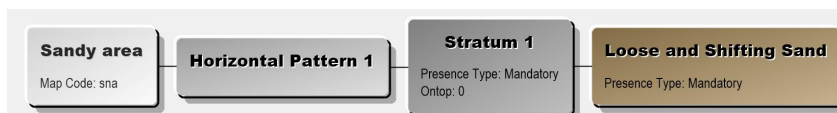


Figure A.12: Sandy area

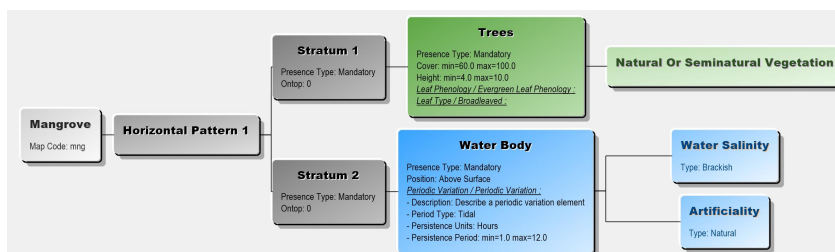


Figure A.13: Mangrove

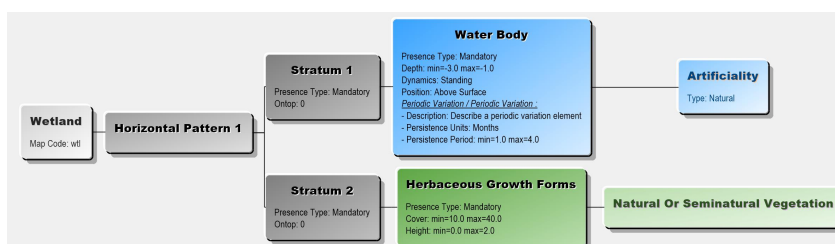


Figure A.14: Wetland

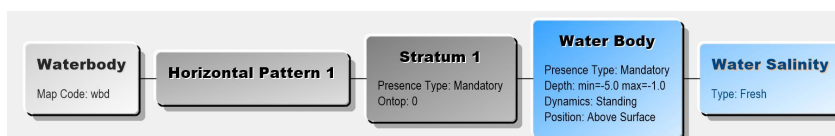


Figure A.15: Water body

The path taken while collecting soil samples

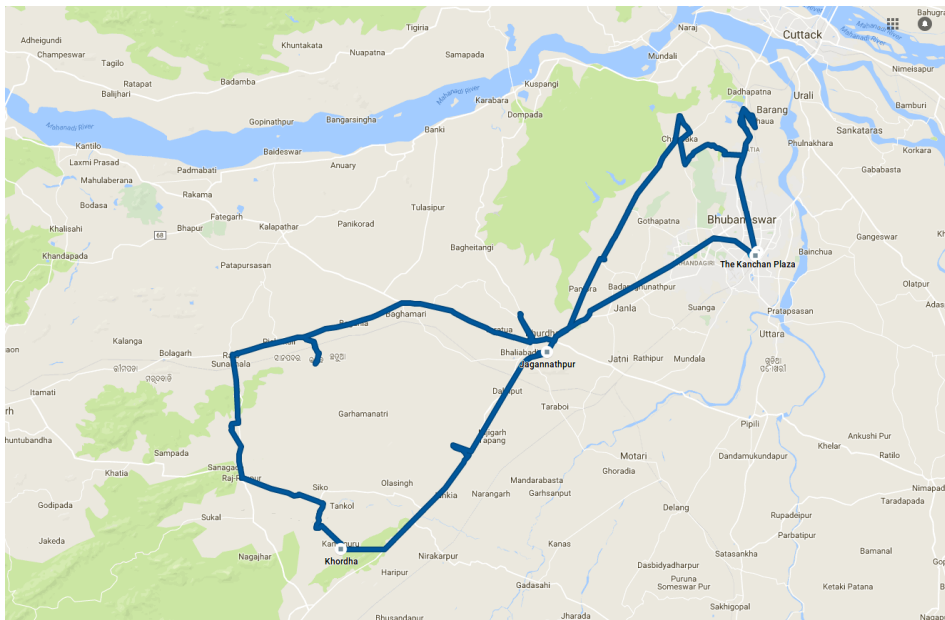


Figure B.1: Trip details for soil sample collection on 03/04/2018: travelled 203 kilometres and visited Bhubaneswar–Chandaka–Ranpur–Khordha

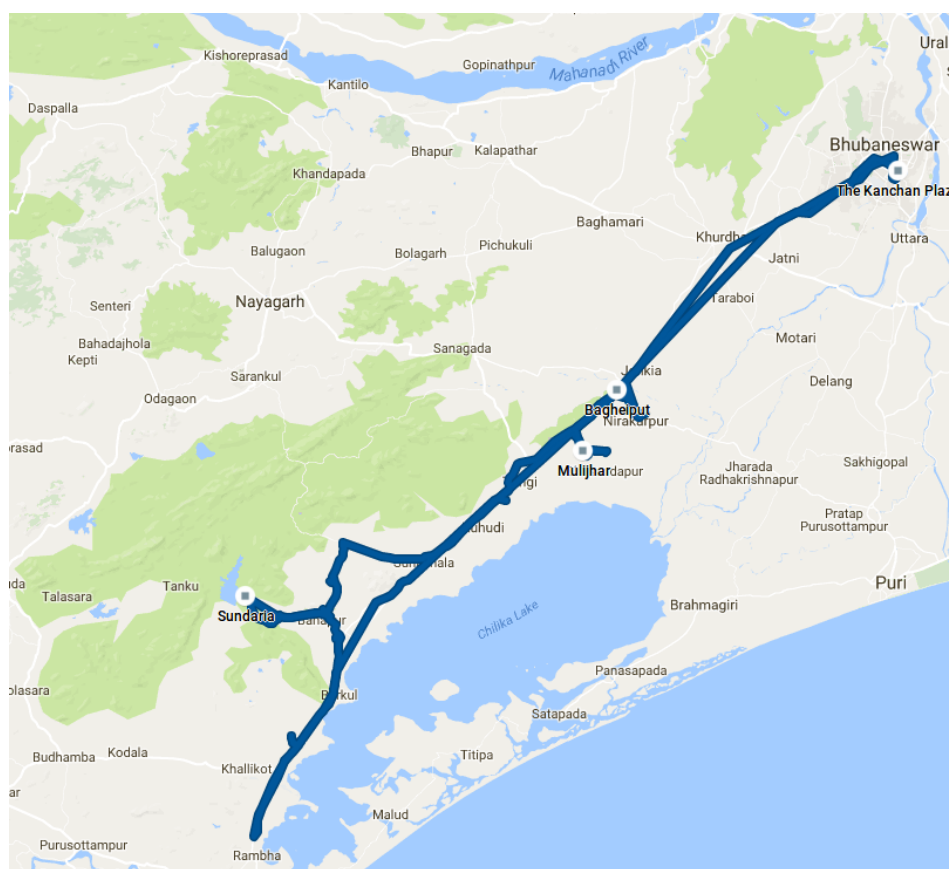


Figure B.2: Trip details for soil sample collection on 04/04/2018: travelled 313 kilometres and visited Bhubaneswar–Rambha–Banpur–Khordha

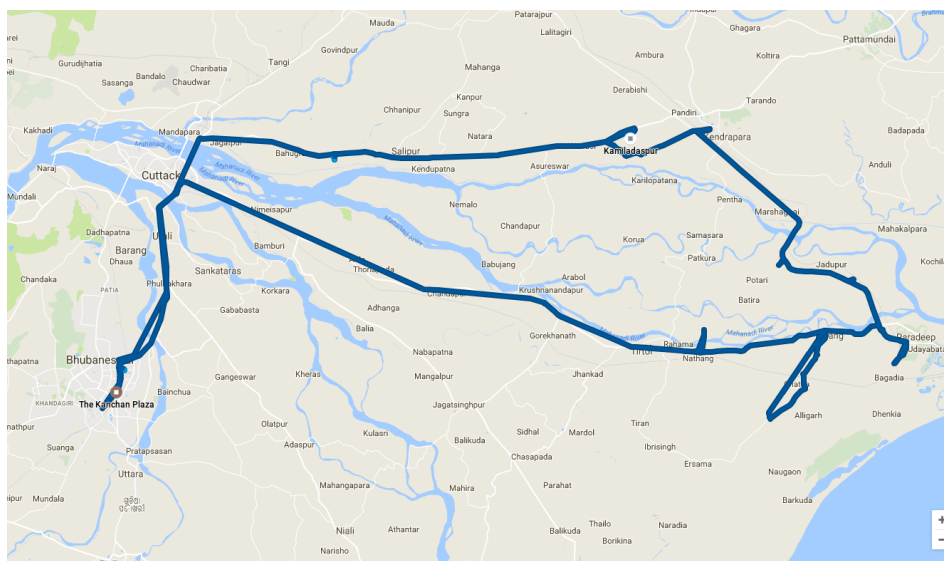


Figure B.3: Trip details for soil sample collection on 05/04/2018: travelled 268 kilometres and visited Bhubaneswar–Salipur–Paradeep–Tritol

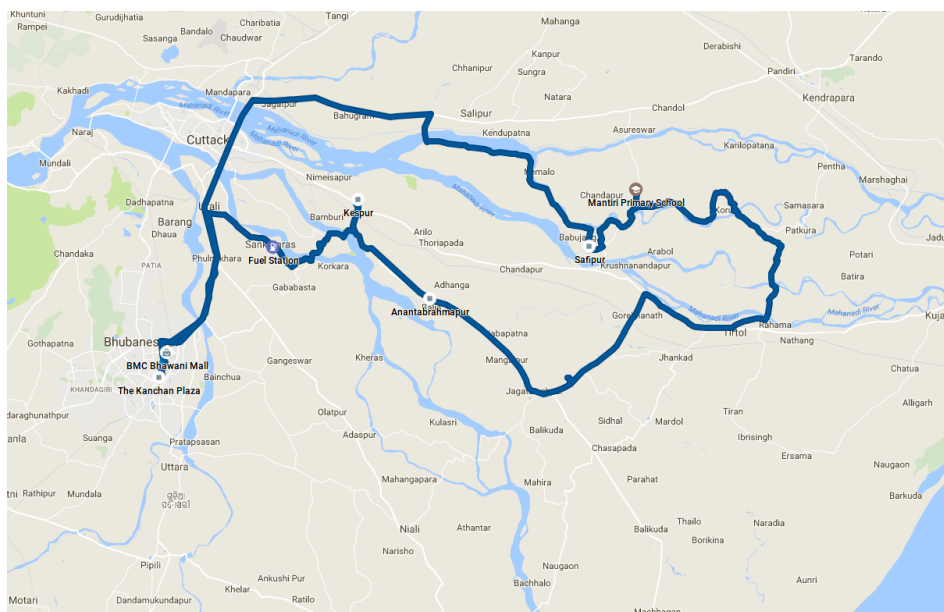


Figure B.4: Trip details for soil sample collection on 06/04/2018: travelled 206 kilometres and visited Bhubaneswar–Salipur–Tritol–Jagatsinghpur

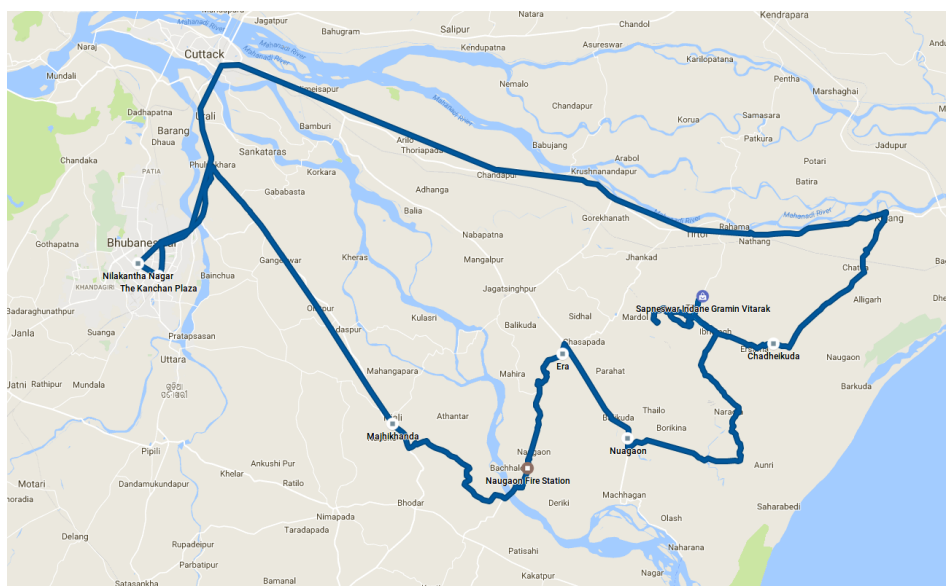


Figure B.5: Trip details for soil sample collection on 07/04/2018: travelled 260 kilometres and visited Bhubaneswar–Paradeep–Nuagaon–Niali



Figure B.6: Trip details for soil sample collection on 08/04/2018: travelled 180 kilometres and visited Bhubaneswar–Niali–Kakatpur–Nimapada

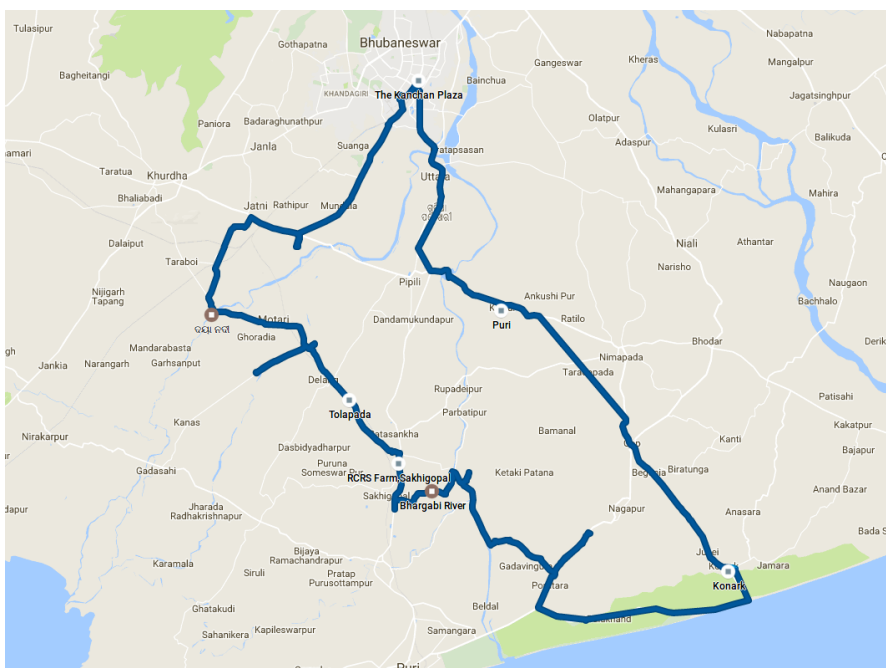


Figure B.7: Trip details for soil sample collection on 09/04/2018: travelled 194 kilometres and visited Bhubaneswar–Gop–Konark–Sakhigopal–Delang

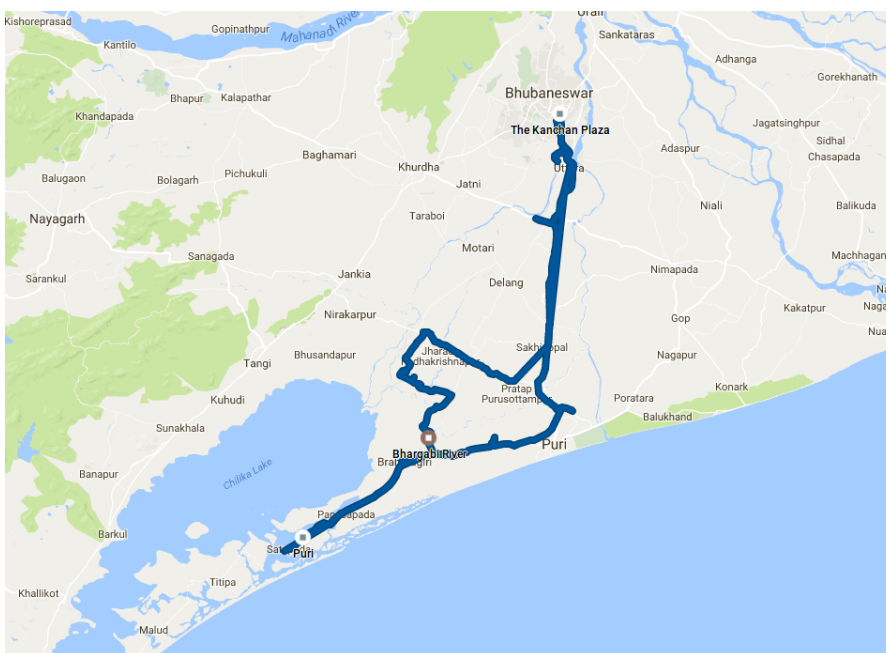


Figure B.8: Trip details for soil sample collection on 11/04/2018: travelled 241 kilometres and visited Bhubaneswar–Puri–Satapada–Sakhigopal

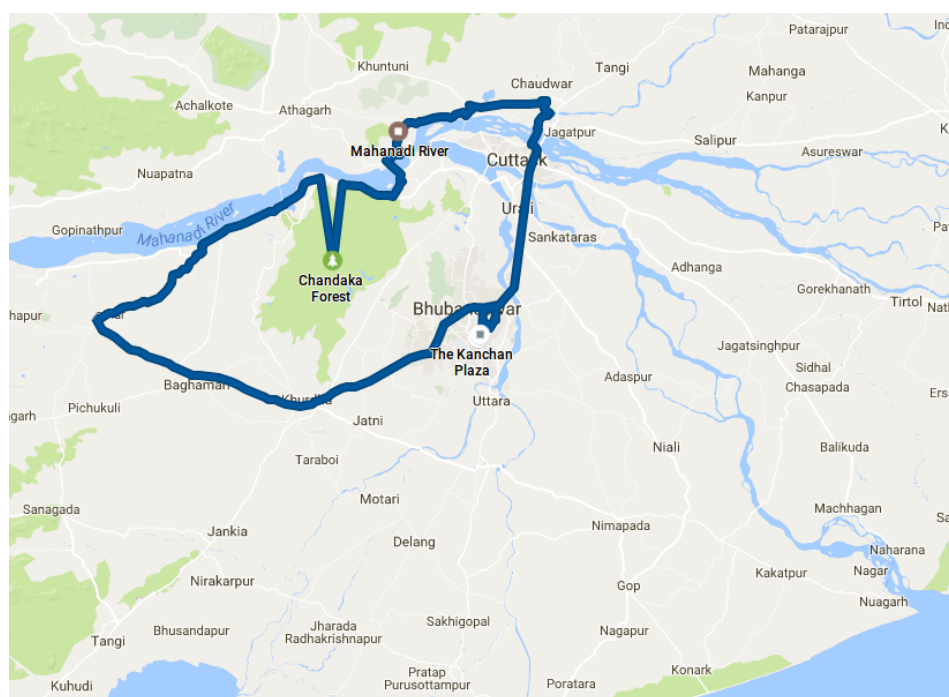


Figure B.9: Trip details for soil sample collection on 12/04/2018: travelled 264 kilometres and visited Bhubaneswar–Cuttack–Naraj–Banki–Kalapathar–Baghmari–Khordha

List of publications

Articles in journals

- **Amit Ghosh**, Shouvik Das, Tuhin Ghosh, and Sugata Hazra. "Risk of extreme events in delta environment: A case study of the Mahanadi delta." *Science of the total environment* (2019).
<https://doi.org/10.1016/j.scitotenv.2019.01.390>
- Anirban Mukhopadhyay, Pramit Ghosh, Abhra Chanda, **Amit Ghosh**, Subhajit Ghosh, Shouvik Das, Tuhin Ghosh, and Sugata Hazra. "Threats to coastal communities of Mahanadi delta due to imminent consequences of erosion Present and near future." *Science of the Total Environment* 637 (2018): 717-729. <https://doi.org/10.1016/j.scitotenv.2018.05.076>
- Somnath Hazra, **Amit Ghosh**, Subhajit Ghosh, Indrajit Pal, and Tuhin Ghosh. "Assessing coastal vulnerability and governance in Mahanadi Delta, Odisha, India." *Progress in Disaster Science* 14 (2022): 100223.
<https://doi.org/10.1016/j.pdisas.2022.100223>
- Abhra Chanda, Sourav Das, Anirban Mukhopadhyay, **Amit Ghosh**, Anirban Akhand, Pramit Ghosh, Tuhin Ghosh, Debashis Mitra, and Sugata Hazra. "Sea surface temperature and rainfall anomaly over the Bay of Bengal during the El Niño-Southern Oscillation and the extreme Indian Ocean Dipole events between 2002 and 2016." *Remote Sensing Applications: Society and Environment* (2018). <https://doi.org/10.1016/j.rsase.2018.08.001>

Book chapters

- Sugata Hazra, Shouvik Das, **Amit Ghosh**, P. Venkat Raju, Amrita Patel, The Mahanadi Delta: A Rapidly Developing Delta in India. In: Nicholls R., Adger W., Hutton C., Hanson S. (eds) Deltas in the Anthropocene. Palgrave Macmillan, Cham, 2020, https://doi.org/10.1007/978-3-030-23517-8_3
- Sugata Hazra, Amrita Patel, Shouvik Das, Asha Hans, **Amit Ghosh**, and Jasmine Giri. "Women-headed households, migration and adaptation to climate change in the Mahanadi Delta, India." In: Hans, Asha, Nitya Rao, Anjal Prakash, and Patel Amrita. Engendering Climate Change: Learnings from South Asia. Taylor & Francis, (2021). 172.

Conference/seminars

- Participated in the International Conference on Mathematical Analysis and Application in Modelling (ICMAAM 2018) at the Department of Mathematics, Jadavpur University during 9–12 January 2018 and presented a contributory talk entitled “**Application of Multivariate Gradients of Covariates for Efficient Soil Sampling Design**”.
- Participated in the 8th DECCMA (Deltas, vulnerability & Climate Change: Migration & Adaptation) Consortium Workshop in 6–9 February 2019 in Dhaka, Bangladesh and presented a talk entitled “**Climate Change impact hotspots in Mahanadi Delta**”.

Notable mentions

Nature published a research highlight using the article "Risk of extreme events in delta environment: A case study of the Mahanadi delta" in their Nature India magazine." <https://www.nature.com/articles/nindia.2019.33>




nature india View all journals Search 🔍 Login

[Explore content](#) [About the journal](#) Sign up for alerts RSS feed

[nature](#) > [nature india](#) > [research highlights](#) > [article](#)

RESEARCH HIGHLIGHT | 19 March 2019

Mahanadi delta high-risk zone for extreme events

The northern part of the Mahanadi delta in eastern India is a high-risk zone for severe cyclones and heavy floods, researchers at Jadavpur University have found¹.

Mahanadi delta in Odisha is drained by three rivers – Mahanadi, Brahmani and Baitarani – that pour into the Bay of Bengal. It has a population of 8 million, and a population density that is higher than that of the state of Odisha.

Sign up to Nature Briefing

An essential round-up of science news, opinion and analysis, delivered to your inbox every weekday.

Email address

Yes! Sign me up to receive the daily *Nature Briefing* email. I agree my information will be processed in accordance with the *Nature* and Springer Nature Limited [Privacy Policy](#).

Sign up

Amit Ghosh Ph.D. Thesis**By: Amit Ghosh**As of: Nov 23, 2022 3:01:05 PM
12,942 words - 66 matches - 35 sources**Similarity Index****4%**Mode: **Similarity Report** ▼**paper text:**

Chapter 1 134429513906500 Introduction The metaphor in the epigraph portrays the anguish of a subsistence farmer who is seeing the flooding of his small farmland. As the natural course to keep a rhythmic climate is 'styled', the experience is shared by the agricultural system as a whole. The climate system that surrounds our very lives is changing. Seemingly, the change is capricious. So, the issue of climate change has sought much attention in recent decades on its causes and consequences to find possible solutions, including adaptive and mitigation measures.

Climate change and agriculture Upon the inception of the IPCC in 1990, it was clear that the concentrations of CO₂ are rising and so are the temperatures (IPCC, 2007). Climate change and global warming are unequivocal, and a mountain of studies confirm that the impacts are very real (IPCC, 2013). It will continue to rise if no proper actions are taken to curb the greenhouse gas emissions (IPCC, 2021). The rising global mean temperature leads to subsequent hydrological and climatological changes. These changes affect the availability of water and surface run-off and thus may affect the hydrological regimes (Middelkoop et al., 2001). Plans for managing water resources are increasingly required to consider the consequences of climate change into account in order to accurately estimate future water availability (Wurbs et al., 2005). On the other hand, frequency of extreme climatic events like flood, cyclone, drought, heat wave are increasing in the warming globe (Rahmstorf and Coumou, 2011). These events pose different challenges on the agricultural sectors and are very complex to address (Cogato et al., 2019; Motha, 2011). The climatic variabilities, especially the extreme events, have been a dilemma for farmers since the inception of agriculture in the fertile earth some millions years ago. Agricultural system is sensitive

to climate change as well as a driver for **climate**

19

change (Prasada et al., 2010). Climate change brings changes in the agro-ecological conditions (Allen et al., 1987) Therefore, variability in temperature, precipitation and soil moisture may act synergistic or antagonistically in determining the optimal temperature and water requirements for biomass production and growth (Karl et al., 2009). Cropping pattern and techniques

have a significant impact on the availability **of water** resources, which is **the**

10

single most critical factor in determining the survival and sustainability of agricultural systems. (Zingaro et al., 2017). The changes and variability of precipitation may affected the sustainability of such cropping practices (Amini Fasakhodi et al., 2010). Changes in the climate and agriculture in the deltas Deltas are formed by alluvial deposits at the edge of a